

UNIVERSIDADE FEDERAL DO RIO GRANDE DO SUL

CENTRO DE BIOTECNOLOGIA

PROGRAMA DE PÓS-GRADUAÇÃO EM BIOLOGIA CELULAR E MOLECULAR

NATHAN ARAUJO CADORE

**PERFIL METABÓLICO DE CÉLULAS HUMANAS DE ADENOCARCINOMA DE
PULMÃO SENSÍVEIS E RESISTENTES À CISPLATINA**

DISSERTAÇÃO DE MESTRADO

PORTO ALEGRE

2020

NATHAN ARAUJO CADORE

**PERFIL METABÓLICO DE CÉLULAS HUMANAS DE ADENOCARCINOMA DE
PULMÃO SENSÍVEIS E RESISTENTES À CISPLATINA**

Dissertação submetida ao Programa de Pós-Graduação em Biologia Celular e Molecular do Centro de Biotecnologia da Universidade Federal do Rio Grande do Sul como requisito parcial para obtenção do título de Mestre.

Orientadora: Profa. Dra. Karina Mariante Monteiro

Porto Alegre

2020

Este trabalho foi realizado no Laboratório de Genômica Estrutural e Funcional e no Laboratório de Biologia Molecular de Cestódeos do Centro de Biotecnologia da UFRGS, sendo financiado pela Coordenação de Aperfeiçoamento de Pessoal de Nível Superior (CAPES), pela Fundação de Amparo em à Pesquisa do Estado do Rio Grande do Sul (FAPERGS) e pelo Conselho Nacional de Desenvolvimento Científico e Tecnológico (CNPq).

AGRADECIMENTOS

Muitas pessoas fizeram parte deste trabalho e foram essenciais para o meu crescimento durante o período do mestrado. Agradeço a todos que me incentivaram de alguma forma e reconheceram a importância desta etapa para mim. Além disso, alguns nomes preciso citar em forma de agradecimento pela participação direta no desenvolvimento deste trabalho.

Agradeço minha orientadora, Profa. Dra. Karina, por me proporcionar um conhecimento imensurável. Agradeço a confiança em mim depositada desde o meu primeiro dia em um laboratório de biologia molecular. Foram alguns anos de muitos ensinamentos que irão comigo para toda a minha carreira científica. Tenho certeza de que este não é o último projeto que estaremos juntos.

Agradeço a Cris pela amizade, parceria, paciência e ensinamentos. Muito obrigado por me ensinar toda a base que constituiu este projeto. Sou muito grato por ter me orientado como IC no início de tudo e por ter sido essa colega incrível durante o mestrado. Agradeço a Lais por ter se tornado uma amiga muito além do laboratório. Muito obrigado por ter me inspirado como cientista e, principalmente, a me aceitar não importa onde eu esteja. Agradeço a May pela amizade que criamos, pelo exemplo de pessoa que é para mim e por ter trazido tanta leveza e conforto aos dias no laboratório. Agradeço a Bruna por ter sido uma grande parceira de bancada. Obrigado pela amizade e por estar sempre ali para me ajudar em cada experimento. Sou muito grato por toda a parceria. Vocês foram muito importantes para mim nessa etapa.

O apoio não se limitou apenas ao laboratório e, por isso, tenho muito a agradecer àqueles que me incentivaram e deram suporte fora dele. Agradeço a Camila e a Lais por um apoio que não consigo descrever em algumas frases. Não tenho palavras para agradecer o quão importante vocês foram para eu concluir esta etapa. Agradeço aos meus biotecs favoritos, Franz e Betina, que participaram de cada segundo desse processo, me ensinam muito a cada dia e tornaram meus dias mais leves. Agradeço ao Cândido por cada dia ao meu lado durante esta etapa, me incentivando e me dando um suporte que jamais vou esquecer.

Todos vocês foram de extrema importância para mim neste processo, por isso, não cabem em palavras meus agradecimentos e aqui fica por mera formalidade.

Agradeço todos os colegas dos laboratórios 204, 206 e 210 que foram muito solícitos em todos os momentos que precisei. Todos vocês agregaram neste projeto e foram essenciais para que eu conseguisse realizá-lo. Agradeço ao Guilherme pelo interesse e esforço na participação do projeto. Apesar do curto tempo, a sua ajuda foi essencial. Agradeço as meninas do OROBOROS, Camila e Bruna, pela ajuda na realização dos experimentos. Agradeço Prof. Dr. Arnaldo Zaha e Prof. Henrique Ferreira pelos diversos ensinamentos e pela construção do meu pensamento crítico. Também, agradeço por proporcionarem a estrutura e materiais necessários para o desenvolvimento deste projeto.

Agradeço aos membros da banca por terem aceitado participar da avaliação deste projeto, Prof. Dr. Eduardo Chiela, Dr. Juciano Gasparotto e Dra. Karine Begnini. Também, ao Prof. Dr. Arnaldo pelas revisões e por fazer parte desta banca. Muito obrigado!

SUMÁRIO

RESUMO.....	6
ABSTRACT.....	7
1. INTRODUÇÃO	9
1.1. O câncer	9
1.2. Tratamento do câncer de pulmão, quimioterapia e cisplatina	12
1.3. Resistência tumoral à CDDP	14
1.4. Metabolismo e necessidades bioenergéticas de células resistentes à CDDP	18
1.5. Modelos celulares para o estudo da resistência tumoral	22
1.6. Justificativa	23
2. OBJETIVOS	25
2.1. Objetivo geral.....	25
2.2. Objetivos específicos.....	25
3. MANUSCRITO	26
4. DISCUSSÃO GERAL.....	87
5. PERSPECTIVAS	95
6. REFERÊNCIAS.....	96
7. CURRÍCULO VITAE RESUMIDO	109

RESUMO

O câncer de pulmão é o tipo de câncer mais incidente e o líder em causas de morte em todo o mundo. O tratamento padrão para pacientes com câncer de pulmão é a quimioterapia, sendo a cisplatina (CDDP) uma das drogas mais utilizadas. Contudo, a resistência do câncer à CDDP é frequente. A resistência à CDDP é um processo complexo e multifatorial. O *fitness* celular e diferentes *trade-offs* bioenergéticos adotados pela célula são exemplos de fatores determinantes na resistência. Estudos prévios do grupo de pesquisa identificaram potenciais alterações bioenergéticas e estratégias de crescimento em células resistentes à CDDP. Portanto, o presente estudo avaliou o perfil metabólico e a regulação de vias bioenergéticas de células sensíveis e resistentes à CDDP. Para isso, células com resistência adquirida à CDDP (A549/CDDP) foram desenvolvidas a partir da exposição de células da linhagem parental A549 a concentrações crescentes da droga. Após, análise da expressão gênica de genes relacionados ao metabolismo foi realizada por RT-qPCR. A dependência por fontes energéticas e efeito de agentes anti- e pró-oxidantes foram avaliados por ensaio de proliferação ou clonogênico. O efeito de inibidores glicolíticos foi avaliado por ensaio de citotoxicidade. Parâmetros do consumo de O₂ mitocondrial foram avaliados por respirometria de alta resolução. A expressão do fator de iniciação eucariótico eIF2 α e de 4E-BP1 e a fosforilação destes foram avaliadas por western blot. Células A549/CDDP apresentaram regulação negativa de genes envolvidos com o metabolismo de glicose e L-glutamina, além da regulação positiva do inibidor de glicólise TIGAR (*TP53-induced glycolysis and apoptosis regulator*), indicando redução da atividade destas vias metabólicas. Também, células resistentes à CDDP apresentaram maior dependência à glicose e L-glutamina para a proliferação. O inibidor 2-DG apresentou maior citotoxicidade em células resistentes, sendo uma consequência da redução de enzimas glicolíticas. Além disso, células A549/CDDP apresentaram respiração mitocondrial reduzida, caracterizando menor atividade da mitocôndria. As linhagens apresentaram semelhança na resposta a agentes anti- e pró-oxidantes, indicando possível semelhança quanto ao equilíbrio redox. Por fim, 4E-BP1 apresentou uma redução na razão da isoforma fosforilada 4E-BP1 (Thr37/46) por 4E-BP1 hipofosforilada em células A549/CDDP. Assim, uma possível regulação global da tradução em células A549/CDDP pode estar atuando como um mecanismo de resistência. Em conjunto, este trabalho descreve uma redução geral do metabolismo em células resistentes à CDDP, possível consequência de uma redução global da tradução. Com isso, o melhor entendimento destas vias na resistência à CDDP poderá proporcionar melhores prognósticos e tratamentos alternativos para o câncer de pulmão.

ABSTRACT

Lung cancer is the most prevalent cancer and the leading cause of death worldwide. The standard treatment of lung cancer is chemotherapy and cisplatin (CDDP) is one of the most used drug. Although CDDP resistance is frequent in lung cancer therapy. CDDP resistance is a complex and multifactorial event. Cell fitness and different bioenergetic trade-offs adopted by cells are examples of determinant factors in cancer resistance. Previous studies of our group identified possible bioenergetics alteration and change in cell growth strategies of CDDP-resistant cells. Thus, the present study evaluated the metabolic profile and regulation of bioenergetic pathways of CDDP-sensitive and -resistant cells. To that end, acquired CDDP-resistant cells (A549/CDDP) were developed by the exposure to increasing drug concentration of A549 parental cell line. Then, gene expression analysis of genes related to bioenergetic metabolism was performed by RT-qPCR. Energy sources dependence and effect of anti- and pro-oxidant agents were evaluated by proliferation or clonogenic assay. The effect of glycolytic inhibitors was accessed by cytotoxicity assay. Parameters of mitochondrial O₂ consumption were evaluated by high-resolution respirometry. Expression of the initiation factor eIF2 α and 4E-BP1, and their phosphorylated isoforms were analyzed by western blot. A549/CDDP cells showed a downregulation of genes involved in glucose and L-glutamine metabolism. Also, the glycolysis inhibitor TIGAR (*TP53-induced glycolysis and apoptosis regulator*) was upregulated in A549/CDDP cells. These results suggest a reduction of glucose and L-glutamine metabolic pathways. Moreover, CDDP-resistant cells showed higher dependence of these substrates for cell proliferation. The glycolysis inhibitor 2-DG showed higher cytotoxicity in A549/CDDP cells, which may be a consequence of reduction in glycolytic enzymes. Furthermore, A549/CDDP cells presented lower mitochondrial respiration featuring decreased mitochondria activity. CDDP-sensitive and -resistant cells showed similar response to anti- and pro-oxidant agents, indicating a possible similarity in redox balance. Lastly, 4E-BP1 showed a reduction in the ratio of phosphorylated isoform 4E-BP1 (Thr37/46) to hypophosphorylated 4E-BP1 in A549/CDDP cells. Thereby, a possible global translation regulation in A549/CDDP cells may be acting as a CDDP-resistance mechanism. Together, this work describes a general reduction in metabolism in CDDP-resistant cells which may be a possible consequence of global translation reduction. Thus, A better understanding of these pathways in CDDP resistance may provide better prognosis and alternative treatments for lung cancer.

LISTA DE ABREVIATURAS

ATP: adenosina trifosfato

BSO: buthionine sulfoximine

CDDP: cisplatina ou cis-diaminodicloroplatina (II)

DEM: diethyl maleate

DNA: ácido desoxirribonucleico

FDA: *Food and Drug Administration*

GSH: glutationa reduzida

MMR: reparo do pareamento errôneo de DNA (do inglês *mismatch repair*)

mtDNA: ácido desoxirribonucleico mitocondrial

NER: reparo por excisão de nucleotídeo (do inglês *nucleotide excision repair*),

NSCLC: câncer de pulmão de células não pequenas (do inglês *non-small cell lung cancer*)

OXPPOS: fosforilação oxidativa

PET-CT: *Positron Emission Tomography–Computed Tomography*

RNA: ácido ribonucleico

ROS: espécies reativas de oxigênio

ROX: consumo de oxigênio residual

RT-qPCR: transcrição reversa seguida de reação em cadeia da polimerase

SCLC: câncer de células pequenas (do inglês *small cell lung cancer*)

UCPs: proteínas de desacoplamento (do inglês *uncoupling proteins*)

2-DG: 2-Deoxi-d-glucose

3-BrP: 3-bromopyruvate

1. INTRODUÇÃO

1.1. O câncer

O câncer é definido como uma doença complexa, onde células de um determinado tecido deixam de responder sinais responsáveis pela regulação da diferenciação, sobrevivência, proliferação e morte celular. Como consequência, estas células se acumulam no tecido formando o tumor, causando um dano local (NATURE, 2020). As células de câncer não se limitam apenas ao tumor, frequentemente migrando para diferentes tecidos e levando à formação de múltiplos tumores no organismo da pessoa acometida pela doença. Este evento, nomeado metástase, é responsável por 90% das mortes relacionadas ao câncer (ZEESHAN; MUTAHIR, 2017).

O câncer é uma doença mundialmente conhecida e amplamente estudada. Hanahan & Weinberg (2011) descrevem dez capacidades essenciais adquiridas pelas células no processo de tumorigênese (Fig. 1). Dentre elas, podem ser destacadas: capacidade de imortalidade replicativa, resistência à morte celular, mutações e instabilidade do genoma, indução de angiogênese e desregulação energética celular. Estas características reforçam a complexidade da formação do tumor, além das características intrínsecas variadas de cada subtipo celular que constituem essa massa tumoral. Levando em consideração estes fatores, é nítida a dificuldade na obtenção de um tratamento universal e eficaz contra o câncer. O melhor entendimento destes mecanismos pode levar à proposição de novas terapias mais eficientes.

A dificuldade no tratamento do câncer leva a uma alta mortalidade relacionada à doença. No último levantamento feito pela Agência Internacional de Pesquisa em Câncer (IARC, do inglês *International Agency for Research on Cancer*) foram estimados 18 milhões de novos casos e 9,5 milhões de mortes relacionadas ao câncer apenas em 2018. O câncer pode ser classificado pelo local primário de desenvolvimento do tumor, destacando-se os cânceres de estômago, próstata, colorretal, mama e pulmão por serem os mais incidentes no mundo em números absolutos. Além disso, dentre estes tipos de tumores, apenas o câncer de próstata não está entre os cinco com maior mortalidade (Fig. 2) (IARC, 2018).

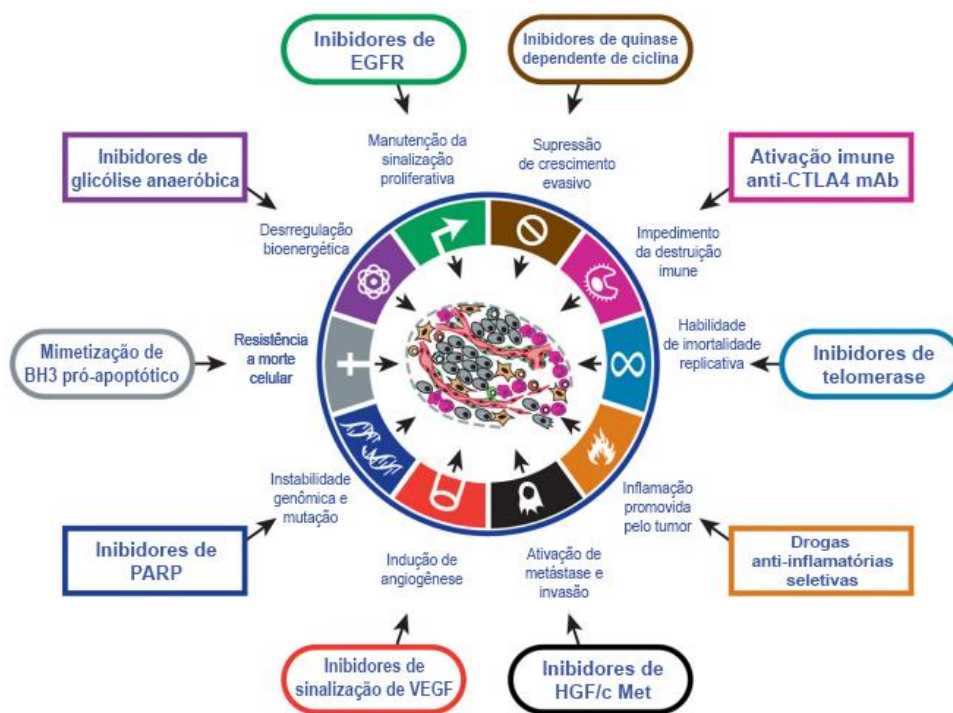


Figura 1: As características (hallmarks) do câncer. Figura ilustrativa de características adquiridas durante a tumorigênese e tratamentos alternativos propostos para a inibição destes processos. EGFR, do inglês *epidermal growth factor receptor*; CTLA4, Proteína T-Linfócito-Associada citotóxico 4; mAb, anticorpo monoclonal; BH3, *B cell lymphoma 2 (BCL2) homology domain 3*; PARP, *Poly (ADP-ribose) polymerase*; VEGF, do inglês *vascular endothelial growth factor*; HGF, Hepatocyte Growth Factor; c-Met, *tyrosine-protein kinase Met*. Adaptada de Hanahan & Weinberg (2011).

1.1.1. O câncer de pulmão

O câncer de pulmão é o tipo de tumor mais incidente em todo o mundo (Fig. 2), sendo o líder na causa de mortes relacionadas ao câncer entre homens e o segundo entre as mulheres. São estimados 1,8 milhões de novos casos de câncer de pulmão por ano em todo o mundo e 1,6 milhões de mortes relacionadas a esta doença (TORRE et al., 2015). Ademais, estes números são crescentes devido ao aumento da população mundial e da estimativa de vida, além da influência de hábitos, como o tabagismo, na saúde dos indivíduos (RAHIB et al., 2014). Além do tabagismo, outros fatores de risco também podem ser determinantes para os números de casos e mortes relacionadas ao câncer de pulmão, como a poluição do ar, o contato com radônio, herança genética, radiação, dieta, entre outros (MAO et al., 2016). No Brasil, o cenário é similar, sendo o câncer de pulmão o tipo mais incidente. Apenas para o ano de 2020, é estimado que existam 30,2 mil casos da doença no país (INCA, 2019).

A alta taxa de mortalidade relacionada ao câncer de pulmão é consequência de diversos fatores relacionados tanto ao diagnóstico quanto ao tratamento. As manifestações clínicas da doença incluem dispneia, embolia pulmonar, pneumotórax, tosses crônicas e dores no peito. Contudo, estas manifestações não estão presentes em estágios iniciais do tumor, além de não serem específicas de câncer (NASIM; SABATH; EAPEN, 2019). Com isso, o diagnóstico do câncer de pulmão é feito, frequentemente, em estágios avançados da doença, o que dificulta o sucesso do tratamento (Fig. 3). O diagnóstico do câncer e a classificação histológica do tumor são passos essenciais para a definição de uma intervenção médica. Entre os principais exames para o diagnóstico do câncer de pulmão devem ser destacados: os exames de tomografia, principalmente o PET-CT (do inglês *Positron Emission Tomography–Computed Tomography*) que permite a identificação da localização do tumor e possíveis tumores em locais secundários, e a biópsia deste tumor (JACOBSEN et al., 2017).

Número estimado da incidência e de mortes pelo mundo, ambos os sexos, todas as idades

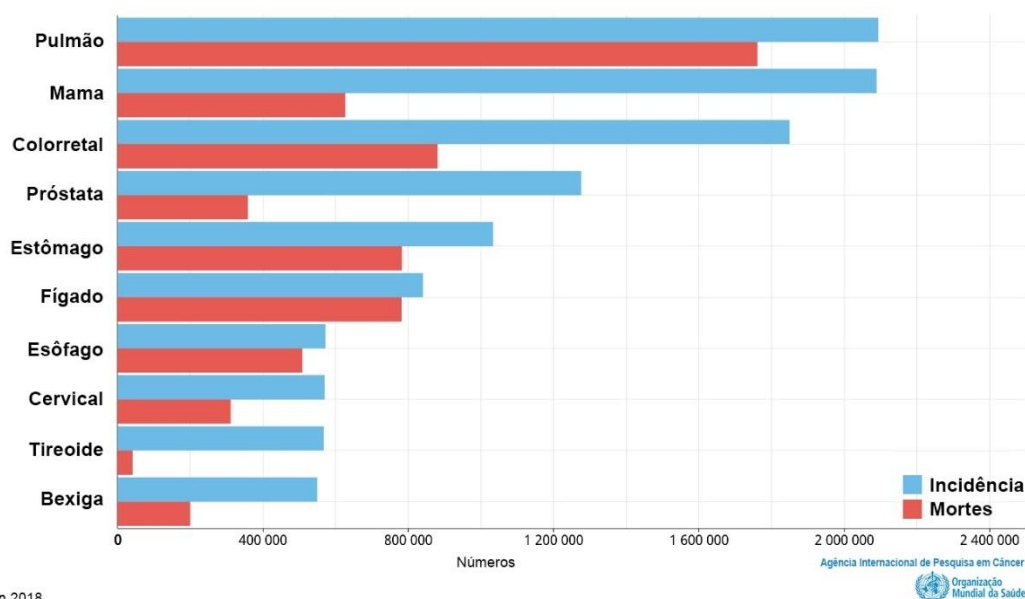


Figura 2: Números de incidência e mortes relacionadas ao câncer no mundo. Números de casos estimados para o ano de 2018 em ambos os sexos e todas as idades (IARC, 2018).

As células de câncer de pulmão podem ser divididas em dois principais grupos histológicos, sendo classificado como câncer de células pequenas (SCLC, do inglês *small cell lung cancer*) e câncer de pulmão de células não pequenas (NSCLC, do inglês *non-small cell lung cancer*), sendo este último responsável por 85% dos casos (SIEGEL; MILLER; JEMAL,

2016). O NSCLC pode ser classificado em três diferentes subtipos: carcinoma de pulmão de células grandes, carcinoma de células escamosas e adenocarcinoma, tendo estes uma frequência de 5-10%, 25-30% e 40%, respectivamente (DENISENKO; BUDKEVICH; ZHIVOTOVSKY, 2018).

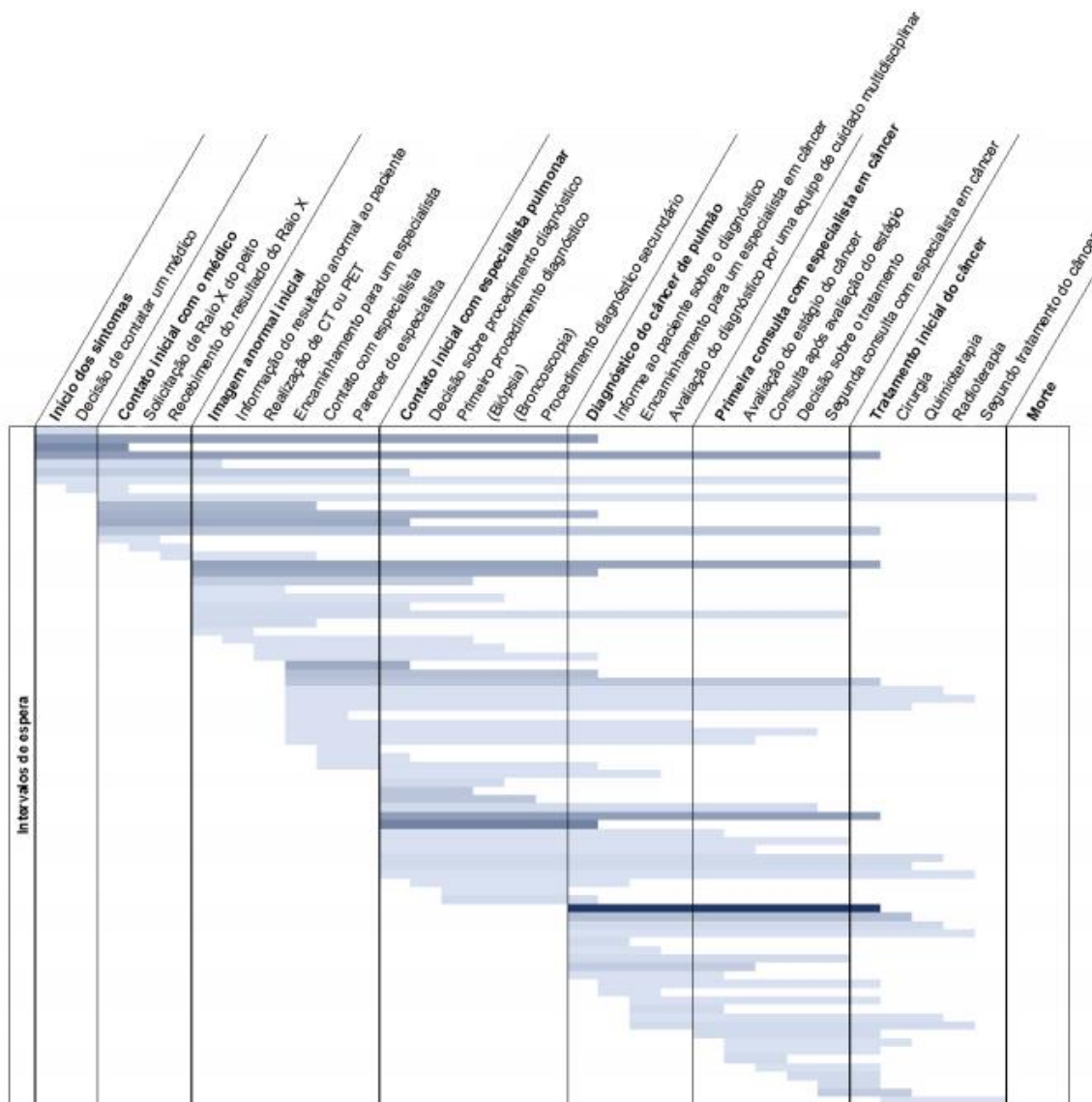


Figura 3: Linha do tempo dos sintomas ao tratamento do câncer de pulmão. Estimativa de tempo relativo dos passos necessários desde o momento dos sintomas ao tratamento do câncer de pulmão. Tons das barras indicam o número de estudos reportando o intervalo de tempo. Adaptado de Jacobsen *et al.* (2017).

1.2. Tratamento do câncer de pulmão, quimioterapia e cisplatina

A escolha da abordagem utilizada no tratamento do câncer de pulmão está diretamente relacionada ao estágio do tumor no momento do diagnóstico. Em estágios iniciais da doença, estágios I e II, a cirurgia e a radioterapia são estratégias efetivas, devido ao tumor estar

localizado. Com a progressão da doença, células tumorais podem migrar do pulmão criando tumores secundários que inviabilizam um tratamento localizado. Como discutido anteriormente, a maioria dos pacientes encontra-se em estágios avançados da doença (estágio III) no momento do diagnóstico, o que faz da quimioterapia o tratamento de escolha para esses pacientes (LEMJABBAR-ALAOUI et al., 2015). Drogas quimioterápicas possuem mecanismos diversos que interferem na divisão celular levando à morte da célula. Um dos principais grupos de quimioterápicos utilizados no tratamento do câncer de pulmão possui como modo de ação a ligação direta com o DNA. Neste grupo estão moléculas alquilantes derivadas de platina, como a cisplatina e a carboplatina, consideradas tratamento padrão de primeira linha contra o NSCLC (WAKELEE; KELLY; EDELMAN, 2014).

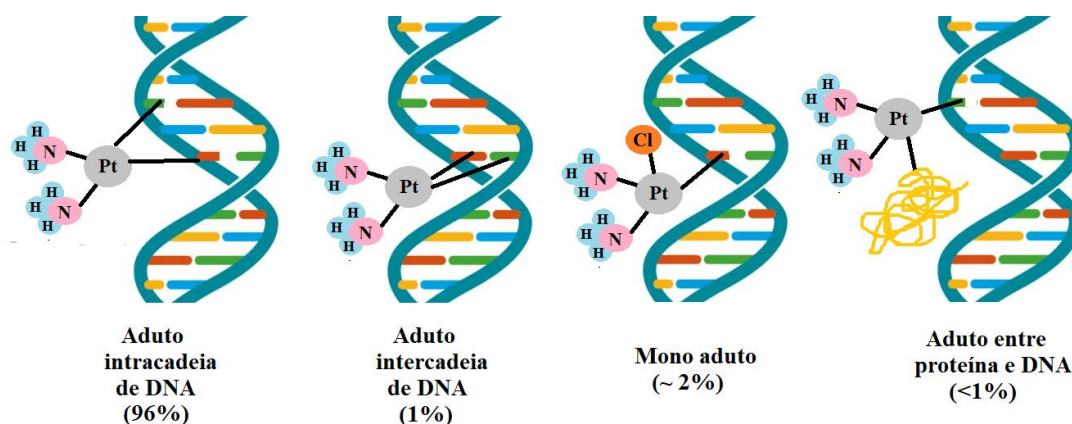


Figura 4: Principais interações da CDDP com o DNA. Diferentes adutos formados pela interação CDDP-DNA e suas frequências de ocorrência.

A cisplatina (CDDP) ou cis-diaminodicloroplatina (II) é uma droga amplamente conhecida e estudada por sua capacidade de interferir na replicação celular, o que permitiu a utilização deste fármaco no tratamento contra o câncer. Os efeitos biológicos da CDDP vem sendo descritos há mais de 60 anos, quando foi observada a sua capacidade de inibir o crescimento celular em *Escherichia coli* (ROSENBERG; VANCAMP; KRIGAS, 1965). A partir da constatação de sua capacidade de inibição replicativa em bactérias, o potencial antitumoral do fármaco foi avaliado (ROSENBERG et al., 1969). Assim, a CDDP foi o primeiro composto derivado de platina aprovado para o tratamento contra o câncer pela agência americana FDA (do inglês *Food and Drug Administration*) em 1978 (KELLAND, 2007). Atualmente, este fármaco é utilizado para o tratamento de diferentes tipos de câncer, incluindo

de bexiga, cabeça e pescoço, ovário, testículo e pulmão (SOCINSKI, 2004). O principal modo de ação da CDDP consiste na ligação direta com átomos N7 de bases purinas do DNA formando adutos. Estas interações preferencialmente são feitas nos sulcos maiores da fita dupla de DNA, onde existe uma maior acessibilidade ao sítio de ligação. A maioria das interações CDDP-DNA resulta em *crosslinks* intracadeia em sítios ApG e GpG, contabilizando 85-90% das interações (Fig. 4). Além disso, podem ser encontrados *crosslinks* intercadeia resultantes da interação com bases de fitas opostas, monoadutos e interação proteína-CDDP-DNA. Contudo, estas formas de interação são menos frequentes (SIDDIK, 2003).

A interação da CDDP com o DNA é o principal modo de ação da droga, contudo, outros mecanismos fazem parte do resultado de sua citotoxicidade. A interação do fármaco com a célula gera um aumento de espécies reativas de oxigênio (ROS) pelo estresse causado, além da interação desse fármaco com moléculas responsáveis pela manutenção do equilíbrio redox, como a glutatona reduzida (GSH) (DASARI; TCHOUNWOU, 2014). Estes mecanismos de citotoxicidade causam a ativação de vias de sinalização apoptótica ou, até mesmo, a necrose das células tumorais (Fig. 5). Contudo, as células tumorais podem utilizar mecanismos de resistência à droga para sobreviver ao tratamento e a alta incidência de resistência à CDDP limita o sucesso do tratamento quimioterápico.

1.3. Resistência tumoral à CDDP

O tumor é constituído de diferentes populações de células que podem possuir fenótipo e genótipo muito distintos entre si (MCGRANAHAN; SWANTON, 2017), o que constitui a heterogeneidade intra-tumoral. Como discutido anteriormente (Subtópico 1.1), essa heterogeneidade pode dificultar o sucesso do tratamento, uma vez que algumas células presentes no tumor podem desenvolver mecanismos relacionados com a resistência ao quimioterápico. A resistência à CDDP é algo relevante na busca do sucesso no tratamento do câncer de pulmão. Durante o tratamento, determinadas populações podem utilizar vias e mecanismos de resistência já ativos para sobreviver ao tratamento, sendo estas consideradas células com resistência intrínseca à droga. Além disso, durante a exposição à CDDP, as células podem ativar mecanismos e alterar vias metabólicas e/ou de sinalização celular que interfiram no efeito biológico do composto, sendo estas consideradas células com resistência adquirida à CDDP. A resistência à CDDP é um processo complexo e multifatorial. Galluzzi et al. (2012) descreve os mecanismos de resistência à droga classificando-os como *pre-target*, *on-target*, *post-target* e *off-target* (Fig. 6).

o balanço do equilíbrio redox da célula, interagindo com moléculas oxidantes, como H_2O_2 . Além disso, este grupamento apresenta afinidade pela CDDP e, assim, pode atuar capturando estas moléculas (PATHAK; DHAR, 2016).

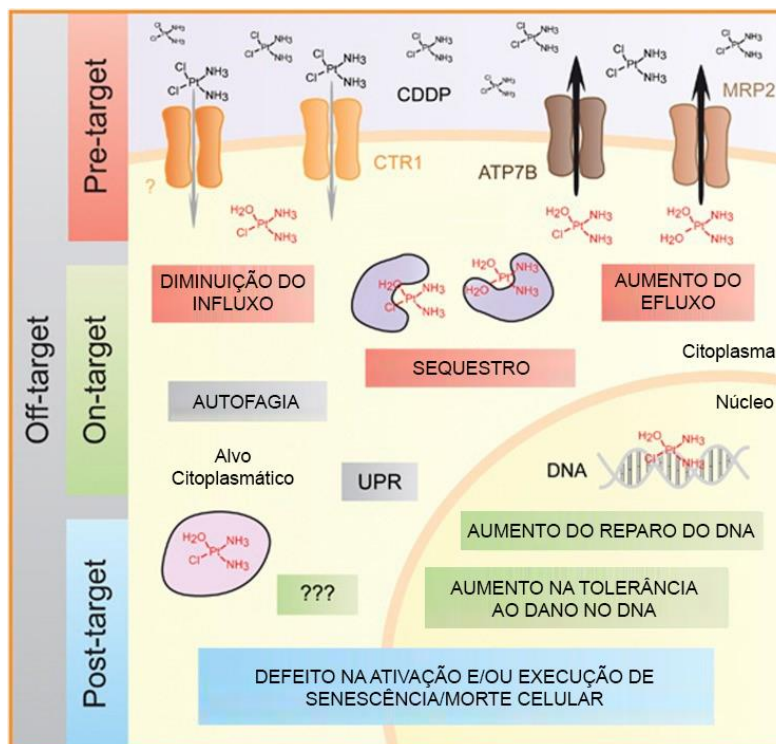


Figura 6: Classificação de mecanismos de resistência à CDDP. Principais mecanismos de resistência à CDDP classificados em *pre-target*, *on-target*, *post-target* e *off-target*. Adaptado de Galluzzi et al. (2014)

1.3.2. Mecanismos de resistência *on-target*

Os principais mecanismos deste grupo incluem a capacidade de reparo de danos causado pela CDDP no DNA e o aumento da tolerância aos danos. A formação dos adutos de CDDP levam à excisão de nucleotídeos, resultando em mutações, inativação de genes essenciais para a sobrevivência, alteração na transcrição e replicação do DNA, além da ativação de genes que respondem a danos e desencadeiam o início do processo de apoptose (HU et al., 2016; MAKOVEC, 2019). Sistemas ativos e eficientes de reparo ao dano no DNA, tais como o reparo por excisão de nucleotídeo (NER, do inglês *nucleotide excision repair*), reparo do pareamento errôneo de DNA (MMR, do inglês *mismatch repair*) e reparo por recombinação homóloga são determinantes no resultado desencadeado pela exposição à CDDP (WEEDEN; ASSELIN-LABAT, 2018). O sistema de NER é conhecido como o principal mecanismo de reparo a danos causados pela CDDP (FURUTA et al., 2002; SHUCK; SHORT; TURCHI, 2008). Como

exemplo, as proteínas ERCC1 (*DNA excision repair protein ERCC-1*) e ERCC2 (*General transcription and DNA repair factor IIIH helicase subunit XPD*) fazem parte desta via de reparo e estão diretamente associadas à resistência ao fármaco.

A resistência à CDDP associada a ERCC1 é consequência do papel essencial desta proteína na via de NER. Durante o reconhecimento do dano no DNA, ERCC1 reconhece a junção ss/dsDNA, interagindo com XPA (*DNA repair protein complementing XP-A cells*) presente no local do dano. A interação física de ERCC1 e XPA é essencial para o recrutamento de XPF (*DNA repair endonuclease XPF*), enzima responsável pela excisão a fita danificada (DUAN et al., 2020). Maior expressão de ERCC1 foi relacionada com a má resposta à terapia utilizando CDDP em diferentes tumores (DU et al., 2016; JUN et al., 2008; OLAUSSEN et al., 2006). Também, a inibição da expressão do gene codificador para esta proteína induz a sensibilidade à CDDP em NSCLC (GUO et al., 2018a).

ERCC2, ou XPD, é outro componente essencial para o sistema NER e frequentemente associado à resposta do tratamento com CDDP. XPD é conhecida pela participação na abertura da hélice de DNA em torno do dano, permitindo o recrutamento de XPA e XPF-ERCC1 (PAJUELO-LOZANO et al., 2018). A maior expressão de XPD também foi relacionada à maiores níveis de resistência em células de glioma (ALOYZ et al., 2002). Ademais, variantes genéticas em *ERCC2* foi associado com o resultado do tratamento com CDDP em pacientes acometidos por osteosarcoma (CARONIA et al., 2009). Ainda, o silenciamento gênico de *ERCC2* em células humanas de câncer de ovário inibe a resistência à CDDP (ZHAO et al., 2016).

1.3.3. Mecanismos de resistência *post-target*

Mecanismos *post-target* são, principalmente, processos envolvidos com vias de transdução de sinal ativadas por CDDP, os quais desencadeiam o processo de apoptose e disfunção na maquinaria de morte celular. Estes eventos estão presentes em células tumorais, visto que são características consideradas *hallmarks* do câncer, como discutido anteriormente. A maior parte de genes e proteínas pertencentes a este grupo de mecanismos de resistência estão, também, indubitavelmente relacionados com a carcinogênese. As proteínas da família BCL-2 são exemplos de proteínas envolvidas nestes mecanismos. Estas podem ser classificadas em pró-apoptóticas, como exemplo Bax (*BCL2 Associated X*), ou anti-apoptóticas, como Bcl-xL (*BCL2 Like 1*). Assim, o equilíbrio entre os diferentes membros desta família é determinante para a decisão entre vida e morte da célula (KNIGHT et al., 2019).

Após a ativação da apoptose pela via intrínseca, onde diversas proteínas da família BCL-2 estão atuando, Bax é ativada oligomerizando com BAK (*Bcl-2 homologous antagonist/killer*), o que resulta na formação de poros na membrana mitocondrial. Este processo resulta na liberação de fatores apoptogênicos no citoplasma (SINGH; LETAI; SAROSIEK, 2019). Sendo assim, Bax é um componente essencial para o desencadeamento desta via apoptótica. A baixa expressão desta proteína já foi relacionada com a maior capacidade de invasão do câncer (PRYCZYNICZ et al., 2014). Também, a ausência de Bax está fortemente relacionada à quimioresistência, visto que este fator é determinante para a morte celular via apoptose intrínseca (GUO et al., 2018b). Por sua vez, Bcl-xL exerce um papel anti-apoptótico, sendo necessária a sua neutralização para que este evento ocorra (DANIAL; KORSMEYER, 2004). O aumento da expressão de Bcl-xL foi relacionado a resistência à CDDP em NSCLC (ZHANG et al., 2016).

1.3.4. Mecanismos de resistência *off-target*

O fenótipo de resistência pode ser suportado por vias de sinalização não diretamente ligadas ao efeito da CDDP. A regulação do crescimento, proliferação e autofagia, alterações de *trade-offs* energéticos, *fitness* celular e manutenção do equilíbrio redox são fenótipos que sustentam a resistência à CDDP (CASTRACANI et al., 2020; HOSSEINI et al., 2019; REN et al., 2010). A proliferação celular reduzida é uma característica de células resistentes à CDDP, uma vez que o DNA destas células é menos disponível para a interação com a droga devido à baixa proliferação e, conseqüentemente, menor taxa de replicação. Também, a replicação lenta permite um maior controle de *checkpoints* do ciclo celular podendo ser determinantes em uma divisão celular errônea, evitando catástrofes mitóticas (SARIN et al., 2017). O equilíbrio redox da célula é outro mecanismo classificado neste grupo, e uma das estratégias selecionadas na célula é a alteração na atividade mitocondrial, visto que a mitocôndria é um dos principais produtores de ROS na célula (ZOROV; JUHASZOVA; SOLLOTT, 2014). Além disso, a presença de moléculas com potencial antioxidante, como GSH, atuam na manutenção do equilíbrio redox da célula sendo fundamental para a sobrevivência (LAN et al., 2018).

1.4. Metabolismo e necessidades bioenergéticas de células resistentes à CDDP

Células tumorais apresentam alta taxa de proliferação e, conseqüentemente, maior demanda de energia para os processos celulares. Nos anos 1920, Otto Warburg descreveu o padrão de metabolismo alterado em células tumorais (WARBURG, 1925). Ele reportou que, mesmo em presença de O₂, existe a produção de ácido láctico por estas células. Este fenômeno

ficou conhecido como efeito Warburg (KOPPENOL et al., 2011; RACKER, 1972). O efeito não está usualmente relacionado com uma disfunção mitocondrial, sendo este apresentado como uma consequência da reprogramação metabólica das células tumorais, onde existe o aumento de expressão de genes relacionados a via glicolítica, transportadores de glicose e fatores reguladores destas vias, como HIF1A (*Hypoxia Inducible Factor 1 Subunit Alpha*) (VAUPEL et al., 2019). Além disso, a mudança do metabolismo oxidativo para o redutor pode ser vantajosa para a manutenção do equilíbrio redox intracelular. A redução na atividade mitocondrial limita a produção de ROS, mantendo concentrações de ROS não tóxicas e letais para a célula. Assim, sustentando processos essenciais para a sobrevivência do tumor como estabilidade genômica, crescimento celular e angiogênese (ICARD et al., 2018). Também, acredita-se que o efeito Warburg é mais vantajoso pela maior facilidade em captar e obter nutriente para a biomassa celular requerida para a geração de uma nova célula (HEIDEN et al., 2009). Com a constatação de Warburg e o avanço de técnicas “-ômicas”, como a proteômica e a metabolômica, foi possível um melhor entendimento da reprogramação metabólica tumoral e a correlação deste fenômeno com o fenótipos de resistência quimioterápica (CHO, 2017; WANG et al., 2018).

Determinadas vias metabólicas, como a glicólise, são essenciais para a progressão e a malignidade de células tumorais (VAUPEL; SCHMIDBERGER; MAYER, 2019). Além de conferir estas características, a reprogramação metabólica e a alteração de necessidades bioenergéticas também estão relacionados com a resistência tumoral. Alterações do perfil metabólico podem definir a capacidade da célula em sobreviver e proliferar em diferentes ambientes, e esta característica são consideradas o *fitness* celular. O *fitness* celular é a aptidão da célula em prosperar em um determinado ambiente, resultado de diferentes parâmetros, incluindo a taxa proliferativa, vias de sinalização ativas, taxa metabólica e regulação transcricional (DI GREGORIO; BOWLING; RODRIGUEZ, 2016). Como exemplo, uma das vantagens ou estratégias selecionadas de células tumorais resistentes à CDDP é a capacidade proliferativa reduzida e, conseqüentemente, uma menor exposição do DNA à droga durante a divisão celular (AKTIPIIS et al., 2013; DUAN et al., 2017). A redução na capacidade proliferativa é normalmente acompanhada de uma maior especialização em mecanismos de sobrevivência.

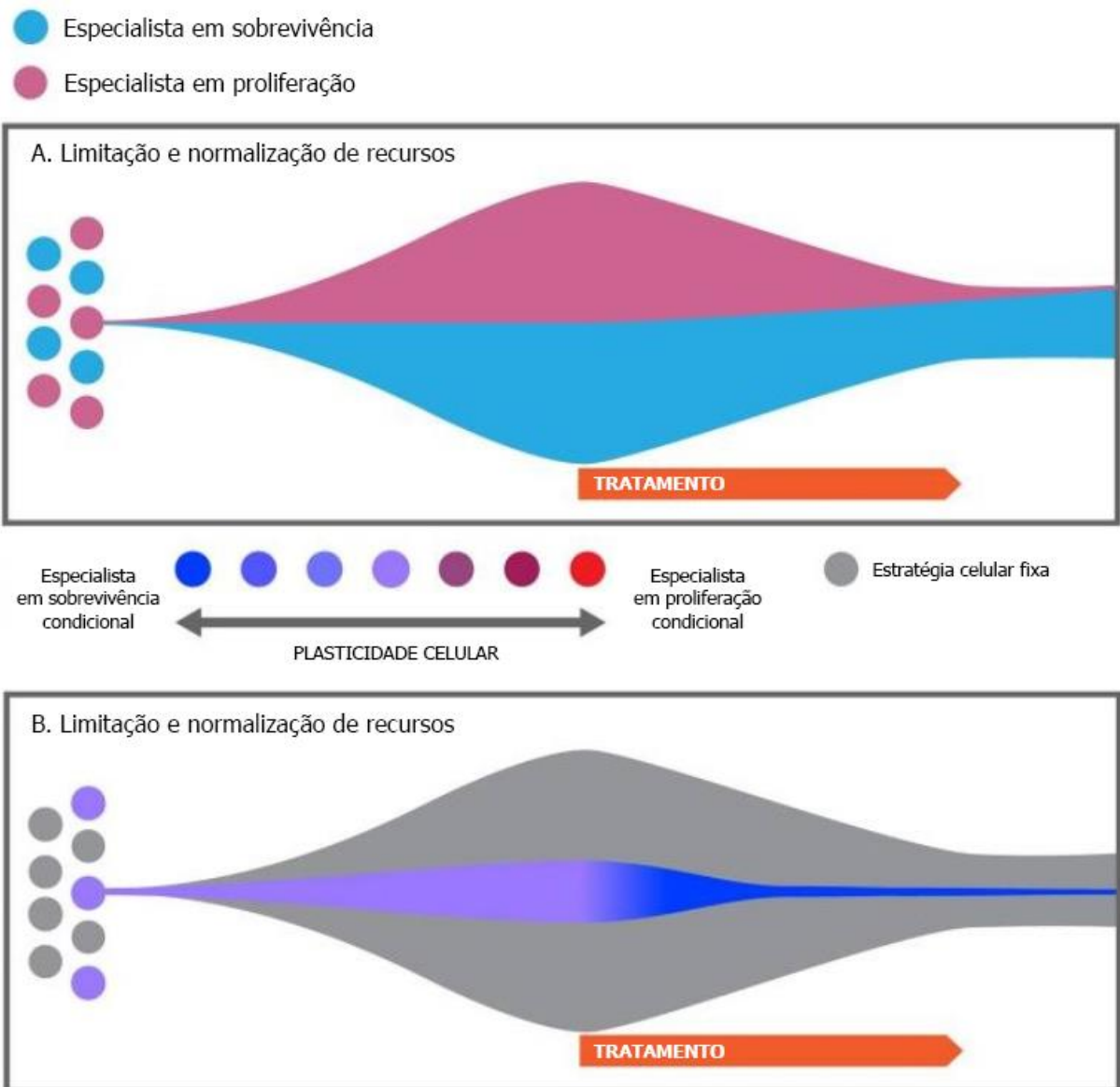


Figura 7: Efeito do tratamento quimioterápico nas estratégias de crescimento de células tumorais. Representação do efeito de tratamentos quimioterápicos longos nas estratégias de crescimento celular. A) células especializadas em máxima proliferação e máxima sobrevivência, antes, durante e após o tratamento. B) plasticidade em estratégias de crescimento e seleção de *trade-offs* relacionados a sobrevivência em células tumorais durante e após o tratamento quimioterápico.

Subpopulações clonais de um mesmo tumor podem apresentar diferenças no *fitness* celular. Entre as diferentes características relacionadas está a alocação de energia, tendo como consequência a seleção de diferentes estratégias celulares, visto que as fontes são finitas (RAFF, 1992). Estas diferentes estratégias celulares selecionadas em decorrência de características do microambiente tumoral são definidas como *trade-offs*. O *fitness* celular e *trade-offs* selecionados não são definitivos, podendo ser alterados em decorrência de mudanças ecológicas

no microambiente tumoral (BODDY; HUANG; AKTIPIIS, 2018). Com isso, a capacidade de adaptação no meio torna-se essencial para determinar a sobrevivência celular em ambientes adversos. Neste contexto, Aktipis et al. (2013) descreve as duas principais estratégias de crescimento encontradas em células tumorais, associando a diferentes *trade-offs* e relaciona estas com a capacidade de sobreviver a ambientes adversos, como a quimioterapia. As principais estratégias de crescimento selecionadas definem as células como especializadas em máxima proliferação ou especializadas em máxima sobrevivência. Células especializadas em proliferação apresentam maior taxa de crescimento, enquanto células especializadas em sobrevivência exibem um crescimento mais lento, contudo, conferindo vantagem para sobreviver a ambientes hostis. Com isso, ao longo do tratamento quimioterápico, as células tendem a adquirir *trade-offs* bioenergéticos para estratégias de sobrevivência e estas são selecionadas após o contato com a droga (Fig. 7).

A seleção de diferentes *trade-offs* inclui, também, a mudança no perfil metabólico e bioenergético da célula. Como discutido anteriormente, estas alterações podem ser determinantes no resultado da exposição da célula a determinado quimioterápico como mecanismos *post-* e *off-target*. A mudança do metabolismo celular como possível mecanismo de resistência à CDDP está descrito na literatura, mas ainda é pouco compreendido. A comparação entre linhagens isogênicas de câncer de ovário sensíveis e resistentes à CDDP indicou a maior atividade da via glicolítica e vias canônicas a glicólise (via das pentoses), em detrimento da fosforilação oxidativa (OXPHOS), como sendo um mecanismo essencial para a resistência tumoral, e um fator determinante para a resistência ao estresse oxidativo (AI et al., 2016; XU et al., 2018). Por outro lado, diversos estudos também demonstram a maior atividade do metabolismo oxidativo mitocondrial como uma característica de células resistentes à CDDP em comparação com suas respectivas linhagens sensíveis (MATASSA et al., 2016; VAZQUEZ et al., 2013; WANGPAICHITR et al., 2012). Também, o aumento da massa mitocondrial já foi relacionado com a resistência à CDDO em NSCLC (GAO et al., 2019). Outras vias de obtenção de energia são também exploradas para o melhor entendimento da resistência tumoral e a busca de intervenções terapêuticas, como a glutaminólise. Glicose e glutamina usualmente constituem as principais fontes de obtenção de energia pelas células tumorais (CANTOR; SABATINI, 2012). O metabolismo de glicose é a fonte usual de obtenção de energia celular e fornecimento de substrato para o ciclo do TCA. Contudo, a utilização de moléculas alternativas como fonte de energia vem sendo amplamente descrita, como o metabolismo de glutamina (CORBET; FERON, 2017). Glutamina é o aminoácido mais abundante circulante no plasma

(BERGSTROM et al., 1974) e sua composição possibilita a doação de carbono e nitrogênio para vias bioenergéticas e biossíntese de componentes celulares, incluindo ácidos nucleicos. No câncer, a utilização de glutamina pode estar envolvida em diferentes aspectos relacionados a malignidade, como manutenção da proliferação, imortalidade replicativa, resistência à morte celular, invasão e metástase (HENSLEY et al., 2013). Diferentes fatores são determinantes para a mudança no perfil metabólico e necessidades bioenergéticas das células tumorais, como alterações de disponibilidade de nutrientes e O₂ no microambiente (OCAÑA et al., 2019), e mutações no mtDNA e genes relacionados ao metabolismo (FERRER et al., 2018; WANG et al., 2016b). Com isso, a compreensão da essencialidade destas alterações na progressão e resistência tumoral permite a busca de intervenções no tratamento do câncer.

1.5. Modelos celulares para o estudo da resistência tumoral

Ensaio *in vitro* são essenciais e amplamente aplicados no estudo da biologia do câncer (BENAM et al., 2015; NIU; WANG, 2015). Entre as diferentes técnicas está o cultivo celular de células tumorais, o qual vem se mostrando uma ótima ferramenta para a prospecção de novos fármacos quimioterápicos e para o melhor entendimento de mecanismos de quimioresistência no intuito de contornar este fenômeno (BUTLER et al., 2017; DING et al., 2018; YONESAKA et al., 2019). Neste contexto, o estabelecimento de linhagens celulares de câncer como modelos de estudo representa uma ferramenta valiosa. Os modelos celulares fornecem maior facilidade em questões práticas e éticas, quando comparadas com modelos *in vivo* e *ex vivo*, além de representarem uma fonte ilimitada de material biológico com o propósito de pesquisa (NEVE et al., 2006). Entre os modelos celulares de câncer de pulmão, a linhagem de células humanas de adenocarcinoma de pulmão A549 tornou-se uma referência para estudos de NSCLC (SUN et al., 2017; YU et al., 2018). Além da utilização desta linhagem para o melhor entendimento da progressão do câncer de pulmão, células A549 são amplamente utilizadas para o entendimento de mecanismos de resistência à CDDP (HORIBE et al., 2018; YU et al., 2017). Apesar de limitações dos diferentes modelos celulares, estes estudos são de extrema importância pois fornecem o conhecimento de potenciais eventos celulares e moleculares presentes em situações clínicas.

O desenvolvimento de sublinhagens com resistência a quimioterápicos a partir de linhagens de células tumorais já estabelecidas vem se tornando uma ferramenta muito poderosa no entendimento de mecanismos envolvidos na quimiorresistência. As estratégias mais comuns

para o desenvolvimento de sublinhagens resistentes tem como base a geração de pares de células isogênicas, sendo a célula parental sensível e a sublinhagem derivada resistente à droga. Células da linhagem sensível são expostas a concentrações crescentes da droga por tempos determinados, permitindo a seleção de células com boa proliferação e tolerância à presença da droga (GARRAWAY; JÄNNE, 2012). Assim, estas linhagens contêm o mesmo *background* genético, diferenciando-se nos mecanismos de resistência adquiridos para o fármaco específico (XAVIER et al., 2016). Ainda, a exposição à CDDP acarreta na acumulação de mutações diferenciando o genótipo das linhagens após um maior período de tratamento (SKOWRON et al., 2019). Muitas destas estratégias utilizam a exposição a altas concentrações da droga por longos tempos de incubação, gerando linhagens com níveis de resistência até 30 vezes maiores que o encontrado na linhagem parental. Contudo, estes níveis de resistência não são usualmente encontrados em pacientes. Modelos celulares utilizando a exposição a concentrações menores do quimioterápico por curtos períodos de tempo geram níveis de resistência menores e são considerados modelos clinicamente relevantes por apresentarem níveis de resistência semelhantes aos encontrados em pacientes (MCDERMOTT et al., 2014).

1.6. Justificativa

O câncer de pulmão é um problema de saúde pública global. Este é o tipo de câncer mais incidente no mundo e o líder nas causas de morte relacionadas a esta doença. O diagnóstico deste tipo de câncer é realizado em estágios avançados da doença, o que limita as opções terapêuticas à quimioterapia. Contudo, a resistência tumoral à quimioterapia é frequente, reduzindo o sucesso do tratamento. A CDDP é a droga utilizada no tratamento de primeira linha contra o câncer de pulmão. Apesar da sua ampla utilização e do conhecimento de mecanismos envolvidos na resistência tumoral à CDDP, tratamentos alternativos para inibir a resistência ao fármaco ainda não foram desenvolvidos. O metabolismo de células tumorais com resistência adquirida à CDDP é alterado, sendo uma consequência da necessidade de adaptação ao ambiente citotóxico causado pela droga. Assim, estas alterações podem fornecer a estas células vantagem na capacidade de sobrevivência. Embora estejam disponíveis na literatura estudos comparativos do metabolismo de células sensíveis e resistentes à CDDP, a regulação do metabolismo bioenergético e o papel deste na resistência tumoral ainda não está claro. Nesse contexto, estudos sobre vias metabólicas ativas, a regulação destas e as necessidades bioenergéticas de linhagens celulares com níveis de resistência à CDDP clinicamente relevantes podem contribuir para o melhor entendimento de mecanismos de resistência tumoral relacionados ao metabolismo bioenergético. Além disso, a investigação do metabolismo de

células resistentes à CDDP permite a identificação de *trade-offs* e *fitness* celular adotados ou selecionados durante o tratamento determinantes para a quimioresistência. Assim, a caracterização de *trade-offs* bioenergéticos associados a resistência à CDDP pode gerar conhecimento para a proposição de um tratamento alternativo contornando este fator limitante no sucesso do tratamento do câncer de pulmão.

2. OBJETIVOS

2.1. Objetivo geral

Análise comparativa do perfil metabólico e necessidades bioenergéticas de células humanas de adenocarcinoma de pulmão sensíveis e resistentes à CDDP

2.2. Objetivos específicos

- i. Desenvolvimento de células A549 com níveis de resistência à CDDP clinicamente relevantes;
- ii. Análise de expressão de genes envolvidos com o metabolismo bioenergético em células A549 sensíveis e resistentes à CDDP;
- iii. Avaliação do efeito de glicose e L-glutamina na proliferação celular das linhagens estudadas;
- iv. Avaliação do perfil de respiração mitocondrial das células A549 sensíveis e resistentes à CDDP;
- v. Comparação da citotoxicidade de inibidores da via glicolítica nas células A549 sensíveis e resistentes à CDDP.
- vi. Comparação da expressão dos fator de iniciação eucariótico eIF2 α e do regulador de iniciação da tradução 4E-BP1, e suas isoformas fosforiladas entre as linhagens.

3. MANUSCRITO

Neste capítulo é apresentado o manuscrito intitulado “*Reduced metabolic activity of cisplatin-resistant A549 non-small cell lung cancer cells*”, resultado do trabalho desenvolvido durante o curso de mestrado. A formatação segue o exigido pela revista *Journal of Cellular Biochemistry* (<https://onlinelibrary.wiley.com/journal/10974644>), para a qual será submetido o trabalho. O desenho experimental foi realizado por NAC, CLM, CSD e KMM. Os experimentos de proteômica incluídos no manuscrito foram realizados previamente a este trabalho de mestrado por CLM, CSD, BVM, NAC e KMM. O desenvolvimento e avaliação das linhagens foram realizados por CLM, CSD e NAC. Os ensaios de respirometria de alta resolução foram planejados e realizados por NAC, CKD, BM e FK. Demais ensaios foram realizados por NAC. As análises de dados foram realizadas por NAC, CLM, CSD, BVM e KMM. A contribuição de materiais, reagentes e equipamentos foi realizada por FK, HBF, AZ e KMM. A redação científica foi realizada por NAC e KMM.

Reduced metabolic activity of cisplatin-resistant A549 non-small cell lung cancer cells

Running title: Metabolism of cisplatin-resistant cancer

Nathan A. Cadore¹, Carolina L. Martello¹, Cristine S. Dutra¹, Bruna V. Meneghetti¹, Camila K. Dias², Bruna Nitzke Minuzzi², Fábio Klamt², Arnaldo Zaha¹, Henrique B. Ferreira¹, Karina M. Monteiro¹

¹ Laboratório de Genômica Estrutural e Funcional, Centro de Biotecnologia, Universidade Federal do Rio Grande do Sul, Avenida Bento Gonçalves, 9500 Porto Alegre, Rio Grande do Sul, Brazil.

² Laboratório 28, Departamento de Bioquímica, Instituto de Ciências Básicas da Saúde, Universidade Federal do Rio Grande do Sul, Rua Ramiro Barcelos 2600, Porto Alegre, Rio Grande do Sul, Brazil.

* Corresponding author

Email address: karina@cbiot.ufrgs.br (Karina M. Monteiro)

Acknowledgments

This work was supported by the Fundação de Amparo à Pesquisa do Estado do Rio Grande do Sul (FAPERGS) [grant number 16/2551-0000 286-0]. NAC is a recipient of a Coordenação de Aperfeiçoamento de Pessoal de Nível Superior (CAPES) fellowship, CLM was recipiente of a Conselho Nacional de Desenvolvimento Científico e Tecnológico (CNPq) fellowship. CSD and BVM are recipients of CNPq fellowships. We thank the Uniprote-MS (Cbiot/UFRGS) for LC-MS/MS analysis.

ABSTRACT

Lung cancer is the most frequent tumor and the leading cause cancer-related deaths worldwide. The main treatment is chemotherapy utilizing platinum-based drugs such as cisplatin (CDDP). However, CDDP resistance is a relevant issue in cancer treatment. Among CDDP resistance mechanisms, cell fitness and bioenergetic trade-offs are strongly related to cell survival. In this work, A549 cells and its CDDP-resistant counterparts A549/CDDP were compared regarding bioenergetic metabolism and cell growth. A downregulation of bioenergetic pathways related to glucose metabolism was observed in A549/CDDP cells by proteomics and RT-qPCR. Also, TP53-induced glycolysis and apoptosis regulator TIGAR was upregulated in CDDP-resistant cells. These cells showed higher dependence of glucose and L-glutamine, and increased vulnerability to 2-DG. Decreased mitochondrial O₂ consumption was observed by high-resolution respirometry in A549/CDDP cells. Proteomics analysis and the reduction of different pathways suggested a global translation inhibition. In addition, western blot analyses showed increased 4E-BP1 presence and reduced rate of phosphorylated isoform. Thus, our evidences suggest a participation of 4E-BP1 in gene expression regulation of CDDP-resistant cells, resulting a global translation reduction. Further investigation of these molecular mechanism in CDDP resistance may lead to a better prognostic and alternative treatments.

Keywords: lung cancer, cisplatin, drug resistance, metabolic reprogramming, proteomics.

1. INTRODUCTION

Lung cancer is the most frequent tumor and the leading cause of cancer-related deaths worldwide (Ferlay et al., 2019). There are two main histological classification of lung cancer: non-small cell lung cancer (NSCLC) and small cell lung cancer. NSCLC is responsible for 85% of all lung cancer cases (Duma, Santana-Davila, & Molina, 2019). In the majority of cases, lung cancer is diagnosed in advanced stages of the disease requiring chemotherapy besides surgery to treatment (Siegel, Miller, & Jemal, 2019). The standard first-line treatment for these patients is chemotherapy with platinum-based drugs such as cisplatin (Hirsch et al., 2017). *Cis-diamminedichloroplatinum (II)* or cisplatin (CDDP) is a well-known chemotherapy compound and the most employed platinum-based drug in cancer therapy. It was the first approved by FDA (Food and Drug Administration) in 1978 for the treatment of testicular and ovarian cancer (Kelland, 2007), and since then has been widely applied in cancer treatment. The main cytotoxic effect of CDDP is the result of its covalent binding to DNA and adducts formation (Fichtinger-Schepman, Lohman, van der Veer, den Hartog, & Reedijk, 1985; Jamieson & Lippard, 1999), leading to inhibition of DNA synthesis, DNA transcription and RNA translation. Nevertheless, CDDP can also bind to proteins, RNA, membrane phospholipids, microfilaments, and thiol-containing molecules altering many biological processes including biosynthesis of cellular compounds and metabolism of bioenergetic sources (MARTINHO et al., 2018).

CDDP resistance is a relevant issue in cancer treatment. Tumor cells may present acquired or intrinsic CDDP resistance. In the former case, cancer cells may shift the expression levels of a broad range of genes leading to the activation of different signaling pathways during drug exposure, which ultimately results in tumor chemoresistance (Siddik, 2003). Subclones can be selected due to the advantage conferred by the activation or silencing of specific signaling pathways that improve survival rate during drug exposure such as Darwinian evolutionary system (Greaves & Maley, 2012). Therefore, tumor heterogeneity is a determining

factor to chemoresistance development during treatment (Bozic et al., 2013) since cell diversity and adaptive capacity are relevant issues for selection of survival strategies.

CDDP resistance is a complex and multifactorial molecular process. The known cellular mechanisms of CDDP resistance include reduced intracellular drug accumulation, increased drug inactivation by thiol-containing molecules, increased DNA damage repair and redox balance (Siddik, 2003). Furthermore, cell fitness and trade-offs can confer adaptive advantage to cell survival in different environments, which can be related to cancer development, progress and chemoresistance (Salgia & Kulkarni, 2018). Several studies have been reporting metabolic alteration and proteins associated to bioenergetic metabolism involved in CDDP resistance (Ai, Lu, Qiu, & Fan, 2016; Roh, Park, Kim, Jang, & Kwon, 2016; Wang et al., 2016). However, metabolic regulation and alterations of CDDP-resistant cells are still poorly understood (Cruz-Bermúdez et al., 2019; D'Alessandro et al., 2019). Studies using *in vitro* cellular models of CDDP resistance and -omics approaches followed by functional studies may be an eminent workflow to a better understanding of cell metabolism and bioenergetics associated with CDDP resistance.

In the present study, a CDDP-resistant NSCLC cell subline with clinical levels of CDDP resistance was developed and characterized. Comparative proteomic and functional annotation analyses of CDDP-sensitive NSCLC cells and its resistant counterpart were performed to identify molecular events potentially involved in CDDP resistance. RT-qPCR analysis confirmed an alteration in glycolysis and L-glutamine metabolism pathways in CDDP-resistant cells. Also, CDDP-resistant cells showed higher dependence of energy sources and vulnerability to metabolic inhibitors in cell survival. Mitochondrial respiration and proton leak were decreased in CDDP-resistant cells. A global translational regulation was proposed and eIF2 α , eIF4E-binding protein 1 (4E-BP1) and phosphorylated isoforms were evaluated. 4E-

BP1 showed a possible involvement in gene expression alteration of A549/CDDP cells. Our results suggest a decreased metabolic activity and global translation inhibition in CDDP-resistant cells, which may be related to CDDP resistance mechanisms.

2. MATERIALS AND METHODS

1. Cell culture and development of CDDP-resistant cells

Human NSCLC A549 cells (ATCC) were maintained in RPMI-1640 medium (Gibco) supplemented with 10% fetal bovine serum (FBS) in the presence of penicillin (100 U/mL) and streptomycin (100 µg/mL) at 37 °C in a humidified atmosphere of 5% CO₂. CDDP-resistant subline A549 (A549/CDDP cells) was developed from A549 cells using a stepwise drug treatment. For that, A549 cells (5×10^5) were continuously exposed to increasing concentration of cisplatin (0.1, 0.2, 0.3, 0.4 and 0.5 µM) for 72 h each. Cisplatin-resistant cells were maintained in culture medium containing 0.5 µM of CDDP until 3 days before the experiments to ensure maintenance of the resistance phenotype. A549/CDDP cells were independently generated three times, which were considered biological replicates in all experiments performed. For A549 cells, the experiments were performed three times considering each a biological replicate. All experiments were performed using technical replicates.

2. Cytotoxicity assay

Cisplatin and glycolysis inhibitors 2-deoxy-D-glucose (2-DG) and 3-bromopyruvate (3-BrP) cytotoxicity were determined by sulforhodamine B (SRB) assay, as described by Vichai & Kirtikara (2006), using from 0.25 to 64 µM of cisplatin (CDDP), from 0.33 to 17.7 mM of 2-DG, and from 4 to 96 µM of 3-BrP. The GI₅₀ (50% of maximal inhibition of growth) value was calculated using a dose (log) vs. normalized response curve with non-linear regression in GraphPad Prism 6.0 software. The assay was performed in triplicate.

3. Population doubling time

Cells were seeded in 24-well plate at 5×10^3 cells/well. The cells were collected by trypsinization at 24, 48, 72, 96, 120 and 144 h after plating and counted using Guava easyCyte flow cytometer (Merck Millipore). Population doubling times were calculated considering all time points using the Cell calculator++ mode of Doubling Time Online Calculator Calculator (<http://www.doubling-time.com/compute.php>).

4. Clonogenic assay

Cells were plated at 500 cells/well in 6-well plate and cultured overnight to adhesion. To evaluate CDDP impact in clonogenic capacity cells were treated with 0, 0.2, 0.3, 0.4, 0.5 or 1.0 μM of CDDP for 72 h and cultured in drug-free medium for further 10 days. To evaluate the effect of reduced glutathione (GSH) on clonogenic capacity, cells were incubated with 4 mM of GSH for 14 days. To evaluate pro-oxidant agents effect, cells were treated with 50 μM of (BSO) or 100 μM of diethyl maleate (DEM) for 24 h and cultured in drug-free medium for further 14 days. Colonies were washed once with PBS 1x, fixed and stained with 6% glutaraldehyde and 0.5% crystal violet solution for at least 30 min, as described by Franken et al. (2006). The wells were washed with water by immersion and dried at room temperature. Colonies were counted using ImageJ (Schneider, Rasband, & Eliceiri, 2012). All images were subjected to visual inspection and manual correction. Plating efficiency (PE) was calculated as the number of colonies formed divided by the number of cells seeded. Surviving fraction (SF) was calculated as the number of colonies formed after treatment divided by the number of cells seeded and multiplied by PE.

5. Protein extraction and sample preparation for mass spectrometry analysis

Cell lysis and protein digestion was performed as described by Pirmoradian et al. (2013), with some modifications. A549 and A549/CDDP cells from confluent culture flasks (~ 2×10^6 cells) were trypsinized and washed with PBS. Aqueous ammonium bicarbonate (50 mM, pH 8.0) was mixed with acetonitrile at a ratio of 9:1 (v:v) to prepare lysis solution containing 0.1% (w/v) Rapigest Surfactant (Waters). Cell pellets were resuspended with lysis solution and samples were incubated with vigorous vortexing for 10 min. The cell lysate was incubated at 95 °C for 5 min and then subjected to 1 h in an ultrasonic bath to improve protein solubility. Samples were centrifuged at 14,000 rpm over 7 min at room temperature and the supernatants were subjected to protein quantitation and digestion. Proteins were quantified using Micro BCA Protein Assay Kit (Thermo Fisher Scientific). Proteins were reduced and alkylated by incubation with 10 mM DTT for 30 min at 60 °C, following addition of 10 mM iodoacetamide for 30 min. Trypsin was added at a ratio of 1:40 (w/w) and samples were incubated at 37 °C for 18 h. Digested protein samples were acidified with 0.5% (v/v) TFA to hydrolyze Rapigest. Samples were incubated at 37 °C for 30 min and centrifuged at 13,000 rpm for 10 minutes. Peptide-containing supernatants were further clean-up with Oasis HLB Extraction Cartridge (Waters).

6. Mass spectrometry analysis

Peptides were analyzed by liquid chromatography-tandem mass spectrometry (LC-MS/MS) using a nanoACQUITY UPLC system coupled to a Xevo G2-XS Q-ToF mass spectrometer (Waters) with a low-flow probe at the source. The peptides were separated by analytical chromatography (Acquity UPLC BEH C18, 1.7 μ m, 2.1 \times 50 mm, Waters), at a flow rate of 8 μ l/min, using a 7-85% water/ACN 0.1% formic acid linear gradient over 90 min. The MS survey scan was set to 0.5 s and recorded from 50 to 2000 m/z. MS/MS scans were acquired from 50 to 2000 m/z, and scan time was set to 1 s. Data were collected in data-independent MS^E

mode of acquisition. Experiment performed in triplicate for each cell line considering each biological replicate as a replica.

7. Data processing and protein identification

LC-MS^E data were processed and searched using ProteinLynx Global Server version 3.0.3 (PLGS 3.0.3, Waters Corporation). The searches were conducted against *Homo sapiens* canonical protein sequences retrieved from the UniProtKB/Swiss-Prot database, with trypsin as enzyme, maximum of one missed cleavage, fixed carbamidomethyl modification for cysteine residues, and oxidation of methionine as variable modification. Peptides and protein tolerance were set as automatic, minimum fragment ion per peptide as 2, minimum fragment ion per protein as 5, minimum peptide matches per proteins as 1 and the false discovery rate (FDR) as 4%. Stringent criteria were used for protein identification and validation, considering only proteins identified in at least two out of three biological replicates were considered for qualitative and quantitative analysis in order to improve confidence. Label-free quantitation analysis was performed from peak intensity measurements (Hi3 method) (Silva et al., 2005) using PGLS Expression^E algorithm. Data sets were normalized using the 60S acidic ribosomal protein P1 (RPLP1, P05386) as reference (housekeeping protein), as this protein was detected in all samples and biological replicates with the lower variance coefficient (<10%). Proteins were taken as differentially expressed between samples if regulation probability (P) was below 0.05 or higher than 0.95.

8. Functional annotation and enrichment analysis

The list of proteins differentially expressed between A549 and A549/CDDP cells was uploaded in DAVID 6.8 (<http://david.abcc.ncifcrf.gov/>) (Huang, Sherman, & Lempicki, 2009) for functional annotation, considering the following databases: COG_ONTOLOGY,

UP_KEYWORDS, UP_SEQ_FEATURE, GOTERM_BP_DIRECT, GOTERM_CC_DIRECT, GOTERM_MF_DIRECT, BBID, BIOCARTA, KEGG_PATHWAY, INTERPRO, PIR_SUPERFAMILY, and SMART. *Homo sapiens* was set as background for the enrichment analysis and functional annotation clustering was performed with classification stringency set to medium, similarity threshold of 0.5, multiple linkage threshold of 0.5, and an EASE enrichment threshold of 1.0. The P-value and the Benjamini-Hochberg FDR were used to determine significance of enrichment or overrepresentation of terms for each annotation.

9. RNA extraction and RT-qPCR

A549 and A549/CDDP cells were cultured in T25 culture flask until approximately 90% confluent (2×10^6 cells), then total RNA was extracted using the Trizol reagent (Thermo Fisher Scientific) following manufacturer's protocol. Extracted RNA was treated with DNase I (Thermo Fisher Scientific) for 15 min at room temperature to remove DNA contamination. The concentration of total RNA was determined using Qubit Quantitation Fluorometer and Qubit RNA HS Assay Kit reagents (Thermo Fisher Scientific). cDNA was synthesized from 5 μ g of total RNA using M-MLV reverse transcriptase (Thermo Fisher Scientific) and random hexamer primes (Thermo Fisher Scientific) as recommended by the supplier. RNaseOUT Recombinant Ribonuclease Inhibitor (Thermo Fisher Scientific) was used as recommended by the supplier. The reverse transcription reaction mixture was incubated at 37 °C for 50 min followed by 70 °C for 15 min to inactivate the reaction. The final cDNA product was diluted 100-fold with nuclease-free water prior to use in qPCR analysis.

Fifteen genes related to glucose and L-glutamine (GLN) metabolism were analyzed by RT-qPCR. Ribosomal 18S RNA and beta actin (ACTB) were used as reference genes. Gene-specific primers were designed using PrimerBlast (Ye et al., 2012) (Table 1). Each qPCR

reaction consisted of 10 μ l of SYBR Select Master Mix (Applied Biosystems), 0.5 μ l of each forward and reverse 10 μ M primer solution, and 9 μ l of diluted cDNA. The analyses were performed in Applied Biosystems 7500 Fast Real-Time PCR System (Applied Biosystems). Statistical analysis was performed by *t*-test comparing the abundance of transcripts for each gene in A549 and A549/CDDP.

10. Cell proliferation assay

Cells were plated in 24-well plates at densities of 2,000 cells/well. After 24 h of culture in complete culture medium, cells were maintained in GLN- or glucose-free medium supplemented with 10% ultrafiltered FBS (Amicon ultra 3 K, Merk) for 7 days. Medium was not changed throughout the course of the experiment and each day was considered a time point. Complete RPMI medium supplemented with 10% ultrafiltered FBS was considered as positive control. At each time point, cells were fixed in 10% formalin for 1 h and stained with 0.1% crystal violet for 30 min. Plate was washed by dH₂O immersion. Dye was extracted with 200 μ l of 10% acetic acid and the relative proliferation was determined by absorbance at 595 nm in 96-well plate (Son et al., 2013). Relative growth was determined by the absorbance value of the indicated condition divided by the positive control. Statistical analysis was performed by multiple *t*-test comparing A549 and A549/CDDP in each time point.

11. High-performance respirometry

The Oxygraph-2k (O2k, OROBOROS Instruments, Innsbruck) was used for measurements of respiration (Makrecka-Kuka, Krumschnabel, & Gnaiger, 2015). 1×10^6 cells were placed into a pre-calibrated chamber in 2 ml of RPMI-1640 media without FBS at 37° C in continuous shaking. First, ROUTINE respiration was determined during oxygen consumption stabilization in normal condition. After stabilization of ROUTINE respiration, the

ATP-synthase inhibitor oligomycin (2 $\mu\text{g}/\text{mL}$) was added to obtain a measure of LEAK respiration. Difference between ROUTINE and LEAK respiration was defined as ATP-linked respiration since oligomycin inhibits this respiration. The experiment was followed by titration of mitochondrial uncoupler FCCP to maximum oxygen flux at optimum uncoupler concentration defined as maximum respiratory capacity. Reserve respiratory capacity was defined by the subtraction of maximum respiratory capacity from the ROUTINE respiration (Desler et al., 2012). Finally, rotenone (0.5 μM) and antimycin A (2.5 μM) were added to obtain residual oxygen consumption (ROX). ROX was discounted to determinate all respiration parameters. Statistical analysis was performed by *t*-test comparing A549 and A549/CDDP in each parameter. The experiment was accomplished by five independent analyzes, the O_2 consumption of A549 and A549 cells was measured simultaneously in each analysis, and cell lines were alternated between chambers.

12. Western blot analysis

A549 and A549/CDDP cells were cultured in T25 culture flask until approximately 90% confluent (2×10^6 cells). Cells were trypsinized and the pellet was resuspended in 300 μL of lysis buffer (40 mM Tris-HCl; 0.1% SDS) containing 2 x Halt Protease and Phosphatase Inhibitor (Thermo Fischer Scientific). Cells were lysed by sonication and soluble proteins were separated by centrifugation. Quantification was performed using a Qubit™ 2.0 quantitation fluorometer (Invitrogen). Samples containing 60 μg of total protein were resolved by sodium dodecyl sulphate-12% polyacrylamide gel electrophoresis (SDS-PAGE) and transferred onto a PVDF membrane for 2 h at 70 V. The membranes were blocked in TBS containing 0.1% Tween 20 and 5% milk powder (blocking solution (BS)) for 1 h. The membrane was incubated with each primary antibody in BS overnight at 4 °C. Dilution of 1:1000 were utilized for eIF2 α Rabbit pAb, Phospho-eIF2 α -S51 Rabbit pAb, [KO Validated] EIF4EBP1, and Phospho-

EIF4EBP1-T37/46 Rabbit pAb (ABclonal). Dilution of 1:8000 was utilized for Actin Monoclonal Antibody (Thermo Fischer Scientific). After incubation, membrane was washed 3 times for 10 min with TBS and secondary antibody was incubated in BS for 1 h. The dilution utilized was 1:10000 to alkaline phosphatase-conjugated anti-rabbit IgG (Thermo Fischer Scientific) or anti-mouse IgG (Invitrogen). The result was revealed using BCIP/NBT Color Development Substrate (Promega).

3. RESULTS

3.1. Generation and characterization of CDDP-resistant A549 cells

A stepwise protocol of CDDP exposure of A549 cells was elaborated aiming to develop acquired CDDP-resistant cells (A549/CDDP cells). After drug exposure, cytotoxicity assay was performed and A549/CDDP ($GI_{50} = 8.793 \mu\text{M}$) cells showed a 3.3-fold increase of GI_{50} value in comparison to A549 ($GI_{50} = 2.656 \mu\text{M}$) cells (Fig. 1A). A significant decrease in A549/CDDP cell proliferation was observed in 96, 120 and 144 h in comparison to A549 cells (Fig. 1B). Also, the doubling time of A549/CDDP subline was significantly higher than that of A549 cells (27.43 and 36.61 h, respectively). Moreover, clonogenicity of A549/CDDP cells in the absence of CDDP was significantly reduced compared to A549 cells (Fig. 1C). However, in the presence of CDDP, A549/CDDP showed higher surviving fraction (SF) in all drug concentrations tested in comparison to A549 cells (Fig. 1D). Clonogenic cell survival data further confirmed the cisplatin-resistant phenotype of A549/CDDP cells.

3.2. Different proteomic profile of CDDP-sensitive and -resistant cells

A comparative proteomic profiling of A549 and A549/CDDP cells was performed aiming to identify alterations in protein expression that may be involved in CDDP resistance. Stringent criteria for protein identification and validation were chosen to increase the chance of identifying proteins and molecular mechanisms consistently involved in drug resistance. LC-MS/MS analysis allowed the identification of a total of 274 proteins, being 203 and 224 proteins identified in A549 and A549/CDDP cells, respectively. Among these proteins, 50 and 71 were exclusively found in A549 and A549/CDDP cells, respectively (Supplementary Figure 1). The 153 proteins shared between cell lines were submitted to quantitative analyses in order to identify expression differences between samples. Quantitative expression analyses performed in PGLS were based on MS precursor intensity values (Hi3 method) and resulted in the

probability of protein regulation (P). Proteins exclusively found in each sample were considered to be upregulated in that sample. Totals of 74 and 196 proteins were identified as up- or downregulated in A549/CDDP cells, respectively (Supplementary Table 1).

Functional annotation and enrichment analysis were performed for proteins found up- and downregulated in A549/CDDP cells. Among upregulated proteins, enriched annotation terms include ‘cell-cell adhesion’, ‘mRNA splicing, via spliceosome’, ‘rRNA processing’, ‘MAPK cascade’, ‘Wnt signaling pathway, planar cell polarity pathway’, ‘regulation of mRNA stability’, ‘gluconeogenesis’, ‘translational’ and ‘protein polyubiquitination’(Supplementary table 2A). Annotation terms enriched among proteins downregulated in A549/CDDP cells include ‘oxidation-reduction process’, ‘cell redox homeostasis’, ‘response to reactive oxygen species’, ‘translational’, ‘tricarboxylic acid cycle’, ‘mitochondrial ATP synthesis coupled proton transport’, ‘ATP biosynthetic process’, ‘mitochondrial matrix’, ‘fatty acid beta-oxidation’, ‘cellular protein metabolic process’, ‘glycolytic process’ and ‘regulation of cellular amino acid metabolic process’ (Supplementary Table 2B). Some GO biological processes and KEGG pathway terms were found in both A549/CDDP up- and downregulated proteins. Thus, enrichment functional analysis parameters of number of genes, fold enrichment, and false discovery rate (FDR) were considered to the comparison of up- and downregulated proteins. Consequently, GO biological processes involving bioenergetic metabolism and RNA translation stood out among A549/CDDP downregulated proteins considering these parameters (Fig. 2A). Also, KEGG pathways showed a relevant downregulation in bioenergetic processes as glycolysis and TCA cycle in A549/CDDP cells (Fig. 2B). These results were intriguing and were explored for further investigation of CDDP-resistant cells metabolism.

3.3. Alteration in the expression of genes related to bioenergetic metabolism

The expression of genes encoding key enzymes and regulators of glucose and GLN metabolism was evaluated by RT-qPCR in order to confirm the results obtained in our proteomic analysis and to better understanding the metabolic reprogramming associated with CDDP resistance (Fig. 3). The expression of glycolytic enzymes hexokinase-2 (HK2) and L-lactate dehydrogenase A chain (LDHA) was found downregulated in A549/CDDP cells, as well as the expression of pentose-phosphate pathway (PPP) enzyme glucose-6-phosphate 1-dehydrogenase (G6PD). These results indicated a downregulation on glucose metabolism, confirming our data from proteomic analysis. Furthermore, negative regulator of glycolysis TIGAR (TP53-inducible glycolysis and apoptosis regulator) was found upregulated in A549/CDDP cells. Enzymes of GLN metabolism aspartate aminotransferase (GOT1) and glutamate dehydrogenase 1 (GLUD1) were found downregulated in A549/CDDP cells. Glucose transporter member 1 (GLUT1), GTPase KRas (KRAS), aspartate aminotransferase (GOT2) enzymes, and bioenergetic regulatory protein SCO2 homolog (SCO2) showed a decreased expression but not statistically significant in A549/CDDP cells. Overall, RNA expression analysis showed a general downregulation of genes related to bioenergetic metabolism in A549/CDDP cells, as observed in proteomic analysis.

3.4. Dependence of GLN and glucose on A549/CDDP cell proliferation

A549/CDDP cells showed higher dependence of GLN and glucose for cellular proliferation in comparison to A549 cells in all time-points of the experiment (Fig. 4A and B). Moreover, A549/CDDP cells were more affected by the glycolysis inhibitor 2-DG. A549/CDDP cells showed reduced GI_{50} (~2.7 mM) for 2-DG compared to A549 cells (~5.7 mM), indicating low tolerance to this glucose analogue (Fig. 4C). No statistically significant differences between A549 and A549/CDDP cells were observed for 3-BrP inhibitor (Fig. 4D).

These results suggest A549/CDDP is more dependent of traditional energy sources and does not show a metabolic plasticity when exposed to limited resources environment.

3.5. Evaluation of redox homeostasis alteration in the clonogenic capacity of A549 and A549/CDDP cells

A549 and A549/CDDP clonogenic capacity were evaluated using SF value after exposure to anti- and pro-oxidant agents. Both cell lines were not affected by GSH presence (Fig. 5A), which suggests that reactive oxygen species (ROS) are not a determinant factor in the reduced clonogenic capacity observed for A549/CDDP cells (Fig. 1B). Also, pro-oxidant drugs BSO and DEM showed the same effect in CDDP-sensitive and -resistant cells, suggesting a similar capacity of detoxification mediated by GSH (Fig. 5B and C).

3.6. Reduced O₂ consumption and ATP-linked respiration in A549/CDDP cells

High-resolution respirometry was performed to investigate O₂ consumption and mitochondrial activity in A549 and A549/CDDP cells. ROUTINE and ATP-linked respiration were found reduced in A549/CDDP cells in comparison to A549 cells (Fig. 6). These results indicate a decreased mitochondrial activity in CDDP-resistant cells. Furthermore, LEAK was found reduced in A549/CDDP cells, which could indicate that a decreased mitochondrial activity is not a consequence of mitochondrial dysfunction. Maximum respiratory capacity was not altered in A549/CDDP cells. Also, reserve respiratory capacity and residual oxygen consumption (ROX) did not show differences between cell lines. These results indicate the mitochondrial capacity remains unaltered in A549/CDDP cells, although, there is a downregulation in mitochondrial activity.

3.7. Evaluation of translation regulation in A549/CDDP cells

Based on the downregulation of various proteins and cellular processes observed in A549/CDDP cells, we investigated determinant factors involved in the regulation of global translation (Fig. 7A). Similar amounts of the initiation factor eIF2 α were found in A549 and A549/CDDP cells (Fig. 7B). Furthermore, the phosphorylation of eIF2 α (Ser51) was similarly found in A549 and A549/CDDP cells (Fig. 7C), indicating no differences in its regulation between A549 and A549/CDDP. The hypophosphorylated isoform of 4E-BP1 showed 2-fold higher expression in A549/CDDP compared to A549 cells (Fig. 7B). However, the difference was not statistically significant. The ratio of phosphorylated isoform phospho-4E-BP1 (Thr37/46) to hypophosphorylated 4E-BP1 was found significantly reduced in A549/CDDP cells (Fig. 7D). These results suggest a higher presence of non-phosphorylated isoform 4E-BP1 in A549/CDDP, which may be regulating a global translation reduction.

4. DISCUSSION

Chemotherapy utilizing CDDP is the first-line treatment of advanced-stage lung cancer. However, during drug exposure, tumor cells can acquire CDDP resistance by altering gene expression, which can confer a survival advantage in the cytotoxic environment. Development of CDDP-resistant cells from a parental cell line has been a powerful tool for the study of molecular mechanisms associated to drug resistance in different cancer types, such as cervical, gastric, ovarian, breast, and lung cancer (Bednarska-Szczepaniak, Krzyżanowski, Klink, & Nowak, 2019; Duan et al., 2018; Qin et al., 2017; B. Wang et al., 2019). In this work, A549 cells with acquired resistance to CDDP (A549/CDDP cells) were developed from A549 parental cells using a stepwise drug treatment, using low drug concentration and short exposure time. Protocols using long periods of treatments and high drug concentrations could lead to resistance rates 10-fold higher when compared to the parental cell line, which may not simulate drug-resistant tumors in patients. Sublines showing 2 to 5-fold resistance higher than their counterparts are considered clinically relevant (McDermott et al., 2014). Thus, the protocol developed in this study generated clinically relevant CDDP-resistant cells compared to those using higher CDDP concentration exposure. Furthermore, A549/CDDP cells showed reduced doubling time and clonogenic capacity compared to A549 parental cells, which are phenotypes frequently associated with CDDP resistance (Annovazzi, Mellai, & Schiffer, 2017; Izumi et al., 2011). Moreover, A549/CDDP cells showed an advantage in clonogenic capacity when exposed to CDDP compared to A549 cells. These results support the CDDP resistant phenotype of the developed subline A549/CDDP.

Proteomics is a powerful tool to monitor protein abundance in distinct samples, offering ultimate information for molecular interactions, signaling pathways, and gene expression alterations in human disease research (Cifani & Kentsis, 2017). Our proteomic analysis showed a marked downregulation of proteins related to cell bioenergetic metabolism in A549/CDDP

cells. Alterations in mitochondrial activity and glycolysis have already been reported as involved in CDDP resistance (Ai, Lu, Qiu, & Fan, 2016; Roh, Park, Kim, Jang, & Kwon, 2016; Wang et al., 2016). Proteins considered key enzymes in the glycolytic pathway were found downregulated in A549/CDDP cells, including GPI, TPI1, GAPDH, PGAM1, PGM1, PGK1, ENO1, PKM, LDHA, and LDHB, which suggests that glucose metabolism is decreased in these cells. G6PD, a key enzyme in the pentose phosphate pathway (PPP), was found downregulated in A549/CDDP cells as well. Furthermore, downregulation of enzymes involved in glycolysis and PPP was confirmed by RNA expression analysis. Relative gene expression performed by RT-qPCR showed a significant decrease of HK2, LDHA, and G6PD RNA levels in A549/CDDP cells. Moreover, TIGAR, a well-known glycolytic repressor, was found upregulated in A549/CDDP cells by RNA expression analysis. TIGAR reduces fructose-2,6-bisphosphate levels in cells, which may lead to downregulation of glycolytic enzymes and a shift from glycolysis to gluconeogenesis through PFK-2/FBPase-2 complex phosphorylation (Bensaad et al., 2006; Okar et al., 2001). Also, TIGAR is associated to increased resistance to cell death. The upregulation of its regulator is related to increment of NADPH intracellular levels and ROS reduction, which may lead to an advantage during drug exposure (Maurer, Heller, Wanka, Rieger, & Steinbach, 2019; Xie et al., 2014). Thus, TIGAR may be involved in glycolysis inhibition and CDDP-resistant cells survival.

Annotation terms related to 'biosynthesis of amino acids' and 'regulation of cellular amino acid metabolic process' were found among proteins down- and upregulated in A549/CDDP cells. Our proteomics and RT-qPCR analyses showed discordant results related to the regulation of GLN metabolism. RT-qPCR analysis found GOT1 and GLUD1 downregulated in A549/CDDP cells. However, GOT1 and GOT2 were found upregulated in A549/CDDP cells by proteomic analysis. The inverse correlation of RNA and protein amount occurs due to the complexity of mechanism of gene expression regulation. Molecular events

such as protein ubiquitination and deubiquitination, regulation of proteasome subunits abundance, macromolecular crowding, and protein localization can determine intracellular protein stability (Cai, Culley, Zhao, & Zhao, 2018; Guzman, Gelman, Tai, & Gruebele, 2014; Lin et al., 2010; Rousseau & Bertolotti, 2018).

Higher glucose and GLN dependence, and the negative impact of 2-DG on cell survival of A549/CDDP compared to A549 suggest a lack of plasticity due to reduced metabolic activity in CDDP-resistant cells. Proliferative cells must be able to adapt their metabolism to use different resources to continuous proliferation (Lehúede, Dupuy, Rabinovitch, Jones, & Siegel, 2016). A549/CDDP cells did not show the capability of using alternative sources. This phenotype can be assumed as a consequence of A549/CDDP trade-offs. Also, higher cytotoxicity of 2-DG in CDDP-resistant cells have been reported and it was associated with lower HK expression, since 2-DG is a competitive inhibitor of glucose for the catalytic sites in HK (Sullivan, Kurtoglu, Brenneman, Liu, & Lampidis, 2014).

Cancer cells can adapt their metabolism to deal with different environmental conditions such as chemotherapy. Some of the major strategies displayed by the cells to deal with CDDP toxic environment include reduction of oxidative stress and alteration of apoptotic pathways (Siddik, 2003), which are mechanisms strongly related to mitochondrial function. Proteomic analysis and high-resolution respirometry indicated a reduced mitochondrial activity in A549/CDDP cells. Proteomic results revealed a downregulation of proteins related to mitochondria activity in A549/CDDP cells, including mitochondrial ATP synthase subunits ATP5A1, ATP5B, and ATP5H as well as mitochondrial cytochrome C oxidase subunit COX5A and cytochrome c1 CYC1. Furthermore, enzymes related to TCA cycle as ACO2, ACO1, CS, IDH1, MDH2 were also found downregulated in A549/CDDP cellular proteome. Biological processes ‘ATP biosynthetic process’, ‘mitochondrial ATP synthesis coupled proton transport’,

‘tricarboxylic acid cycle’, and KEGG pathways ‘oxidative phosphorylation’, ‘citrate cycle’ were found enriched in A549/CDDP downregulated proteins. These results strongly suggest a downregulation in mitochondrial activity of CDDP-resistant cells. Moreover, A549/CDDP cells showed decreased ROUTINE and ATP-linked respiration in high-resolution respirometry analysis, demonstrating a reduced mitochondrial activity in comparison to A549 cells. LEAK was also found reduced in CDDP-resistant cells. LEAK is strongly associated to mitochondrial integrity and a higher rate may be associated to mitochondrial dysfunction (Baffy, 2017). Thus, our results suggest that ROUTINE and ATP-linked respiration is not a consequence of mitochondrial dysfunction. Furthermore, we did not observe an increase in maximum and reserve respiratory capacity of A549/CDDP cells, which indicate a similar energetic demand on mitochondria. Considering mitochondria as the major producers of ROS (Zorov, Juhaszova, & Sollott, 2014), a reduction of mitochondrial activity may also reduce mitochondrial ROS (mtROS), which could be a mechanism of CDDP resistance in lung cancer cells.

The selection of different bioenergetic trade-offs in cancer cells may determinate different growth strategies. Cells can be classified as proliferation specialist or survival specialist according to the growth strategy adopted (Aktipis et al., 2013). During increasing drug exposure, survival specialist A549 cells may be selected, and the reduced glycolysis and mitochondrial metabolism may be related to A549/CDDP trade-offs (Gao et al., 2019). Reduced metabolism could be related to the reduced growth rate observed for A549/CDDP cells. Although the reduced clonogenic capacity of CDDP-resistant cells has been reported as a consequence of higher ROS concentration (Duan et al., 2017), we did not observe an increment in clonogenic capacity of A549/CDDP cells treated with GSH. Also, ROX did not show a difference between cell lines, and its parameter is strongly related with ROS presence (Wagner, Venkataraman, & Buettner, 2011). The results did not correlate ROS presence with the reduced growth of A549/CDDP. Thus, the hypothesis of stress-inducing the reduced cell growth may

be discarded, reinforcing the idea of a selected phenotype as a growth strategy (Boddy; Huang & Aktipis, 2018). For sustaining cell growth, signaling pathways that stimulate cell proliferation must also participate in the reorganization of metabolic activity that allows quiescent cells to begin to proliferate (DeBerardinis, Lum, Hatzivassiliou, & Thompson, 2008). PI3K/Akt/mTOR pathway is an example of signal transduction pathway responsible for inducing cell growth and metabolic activity to support cellular biosynthesis (Ersahin, Tuncbag, & Cetin-Atalay, 2015). ERK-MAPK signaling pathway is also associated with cell proliferation induction, and its activation results in an upregulation of positive regulator of glycolysis (Papa, Choy, & Bubici, 2019). Considering this scenario, it is possible that reduced bioenergetic metabolism and cell growth may be regulated by mechanisms in common. Also, a reduced metabolic rate could be advantageous to A549/CDDP cells. A decreased metabolic rate is a characteristic of quiescent cells and the quiescence have been associated as an innate drug resistance mechanism in solid cancers (Brown et al., 2017).

The number of proteins and biological processes found downregulated in A549/CDDP cells suggested a possible global translation inhibition. Translation can be regulated globally or at a transcript-specific level. Ribosomal profile and alteration of translational initiation factors expression and phosphorylation may be determinant to regulate translational in a global perspective (Hershey, Sonenberg, & Mathews, 2012; Marcon et al., 2017). Thus, to access a possible alteration in RNA translation between A549 and A549/CDDP cells, eukaryotic initiation factor eIF2 α and eIF4E-binding protein 1 (4E-BP1) as well as their phosphorylated isoforms were compared between cell lines. The initiation factor eIF2 α transfers methionyl-initiator tRNA (Met) to the small ribosomal subunit and its phosphorylation (Ser51) prevents the eIF2 complex recycling, thus limiting translation initiation (Krishnamoorthy, Pavitt, Zhang, Dever, & Hinnebusch, 2001). 4E-BP1 is one of the main regulators responsible for global translation inhibition. The protein directly interacts with eIF4E, which is a limiting component

of the complex that recruits 40S ribosomal subunits (Qin, Jiang, & Zhang, 2016). However, 4E-BP1 phosphorylation may alter the affinity to eIF4E avoiding the interaction of these proteins. Then, increasing eIF4E availability for its interacting partner EIF4G, which is involved in mRNA recruitment to the ribosomes for protein translation (Sonenberg & Hinnebusch, 2009). eIF2 α and phospho-eIF2 α (Ser51) did not show differences between A549 and A549/CDDP cells, suggesting a similarity in regulation activity of its initiation factor in global translation. However, 4E-BP1 was found 2-fold higher in A549/CDDP compared to A549 cells. The difference of 4E-BP1 was not significant and it was a consequence of variance between A549/CDDP biological replicates. Furthermore, the ratio of phospho-4E-BP1 (Thr37/46) to 4E-BP1 was significantly decreased in A549/CDDP. These findings strongly suggest an alteration in 4E-BP1 regulation and phosphorylation, which may be inhibiting global translation and leading to a reduced metabolic activity of A549/CDDP.

In conclusion, A549/CDDP cells largely differed from A549 cells regarding metabolism. Glycolysis, the major use of glucose for energy obtaining was found downregulated in A549/CDDP cells. In addition, mitochondrial activity was also found downregulated in A549/CDDP cells. Our results indicated that CDDP-resistant cells have a higher dependence on common energy sources glucose and GLN due to a lack of plasticity of their reduced metabolism. The decreased metabolic rate observed for A549/CDDP cells may result in reduced cell growth and ROS production, which could represent a mechanism of CDDP resistance in these cells. Finally, we observed higher levels of 4E-BP1 and decreased ratio of phospho-4E-BP1 to 4E-BP1 suggesting a reduction of global translation in A549/CDDP.

5. REFERENCES

- Ai, Z., Lu, Y., Qiu, S., & Fan, Z. (2016). Overcoming cisplatin resistance of ovarian cancer cells by targeting HIF-1-regulated cancer metabolism. *Cancer Letters*, 373(1), 36–44. <https://doi.org/10.1016/j.canlet.2016.01.009>
- Aktipis, C. A., Boddy, A. M., Gatenby, R. A., Brown, J. S., & Maley, C. C. (2013, November 11). Life history trade-offs in cancer evolution. *Nature Reviews Cancer*, Vol. 13, pp. 883–892. <https://doi.org/10.1038/nrc3606>
- Annovazzi, L., Mellai, M., & Schiffer, D. (2017). Chemotherapeutic drugs: DNA damage and repair in glioblastoma. *Cancers*, 9(6). <https://doi.org/10.3390/cancers9060057>
- Baffy, G. (2017). Mitochondrial uncoupling in cancer cells: Liabilities and opportunities. *Biochimica et Biophysica Acta - Bioenergetics*, 1858(8), 655–664. <https://doi.org/10.1016/j.bbabi.2017.01.005>
- Bednarska-Szczepaniak, K., Krzyżanowski, D., Klink, M., & Nowak, M. (2019). Adenosine Analogues as Opposite Modulators of the Cisplatin Resistance of Ovarian Cancer Cells. *Anti-Cancer Agents in Medicinal Chemistry*, 19(4), 473–486. <https://doi.org/10.2174/1871520619666190118113201>
- Bensaad, K., Tsuruta, A., Selak, M. A., Vidal, M. N. C., Nakano, K., Bartrons, R., ... Vousden, K. H. (2006). TIGAR, a p53-Inducible Regulator of Glycolysis and Apoptosis. *Cell*, 126(1), 107–120. <https://doi.org/10.1016/j.cell.2006.05.036>
- Boddy, A. M., Huang, W., & Aktipis, A. (2018). Life History Trade-Offs in Tumors. *Current Pathobiology Reports*, Vol. 6, pp. 201–207. <https://doi.org/10.1007/s40139-018-0188-4>
- Bozic, I., Reiter, J. G., Allen, B., Antal, T., Chatterjee, K., Shah, P., ... Nowak, M. A. (2013). Evolutionary dynamics of cancer in response to targeted combination therapy. *ELife*, 2013(2). <https://doi.org/10.7554/eLife.00747>
- Brown, J. A., Yonekubo, Y., Hanson, N., Sastre-Perona, A., Basin, A., Rytlewski, J. A., ... Schober, M. (2017). TGF- β -Induced Quiescence Mediates Chemoresistance of Tumor-Propagating Cells in Squamous Cell Carcinoma. *Cell Stem Cell*, 21(5), 650-664.e8. <https://doi.org/10.1016/j.stem.2017.10.001>
- Cai, J., Culley, M. K., Zhao, Y., & Zhao, J. (2018). The role of ubiquitination and deubiquitination in the regulation of cell junctions. *Protein and Cell*, 9(9), 754–769. <https://doi.org/10.1007/s13238-017-0486-3>
- Cifani, P., & Kentsis, A. (2017). Towards comprehensive and quantitative proteomics for diagnosis and therapy of human disease. *Proteomics*, Vol. 17. <https://doi.org/10.1002/pmic.201600079>
- Cruz-Bermúdez, A., Laza-Briviesca, R., Vicente-Blanco, R. J., García-Grande, A., Coronado, M. J., Laine-Menéndez, S., ... Provencio, M. (2019). Cisplatin resistance involves a metabolic reprogramming through ROS and PGC-1 α in NSCLC which can be overcome by OXPHOS inhibition. *Free Radical Biology and Medicine*, 135, 167–181. <https://doi.org/10.1016/j.freeradbiomed.2019.03.009>
- D'Alessandro, G., Quaglio, D., Monaco, L., Lauro, C., Ghirga, F., Ingallina, C., ... Limatola, C. (2019). 1H-NMR metabolomics reveals the Glabrescione B exacerbation of glycolytic metabolism beside the cell growth inhibitory effect in glioma. *Cell Communication and Signaling*, 17(1). <https://doi.org/10.1186/s12964-019-0421-8>

- DeBerardinis, R. J., Lum, J. J., Hatzivassiliou, G., & Thompson, C. B. (2008). The Biology of Cancer: Metabolic Reprogramming Fuels Cell Growth and Proliferation. *Cell Metabolism*, 7(1), 11–20. <https://doi.org/10.1016/j.cmet.2007.10.002>
- Desler, C., Hansen, T. L., Frederiksen, J. B., Marcker, M. L., Singh, K. K., & Juel Rasmussen, L. (2012). Is There a Link between Mitochondrial Reserve Respiratory Capacity and Aging? *Journal of Aging Research*, 2012, 192503. <https://doi.org/10.1155/2012/192503>
- Duan, G., Shi, M., Xie, L., Xu, M., Wang, Y., & Yan, H. (2018). Increased Glutamine Consumption in Cisplatin-Resistant Cells Has a Negative Impact on Cell Growth. *Scientific Reports*, (February), 1–11. <https://doi.org/10.1038/s41598-018-21831-x>
- Duan, G., Tang, Q., Yan, H., Xie, L., Wang, Y., Zheng, X. E., ... Zou, X. (2017). A Strategy to Delay the Development of Cisplatin Resistance by Maintaining a Certain Amount of Cisplatin-Sensitive Cells. *Scientific Reports*, 7(1). <https://doi.org/10.1038/s41598-017-00422-2>
- Duma, N., Santana-Davila, R., & Molina, J. R. (2019, August 1). Non-Small Cell Lung Cancer: Epidemiology, Screening, Diagnosis, and Treatment. *Mayo Clinic Proceedings*, Vol. 94, pp. 1623–1640. <https://doi.org/10.1016/j.mayocp.2019.01.013>
- Ersahin, T., Tuncbag, N., & Cetin-Atalay, R. (2015). The PI3K/AKT/mTOR interactive pathway. *Molecular BioSystems*, 11(7), 1946–1954. <https://doi.org/10.1039/c5mb00101c>
- Ferlay, J., Colombet, M., Soerjomataram, I., Mathers, C., Parkin, D. M., Piñeros, M., ... Bray, F. (2019, April 15). Estimating the global cancer incidence and mortality in 2018: GLOBOCAN sources and methods. *International Journal of Cancer*, Vol. 144, pp. 1941–1953. <https://doi.org/10.1002/ijc.31937>
- Fichtinger-Schepman, A. M. J., Lohman, P. H. M., van der Veer, J. L., den Hartog, J. H. J., & Reedijk, J. (1985). Adducts of the Antitumor Drug cis-Diamminedichloroplatinum(II) with DNA: Formation, Identification, and Quantitation. *Biochemistry*, 24(3), 707–713. <https://doi.org/10.1021/bi00324a025>
- Franken, N. A. P., Rodermond, H. M., Stap, J., Haveman, J., & van Bree, C. (2006). Clonogenic assay of cells in vitro. *Nature Protocols*, 1(5), 2315–2319. <https://doi.org/10.1038/nprot.2006.339>
- Gao, Y., Dorn, P., Liu, S., Deng, H., Hall, S. R. R., Peng, R.-W., Schmid, R. A., & Marti, T. M. (2019). Cisplatin-resistant A549 non-small cell lung cancer cells can be identified by increased mitochondrial mass and are sensitive to pemetrexed treatment. *Cancer Cell International*, 19, 317. <https://doi.org/10.1186/s12935-019-1037-1>
- Greaves, M., & Maley, C. C. (2012). Clonal evolution in cancer. *Nature*, 481(7381), 306–313. <https://doi.org/10.1038/nature10762>
- Guzman, I., Gelman, H., Tai, J., & Gruebele, M. (2014). The extracellular protein VlsE is destabilized inside cells. *Journal of Molecular Biology*, 426(1), 11–20. <https://doi.org/10.1016/j.jmb.2013.08.024>
- Hershey, J. W. B., Sonenberg, N., & Mathews, M. B. (2012). Principles of Translational Control: An Overview. *Cold Spring Harbor Perspectives in Biology*, 4(12), a011528–a011528. <https://doi.org/10.1101/cshperspect.a011528>
- Hirsch, F. R., Scagliotti, G. V., Mulshine, J. L., Kwon, R., Curran, W. J., Wu, Y. L., & Paz-Ares, L. (2017, January 21). Lung cancer: current therapies and new targeted treatments. *The Lancet*, Vol. 389, pp. 299–311. [https://doi.org/10.1016/S0140-6736\(16\)30958-8](https://doi.org/10.1016/S0140-6736(16)30958-8)

- Huang, D. W., Sherman, B. T., & Lempicki, R. A. (2009). Bioinformatics enrichment tools: Paths toward the comprehensive functional analysis of large gene lists. *Nucleic Acids Research*, 37(1), 1–13. <https://doi.org/10.1093/nar/gkn923>
- Izumi, H., Yasuniwa, Y., Akiyama, M., Yamaguchi, T., Kuma, A., Kitamura, N., & Kohno, K. (2011). Forced expression of ZNF143 restrains cancer cell growth. *Cancers*, 3(4), 3909–3920. <https://doi.org/10.3390/cancers3043909>
- Jamieson, E. R., & Lippard, S. J. (1999). Structure, recognition, and processing of cisplatin-DNA adducts. *Chemical Reviews*, 99(9), 2467–2498. <https://doi.org/10.1021/cr980421n>
- Kelland, L. (2007). The resurgence of platinum-based cancer chemotherapy. *Nature Reviews Cancer*, 7(8), 573–584. <https://doi.org/10.1038/nrc2167>
- Krishnamoorthy, T., Pavitt, G. D., Zhang, F., Dever, T. E., & Hinnebusch, A. G. (2001). Tight Binding of the Phosphorylated α Subunit of Initiation Factor 2 (eIF2 α) to the Regulatory Subunits of Guanine Nucleotide Exchange Factor eIF2B Is Required for Inhibition of Translation Initiation. *Molecular and Cellular Biology*, 21(15), 5018–5030. <https://doi.org/10.1128/mcb.21.15.5018-5030.2001>
- Lehúede, C., Dupuy, F., Rabinovitch, R., Jones, R. G., & Siegel, P. M. (2016, September 15). Metabolic plasticity as a determinant of tumor growth and metastasis. *Cancer Research*, Vol. 76, pp. 5201–5208. <https://doi.org/10.1158/0008-5472.CAN-16-0266>
- Lin, W. S., Lu, K. M., Chung, M. H., Liu, S. T., Chen, H. H., Chang, Y. L., ... Huang, S. M. (2010). The subcellular localization and protein stability of mouse alpha-actinin 2 is controlled by its nuclear receptor binding motif in C2C12 cells. *International Journal of Biochemistry and Cell Biology*, 42(12), 2082–2091. <https://doi.org/10.1016/j.biocel.2010.09.024>
- Makrecka-Kuka, M., Krumschnabel, G., & Gnaiger, E. (2015). High-resolution respirometry for simultaneous measurement of oxygen and hydrogen peroxide fluxes in permeabilized cells, tissue homogenate and isolated mitochondria. *Biomolecules*, 5(3), 1319–1338. <https://doi.org/10.3390/biom5031319>
- Marcon, B. H., Holetz, F. B., Eastman, G., Origa-Alves, A. C., Amorós, M. A., de Aguiar, A. M., ... Dallagiovanna, B. (2017). Downregulation of the protein synthesis machinery is a major regulatory event during early adipogenic differentiation of human adipose-derived stromal cells. *Stem Cell Research*, 25, 191–201. <https://doi.org/10.1016/j.scr.2017.10.027>
- Maurer, G. D., Heller, S., Wanka, C., Rieger, J., & Steinbach, J. P. (2019). Knockdown of the TP53-induced glycolysis and apoptosis regulator (TIGAR) sensitizes glioma cells to hypoxia, irradiation and temozolomide. *International Journal of Molecular Sciences*, 20(5). <https://doi.org/10.3390/ijms20051061>
- McDermott, M., Eustace, A. J., Busschots, S., Breen, L., Crown, J., Clynes, M., ... Stordal, B. (2014). In vitro Development of Chemotherapy and Targeted Therapy Drug-Resistant Cancer Cell Lines: A Practical Guide with Case Studies. *Frontiers in Oncology*, 4, 40. <https://doi.org/10.3389/fonc.2014.00040>
- Okar, D. A., Lange, A. J., Manzano, À., Navarro-Sabatè, A., Riera, L., & Bartrons, R. (2001). PFK-2/FBPase-2: Maker and breaker of the essential biofactor fructose-2,6-bisphosphate. *Trends in Biochemical Sciences*, 26(1), 30–35. [https://doi.org/10.1016/S0968-0004\(00\)01699-6](https://doi.org/10.1016/S0968-0004(00)01699-6)
- Papa, S., Choy, P. M., & Bubici, C. (2019). The ERK and JNK pathways in the regulation of metabolic reprogramming. *Oncogene*, 38(13), 2223–2240. <https://doi.org/10.1038/s41388-018-0582-8>

- Pirmoradian, M., Budamgunta, H., Chingin, K., Zhang, B., Astorga-Wells, J., & Zubarev, R. A. (2013). Rapid and deep human proteome analysis by single-dimension shotgun proteomics. *Molecular and Cellular Proteomics*, 12(11), 3330–3338. <https://doi.org/10.1074/mcp.O113.028787>
- Qin, X., Jiang, B., & Zhang, Y. (2016). 4E-BP1, a multifactor regulated multifunctional protein. *Cell Cycle*, 15(6), 781–786. <https://doi.org/10.1080/15384101.2016.1151581>
- Qin, X., Yu, S., Zhou, L., Shi, M., Hu, Y., Xu, X., ... Feng, J. (2017). Cisplatin-resistant lung cancer cell-derived exosomes increase cisplatin resistance of recipient cells in exosomal miR-100-5p-dependent manner. *International Journal of Nanomedicine*, 12, 3721–3733. <https://doi.org/10.2147/IJN.S131516>
- Roh, J. L., Park, J. Y., Kim, E. H., Jang, H. J., & Kwon, M. (2016). Activation of mitochondrial oxidation by PDK2 inhibition reverses cisplatin resistance in head and neck cancer. *Cancer Letters*, 371(1), 20–29. <https://doi.org/10.1016/j.canlet.2015.11.023>
- Rousseau, A., & Bertolotti, A. (2018). Regulation of proteasome assembly and activity in health and disease. *Nature Reviews Molecular Cell Biology*, 19(11), 697–712. <https://doi.org/10.1038/s41580-018-0040-z>
- Salgia, R., & Kulkarni, P. (2018). The Genetic/Non-genetic Duality of Drug ‘Resistance’ in Cancer. *Trends in Cancer*, 4(2), 110–118. <https://doi.org/10.1016/j.trecan.2018.01.001>
- Schneider, C. A., Rasband, W. S., & Eliceiri, K. W. (2012). NIH Image to ImageJ: 25 years of image analysis. *Nature Methods*, 9(7), 671–675. <https://doi.org/10.1038/nmeth.2089>
- Siddik, Z. H. (2003). Cisplatin: mode of cytotoxic action and molecular basis of resistance. *Oncogene*, 22(47), 7265–7279. <https://doi.org/10.1038/sj.onc.1206933>
- Siegel, R. L., Miller, K. D., & Jemal, A. (2019). Cancer statistics, 2019. *CA: A Cancer Journal for Clinicians*, 69(1), 7–34. <https://doi.org/10.3322/caac.21551>
- Son, J., Lyssiotis, C. A., Ying, H., Wang, X., Hua, S., Ligorio, M., ... Kimmelman, A. C. (2013). Glutamine supports pancreatic cancer growth through a KRAS-regulated metabolic pathway. *Nature*, 496(7443), 101–105. <https://doi.org/10.1038/nature12040>
- Sonenberg, N., & Hinnebusch, A. G. (2009). Regulation of Translation Initiation in Eukaryotes: Mechanisms and Biological Targets. *Cell*, 136(4), 731–745. <https://doi.org/10.1016/j.cell.2009.01.042>
- Sullivan, E. J., Kurtoglu, M., Brenneman, R., Liu, H., & Lampidis, T. J. (2014). Targeting cisplatin-resistant human tumor cells with metabolic inhibitors. *Cancer Chemotherapy and Pharmacology*, 73(2), 417–427. <https://doi.org/10.1007/s00280-013-2366-8>
- Vichai, V., & Kirtikara, K. (2006). Sulforhodamine B colorimetric assay for cytotoxicity screening. *Nature Protocols*, 1(3), 1112–1116. <https://doi.org/10.1038/nprot.2006.179>
- Xie, J. M., Li, B., Yu, H. P., Gao, Q. G., Li, W., Wu, H. R., & Qin, Z. H. (2014). TIGAR has a dual role in cancer cell survival through regulating apoptosis and autophagy. *Cancer Research*, 74(18), 5127–5138. <https://doi.org/10.1158/0008-5472.CAN-13-3517>
- Wagner, B. A., Venkataraman, S., & Buettner, G. R. (2011). The rate of oxygen utilization by cells. *Free Radical Biology and Medicine*, 51(3), 700–712. <https://doi.org/10.1016/j.freeradbiomed.2011.05.024>
- Wang, B., Zhang, Y., Ye, M., Wu, J., Ma, L., & Chen, H. (2019). Cisplatin-resistant MDA-MB-231 Cell-derived Exosomes Increase the Resistance of Recipient Cells in an Exosomal miR-423-5p-

dependent Manner. *Current Drug Metabolism*, 20(10), 804–814.
<https://doi.org/10.2174/1389200220666190819151946>

Wang, S. F., Chen, M. S., Chou, Y. C., Ueng, Y. F., Yin, P. H., Yeh, T. S., & Lee, H. C. (2016). Mitochondrial dysfunction enhances cisplatin resistance in human gastric cancer cells via the ROS-activated GCN2-eIF2 α -ATF4-xCT pathway. *Oncotarget*, 7(45), 74132–74151.
<https://doi.org/10.18632/oncotarget.12356>

Ye, J., Coulouris, G., Zaretskaya, I., Cutcutache, I., Rozen, S., & Madden, T. L. (2012). Primer-BLAST: a tool to design target-specific primers for polymerase chain reaction. *BMC Bioinformatics*, 13, 134. <https://doi.org/10.1186/1471-2105-13-134>

Zorov, D. B., Juhaszova, M., & Sollott, S. J. (2014, July 1). Mitochondrial reactive oxygen species (ROS) and ROS-induced ROS release. *Physiological Reviews*, Vol. 94, pp. 909–950.
<https://doi.org/10.1152/physrev.00026.2013>

FIGURES

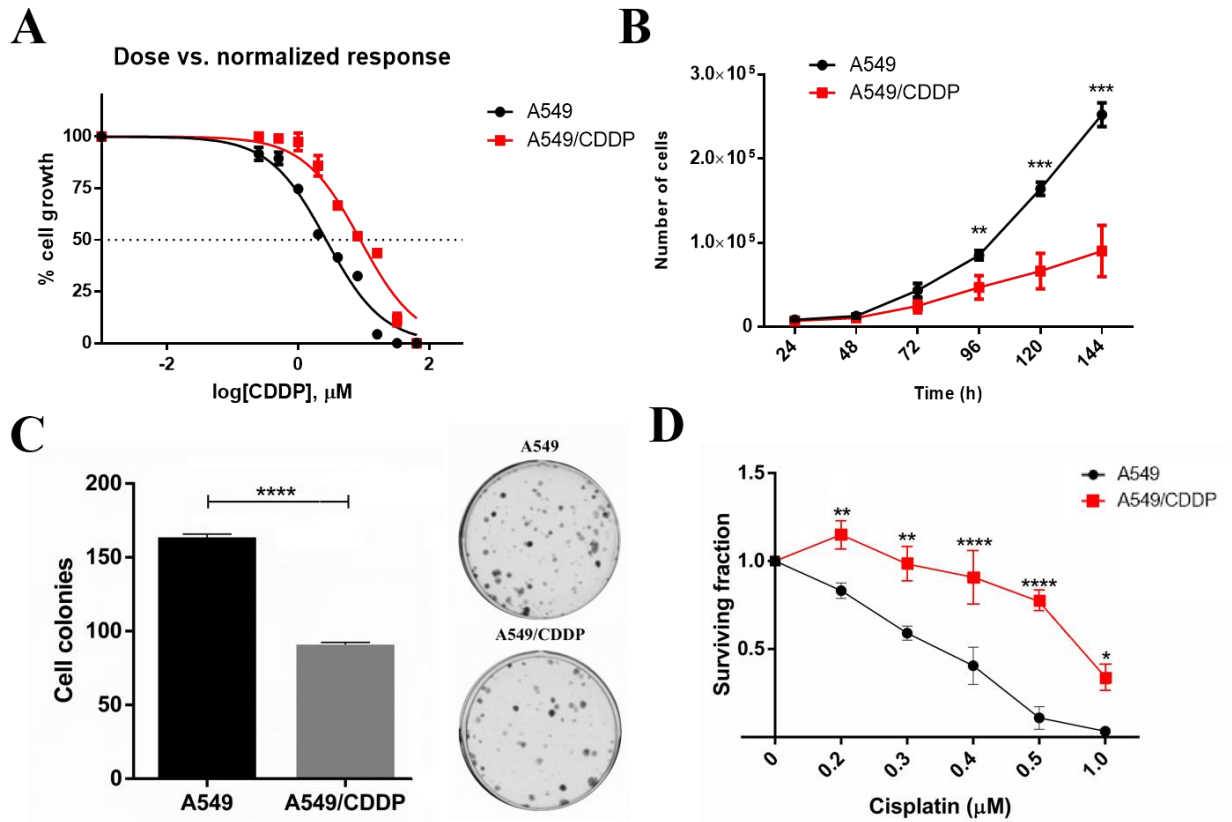


Figure 1: Comparison of CDDP cytotoxicity, proliferative and clonogenic capacities of A549 and A549/CDDP cells. A) Cytotoxicity assay showing CDDP concentration vs. cell inhibition growth of A549 and A549/CDDP cells after 72 h. The concentration that results in inhibiting cell growth by 50% (GI_{50}) was calculated and used to compare cisplatin resistance of each cell line. A549 $GI_{50} = 2.656 \mu\text{M}$; A549/CDDP $GI_{50} = 8.793 \mu\text{M}$. B) Cell proliferation and C) colony formation in the absence of CDDP. D) Surviving fraction (SF) of A549 and A549/CDDP cells upon CDDP exposure. Number of cells (B) and SF (D) were compared by multiple t test one per row, corrected for multiple comparisons using the Holm-Sidak method. Cell colonies (C) were compared using t test. * $p < 0.05$, ** $p < 0.01$, *** $p < 0.001$, **** $p < 0.0001$.

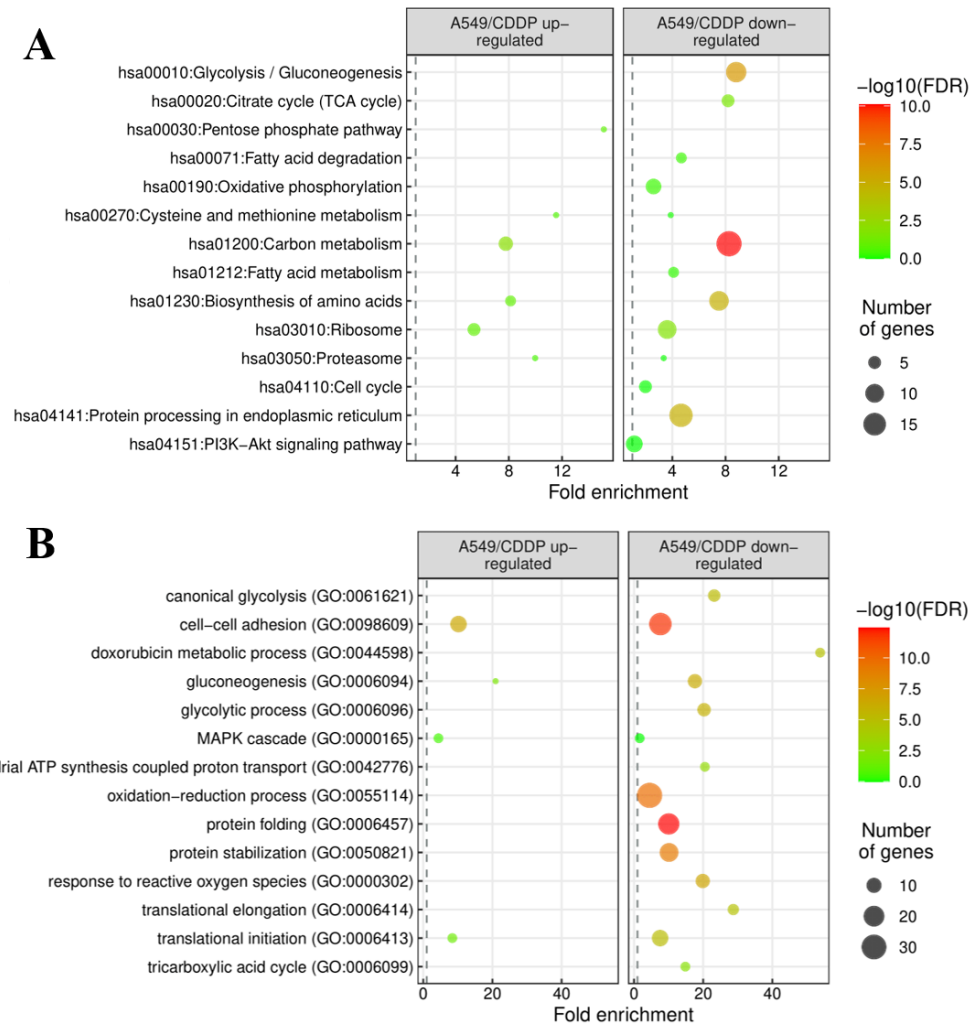


Figure 2: GO biological processes and KEGG pathways enriched in functional annotation analysis of proteins found up- and downregulated in A549/CDDP cells. Main terms enriched in proteins up- and downregulated in A549/CDDP cells. Terms are sorted by fold enrichment, whose significance is indicated by the dot color ($-\log_{10}$ (False Discovery Rate (FDR) - corrected p-values)). The dot size indicates the number of proteins associated with each process. The vertical grey dashed line represents a fold enrichment of 1.

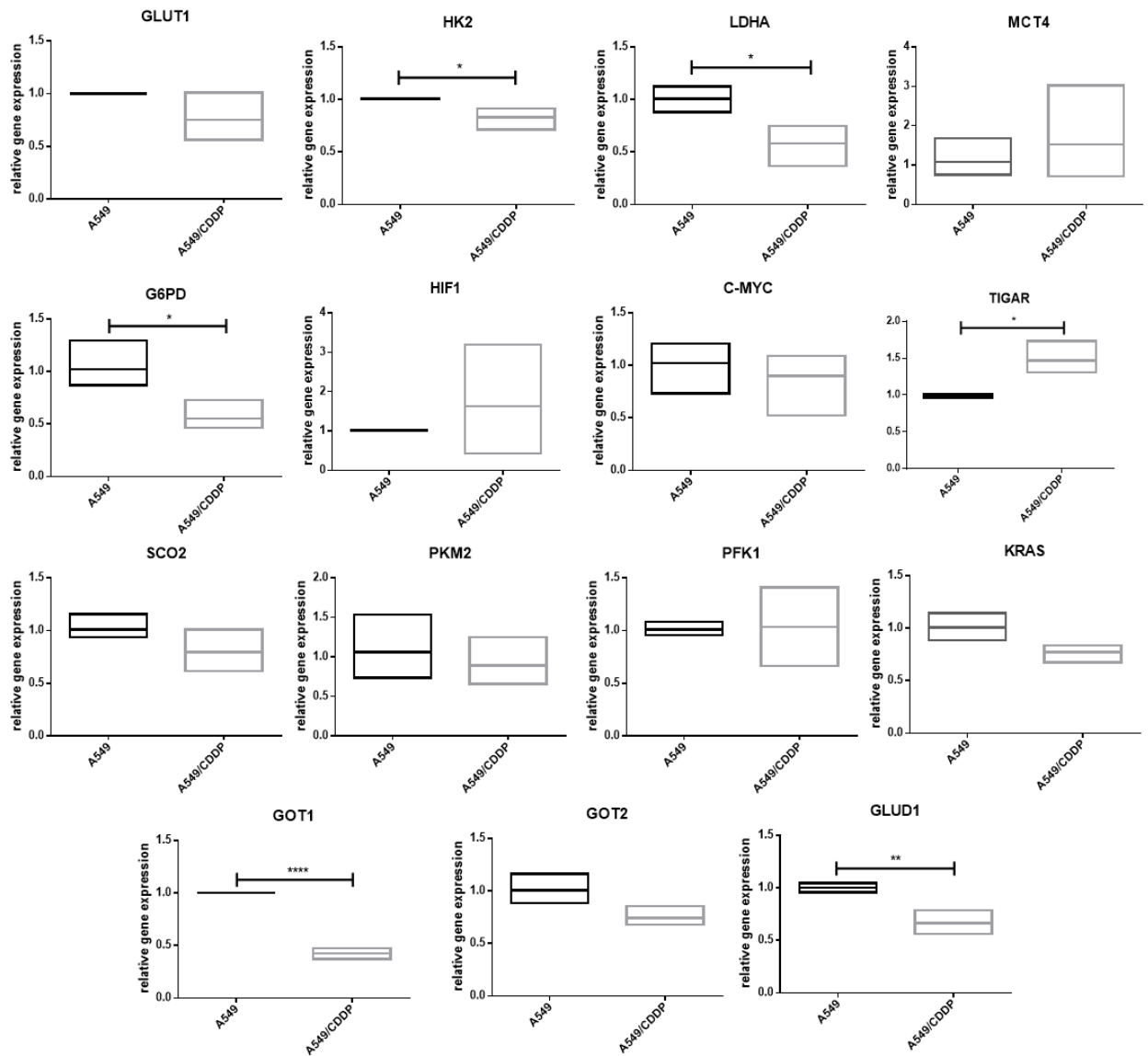


Figure 3: Relative gene expression of A549/CDDP cells in compared to A549 cells. Relative gene expression analysis by RT-qPCR from total RNA of A549 and A549/CDDP cells. Data shown are the means \pm SD of triplicate analyses. Statistical significance was determined by Mann-Whitney test. * $p < 0.05$, ** $p < 0.01$, **** $p < 0.0001$.

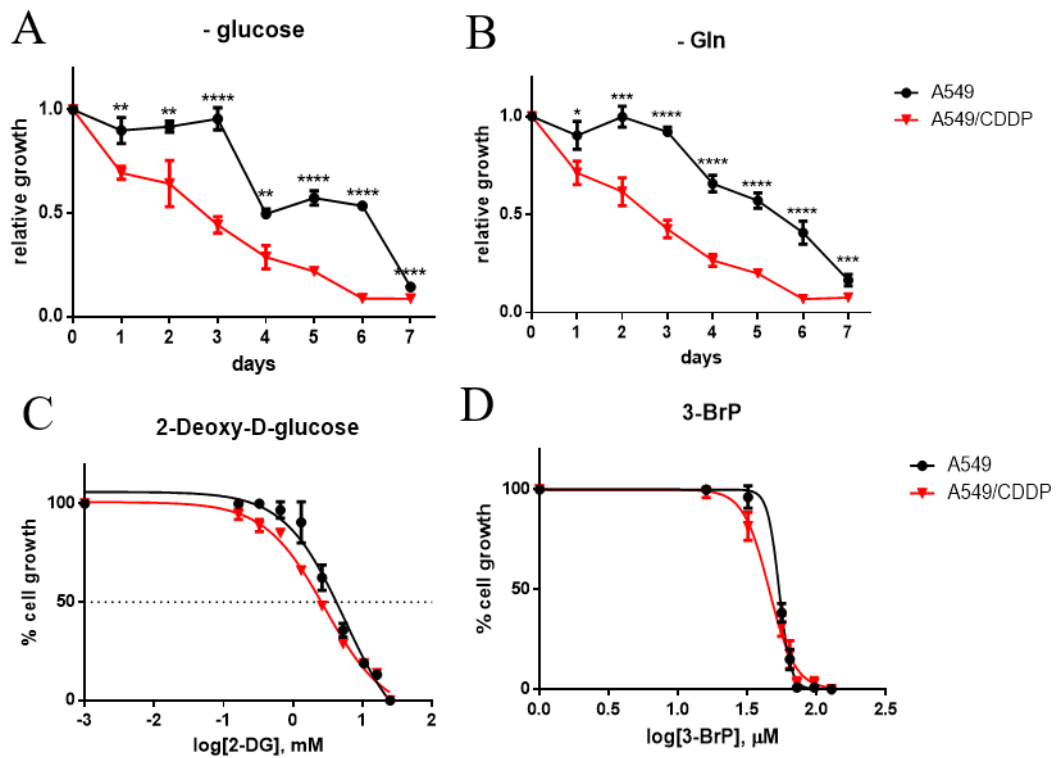


Figure 4: Effects of Gln, glucose and glycolysis inhibitors on the proliferation of A549 and A549/CDDP cells. Relative growth of A549 and A549/CDDP cells in the presence and in the absence of A) glucose and B) GLN. Time points were compared by multiple t test one per row, corrected for multiple comparisons using the Holm-Sidak method. Cytotoxicity assay of A549 and A549/CDDP cells exposed to glycolysis inhibitors C) 2-DG and D) 3-BrP. Mean and standard deviation from a representative experiment. * $p < 0.05$, ** $p < 0.01$, *** $p < 0.001$, **** $p < 0.0001$.



Figure 5: Effect of anti- and pro-oxidant molecules on the clonogenic capacity of A549 and A549/CDDP cells. SF of A549 and A549/CDDP cells after treatment for 24 h with A) GSH (4 mM), B) BSO (50 μ M), C) DEM (100 μ M). Data shown are the means \pm SD of triplicate analyses. Statistical significance was determined by t test.

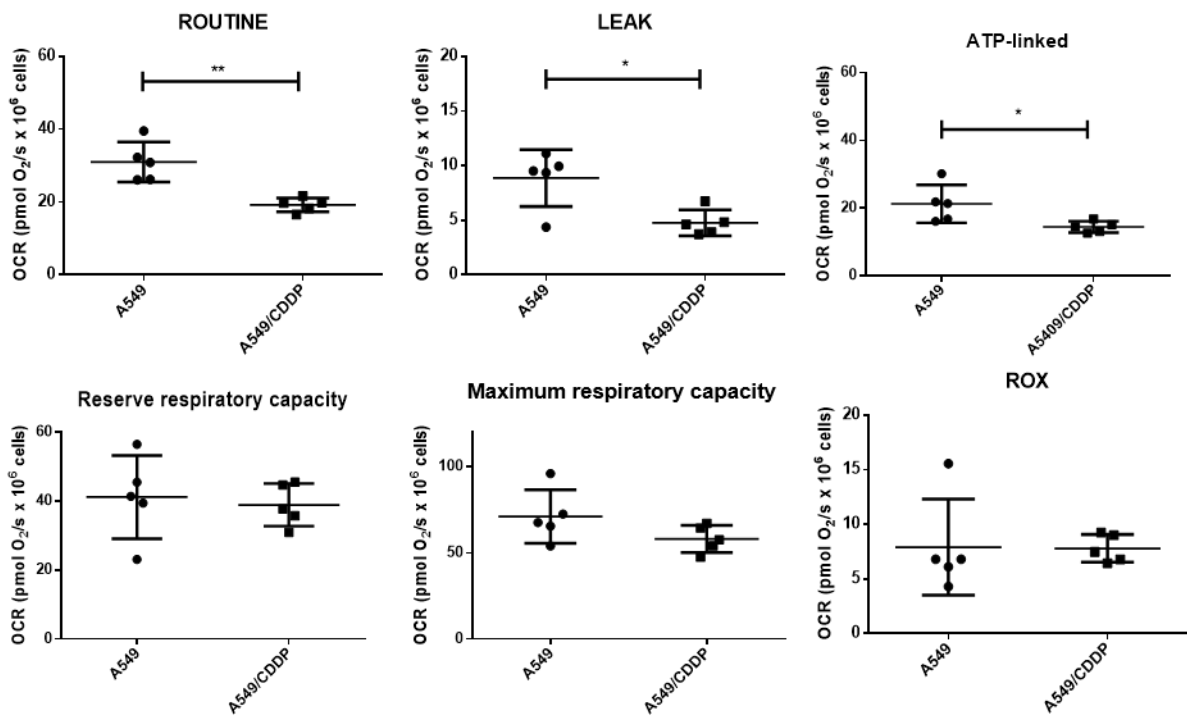


Figure 6: High-performance respirometry analysis comparing A549 and A549/CDDP cells. Oxygen consumption rate (OCR) expressed as pmol O₂/s x 10⁶ cells, mean \pm SD of N = 5 independent cultures. Statistical significance was determined by t test. * p < 0.05, ** p < 0.01.

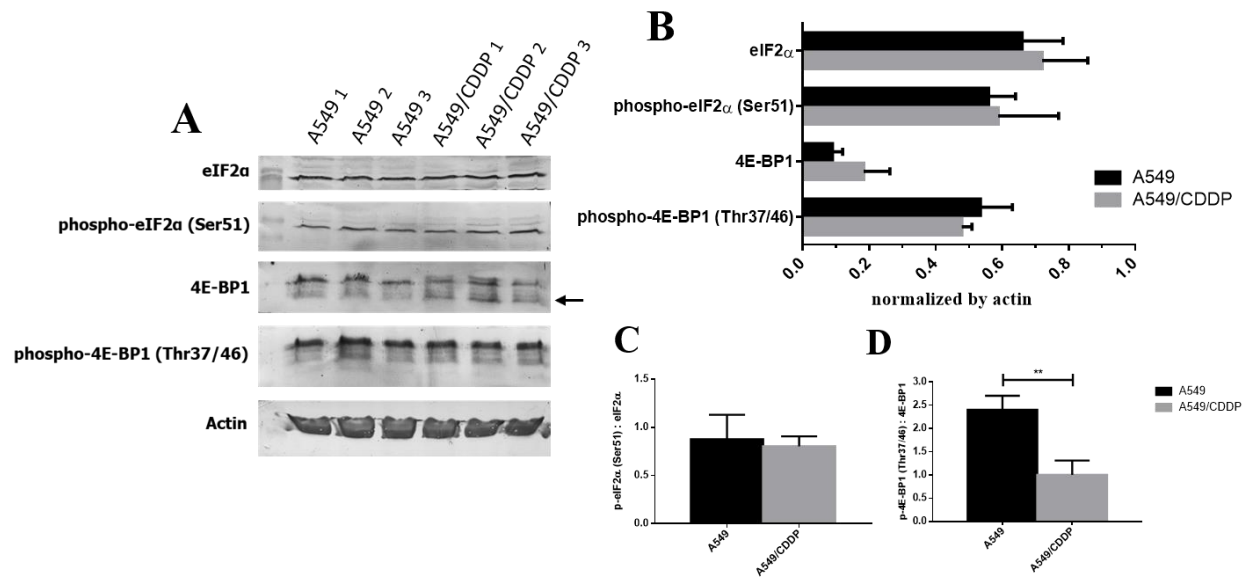


Figure 7: Analysis of eIF2 α and 4E-BP1 expression and phosphorylation in A549 and A549/CDDP cells. A) Western blot analysis of A549 and A549/CDDP replicates. Arrow represents hypophosphorylated isoform of 4E-BP1. B) quantification of eIF2 α , phospho-eIF2 α (Ser51), 4E-BP1, phospho-4E-BP1 (Thr37/46) relative to actin intensity. C) ratio of phospho-eIF2 α : eIF2 α intensity. D) ratio of phospho-4E-BP1 (Thr37/46): 4E-BP1. Statistical significance was determined by multiple t test, corrected for multiple comparisons using the Holm-Sidak method. ** p < 0.01.

TABLES

Table 1: Primers sequences utilized for RT-qPCR

Gene	Primers Sequence (5' – 3')
SLC2A1 (GLUT1)	F: GAACTCTTCAGCCAGGGTCC R: ACCACACAGTTGCTCCACAT
HK2	F: CCCCTGCCACCAGACTAAAC R: CAAAGTCCCCTCTCCTCTGG
PKM2	F: ATCGGTCTCACCAAGTCTGG R: GAAGATGCCACGGTACAGGT
G6PD	F: ACGACGAAGCGCAGACAG R: TCCGACTGATGGAAGGCATC
LDHA	F: AGCTGTTCCACTTAAGGCC R: TGGAACCAAAAGGAATCGGGA
HIF1A	F: GACCGATTACCATGGAGGG R: GTGGCAACTGATGAGCAAGC
C-MYC	F: GGACCCGCTTCTCTGAAAGG R: TAACGTTGAGGGGCATCGTC
TIGAR	F: CTCTGACTGTTGTCCGGCAT R: TGCATGGTCTGCTTTGTCCT
SLC16A4 (MCT4)	F: ACAGCCTGGATCTCCTCCAT R: ATGATGCTCCGGCAAAGGA
PFKM	F: TGGGACTAAAAGGACTCTACCC R: CCCTGTGTAAGCCTCAAAGC
SCO2	F: TGGACCACTCCATTGCCATC R: AGACAGGACACTGCGGAAAG
GOT1	F: CTCTCGATATGGCACCTCCG R: AAAACCCAGGGATGGCAGTC
GOT2	F: CATGGCTGACCGCATCATTG R: AGAACTCCTTGATCAGCCGC
GLUD1	F: GACATCGTGCCTCTGGCT R: AGGTCACACCAGCTTCATTGT
KRAS	F: GCCTTGACGATACAGCTAAT R: TGACCTGCTGTGTCGAGAAT
ACTB	F: CCTGGCACCCAGCACAAT R: GACTCGTCATACTCCTGCTTG
18S	F: TCGGAACTGAGGCCATGATT R: CCTCCGACTTTCGTTCTTGATT

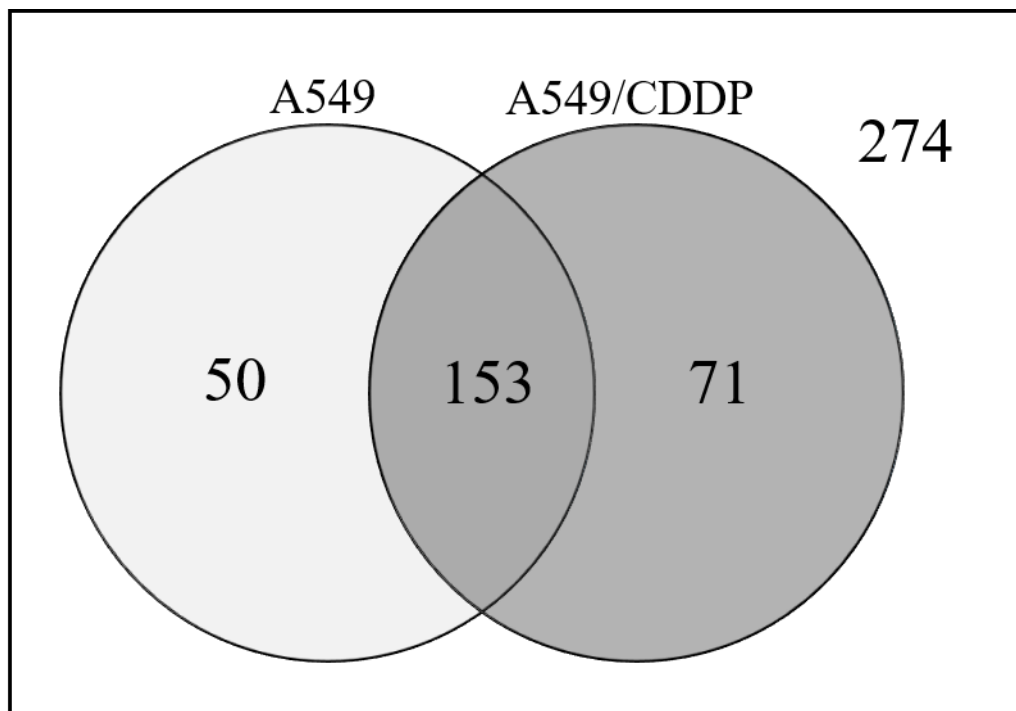
SUPPLEMENTARY MATERIALS

Supplementary Figure 1: Overview of the proteins identified from A549 and A549/CDDP cells.

Venn diagrams of proteins identified by LC-MS/MS analysis. Diagrams revealed total, exclusive, and shared proteins identified in A549 and A54/CDDP.

Supplementary Table 1: Quantitative protein expression analysis between A549 and A549/CDDP cells.

Supplementary Table 2: Functional annotation clustering and gene-term enrichment analysis for proteins found A) upregulated and B) downregulated in A549/CDDP cells in comparison to A549 cells.



SUPPLEMENTARY FIGURE 1: Overview of the proteins identified from A549 and A549/CDDP cells. Venn diagrams of proteins identified by LC-MS/MS analysis. Diagrams revealed total, exclusive, and shared proteins identified in A549 and A54/CDDP.

SUPPLEMENTARY TABLE 1: Quantitative protein expression analysis between A549 and A549/CDDP cells.

Protein name	Gene name	Accession No	Score	A549:A549/CDDP		
				Ratio	Probability	Overexpression
10 kDa heat shock protein_mitochondrial	HSPE1	P61604	5455.63	5.36	1.00	A549
14-3-3 protein epsilon	YWHAE	P62258	1015.06	-	-	A549
14-3-3 protein gamma	YWHAG	P61981	7545.14	4.66	1.00	A549
14-3-3 protein sigma	SFN	P31947	2146.96	-	-	A549/CDDP
14-3-3 protein theta	YWHAQ	P27348	1817.00	2.61	1.00	A549
14-3-3 protein zeta/delta	YWHAZ	P63104	5249.27	2.27	1.00	A549
26S protease regulatory subunit 6A	PSMC3	R4GNH3	995.51	-	-	A549/CDDP
26S protease regulatory subunit 6B	PSMC4	P43686	1906.86	-	-	A549
3-hydroxyacyl-CoA dehydrogenase type-2	HSD17B10	Q99714	2197.71	3.03	1.00	A549
3-hydroxyisobutyrate dehydrogenase_mitochondrial	HIBADH	P31937	2002.81	3.60	1.00	A549
40S ribosomal protein S13	RPS13	J3KMX5	884.71	-	-	A549/CDDP
40S ribosomal protein S15	RPS15	K7ELC2	4797.85	-	-	A549
40S ribosomal protein S17	RPS17	P08708	8189.89	1.55	1.00	A549
40S ribosomal protein S28	RPS28	P62857	2730.54	-	-	A549/CDDP
40S ribosomal protein S4_X isoform	RPS4X	P62701	2537.10	1.97	1.00	A549
40S ribosomal protein S7	RPS7	P62081	5197.85	1.08	0.96	A549
40S ribosomal protein SA (Fragment)	RPSA	C9J9K3	4825.64	1.30	1.00	A549
4F2 cell-surface antigen heavy chain	SLC3A2	P08195	2618.66	-	-	A549
6-phosphogluconate dehydrogenase_decarboxylating	PGD	P52209	18383.40	2.20	1.00	A549
6-phosphogluconolactonase	PGLS	O95336	1219.28	-	-	A549/CDDP
60 kDa heat shock protein_mitochondrial	HSPD1	P10809	12125.92	5.05	1.00	A549
60S acidic ribosomal protein P0	RPLP0	P05388	3429.00	5.10	1.00	A549
60S acidic ribosomal protein P1	RPLP1	P05386	51512.98	Normalizing protein		
60S acidic ribosomal protein P2	RPLP2	P05387	8938.10	-	-	A549

60S ribosomal protein L11	RPL11	P62913	3202.81	-	-	A549/CDDP
60S ribosomal protein L22	RPL22	P35268	4910.75	3.29	1.00	A549
60S ribosomal protein L24	RPL24	C9JXB8	1210.21	-	-	A549/CDDP
60S ribosomal protein L4	RPL4	P36578	1136.77	2.27	1.00	A549
60S ribosomal protein L8 (Fragment)	RPL8	E9PKZ0	1267.90	-	-	A549/CDDP
78 kDa glucose-regulated protein	HSPA5	P11021	5102.34	4.62	1.00	A549
Acetyl-CoA acetyltransferase_mitochondrial	ACAT1	P24752	2412.25	2.58	1.00	A549
Aconitate hydratase_mitochondrial	ACO2	Q99798	1153.82	-	-	A549
Actin_alpha cardiac muscle 1	ACTC1	P68032	918.27	-	-	A549/CDDP
Actin_cytoplasmic 1	ACTB	P60709	30879.36	-	-	A549/CDDP
Actin_cytoplasmic 2	ACTG1	P63261	31803.16	-	-	A549
Actin-related protein 3	ACTR3	P61158	1688.38	-	-	A549
Adenylyl cyclase-associated protein 1	CAP1	Q01518	1365.23	1.52	1.00	A549
ADP-ribosylation factor 3	ARF3	P61204	5358.78	-	-	A549/CDDP
ADP-ribosylation factor 4	ARF4	P18085	3140.52	-	-	A549
ADP/ATP translocase 1	SLC25A4	P12235	4210.19	-	-	A549/CDDP
Alanine--tRNA ligase_cytoplasmic	AARS	P49588	1769.41	1.90	1.00	A549
Aldehyde dehydrogenase_dimeric NADP-preferring	ALDH3A1	P30838	13070.40	8.33	1.00	A549
Aldehyde dehydrogenase_mitochondrial	ALDH2	P05091	1849.62	3.19	1.00	A549
Aldo-keto reductase family 1 member B10	AKR1B10	O60218	18093.57	4.57	1.00	A549
Aldo-keto reductase family 1 member C1	AKR1C1	Q04828	20069.67	2.64	1.00	A549
Aldo-keto reductase family 1 member C2	AKR1C2	P52895	911.52	6.17	1.00	A549
Aldo-keto reductase family 1 member C3	AKR1C3	A0A0A0MS S8	16352.93	9.78	1.00	A549
Aldose reductase	AKR1B1	P15121	2937.44	2.61	1.00	A549
Alpha-actinin-4	ACTN4	O43707	8139.03	2.01	1.00	A549
Alpha-enolase	ENO1	P06733	14101.80	2.14	1.00	A549
Annexin A1	ANXA1	P04083	19702.07	2.83	1.00	A549
Annexin A2	ANXA2	P07355	8074.46	7.17	1.00	A549
Annexin A4	ANXA4	P09525	5638.42	7.32	1.00	A549

Annexin A5	ANXA5	P08758	1957.23	7.24	1.00	A549
Anterior gradient protein 2 homolog	AGR2	O95994	4034.07	37,71	1.00	A549
AP-2 complex subunit beta	AP2B1	P63010	997.48	-	-	A549
Aspartate aminotransferase_cytoplasmic	GOT1	P17174	1177.14	-	-	A549/CDDP
Aspartate aminotransferase_mitochondrial	GOT2	P00505	3530.26	-	-	A549/CDDP
ATP synthase subunit alpha_mitochondrial	ATP5A1	P25705	5307.70	3.82	1.00	A549
ATP synthase subunit beta_mitochondrial	ATP5B	P06576	10118.14	3.19	1.00	A549
ATP synthase subunit d_mitochondrial	ATP5H	O75947	4942.79	2.01	1.00	A549
ATP synthase subunit O_mitochondrial	ATP5O	P48047	1350.35	-	-	A549/CDDP
ATP-citrate synthase	ACLY	P53396	1449.09	-	-	A549/CDDP
BAG family molecular chaperone regulator 3	BAG3	O95817	1499.14	-	-	A549/CDDP
Barrier-to-autointegration factor	BANF1	O75531	22563.58	1.17	1.00	A549
Calcium-binding mitochondrial carrier protein Aralar2	SLC25A13	Q9UJS0	1201.75	-	-	A549
Calmodulin	CALM1	P62158	8614.13	-	-	A549/CDDP
Calnexin	CANX	P27824	1768.14	3.42	1.00	A549
Calpastatin	CAST	A0A0C4DG B5	861.61	-	-	A549/CDDP
Calreticulin	CALR	P27797	2827.32	2.86	1.00	A549
Carbonic anhydrase 12	CA12	O43570	4085.37	-	-	A549/CDDP
Carbonyl reductase [NADPH] 1	CBR1	P16152	2540.17	2.05	1.00	A549
Chloride intracellular channel protein 1	CLIC1	O00299	2659.74	-	-	A549/CDDP
Citrate synthase	CS	B4DJV2	1161.70	6.42	1.00	A549
Clathrin heavy chain	CLTC	A0A087WV Q6	1002.98	-	-	A549/CDDP
Cleavage and polyadenylation specificity factor subunit 5	NUDT21	O43809	2785.87	2.29	1.00	A549
Coatomer subunit alpha	COPA	P53621	893.07	-	-	A549/CDDP
Cofilin-1	CFL1	E9PK25	14408.48	1.75	1.00	A549
Complement component 1 Q subcomponent-binding protein_mitochondrial	C1QBP	Q07021	1780.33	1.58	1.00	A549

Cystatin-B	CSTB	P04080	2003.60	-	-	A549
Cytochrome b-c1 complex subunit Rieske_mitochondrial	UQCRFS1	P47985	2570.11	1.52	1.00	A549
Cytochrome c oxidase subunit 5A_mitochondrial	COX5A	H3BNX8	1299.02	-	-	A549
Cytochrome c1_heme protein_mitochondrial	CYC1	P08574	1029.55	-	-	A549
Cytoplasmic aconitate hydratase	ACO1	P21399	5708.51	1.07	0.96	A549
Dihydropyrimidinase-related protein 2	DPYSL2	A0A1C7CYX9	1757.27	-	-	A549
DNA-(apurinic or apyrimidinic site) lyase	APEX1	P27695	1251.79	1.92	1.00	A549
Dolichyl-diphosphooligosaccharide--protein glycosyltransferase subunit 2	RPN2	P04844	1039.72	-	-	A549/CDDP
Electron transfer flavoprotein subunit alpha_mitochondrial	ETFA	P13804	6095.82	-	-	A549
Elongation factor 1-alpha 2	EEF1A2	Q05639	3475.46	1.26	1.00	A549
Elongation factor 1-beta	EEF1B2	P24534	2157.17	2.39	1.00	A549
Elongation factor 2	EEF2	P13639	5972.93	2.05	1.00	A549
Elongation factor Tu_mitochondrial	TUFM	P49411	3268.56	2.97	1.00	A549
Endoplasmic reticulum resident protein 29	ERP29	P30040	2337.15	-	-	A549
Endoplasmic	HSP90B1	P14625	5351.34	4.18	1.00	A549
Enoyl-CoA hydratase_mitochondrial	ECHS1	P30084	1514.01	4.71	1.00	A549
Epoxide hydrolase 1	EPHX1	P07099	1510.14	4.57	1.00	A549
Erythrocyte band 7 integral membrane protein	STOM	P27105	2011.27	2.92	1.00	A549
Eukaryotic initiation factor 4A-II	EIF4A2	Q14240	1486.17	3.60	1.00	A549
Eukaryotic translation initiation factor 5A-1	EIF5A	I3L504	1873.92	1.93	1.00	A549
Eukaryotic translation initiation factor 6	EIF6	P56537	1682.25	1.38	1.00	A549
Far upstream element-binding protein 2	KHSRP	A0A087WTP3	1026.40	-	-	A549/CDDP
Filamin-A	FLNA	P21333	2844.22	1.54	1.00	A549
Flavin reductase (NADPH)	BLVRB	P30043	2100.98	-	-	A549/CDDP
Fructose-bisphosphate aldolase A	ALDOA	P04075	9896.66	-	-	A549/CDDP

Galectin-1	LGALS1	P09382	897.23	3.32	1.00	A549
Glucose-6-phosphate 1-dehydrogenase	G6PD	P11413	5453.06	3.82	1.00	A549
Glucose-6-phosphate isomerase (Fragment)	GPI	A0A0A0MTS2	11408.26	3.71	1.00	A549
Glutathione S-transferase P	GSTP1	P09211	39906.52	2.25	1.00	A549
Glyceraldehyde-3-phosphate dehydrogenase	GAPDH	P04406	28056.91	3.16	1.00	A549
Glyoxylate reductase/hydroxypyruvate reductase	GRHPR	Q9UBQ7	2488.14	-	-	A549
GTP-binding nuclear protein Ran	RAN	B5MDF5	1000.37	-	-	A549
GTP-binding protein SAR1a	SAR1A	Q9NR31	1890.22	-	-	A549
Heat shock 70 kDa protein 1B	HSPA1B	A0A0G2JIW1	18344.75	3.42	1.00	A549
Heat shock 70 kDa protein 4	HSPA4	P34932	3229.50	1.05	0.94	-
Heat shock cognate 71 kDa protein	HSPA8	P11142	15891.42	3.39	1.00	A549
Heat shock protein beta-1	HSPB1	P04792	12113.59	1.51	1.00	A549
Heat shock protein HSP 90-alpha	HSP90AA1	P07900	14893.04	2.58	1.00	A549
Heat shock protein HSP 90-beta	HSP90AB1	P08238	4996.02	2.72	1.00	A549
Heterogeneous nuclear ribonucleoprotein F	HNRNPF	P52597	1135.86	-	-	A549
Heterogeneous nuclear ribonucleoprotein K	HNRNPK	P61978	14853.93	2.18	1.00	A549
Heterogeneous nuclear ribonucleoprotein Q	SYNCRIP	O60506	791.14	-	-	A549/CDDP
Heterogeneous nuclear ribonucleoprotein U	HNRNPU	Q00839	1657.69	-	-	A549/CDDP
Heterogeneous nuclear ribonucleoproteins A2/B1	HNRNPA2B1	P22626	1161.72	2.41	1.00	A549
Histidine triad nucleotide-binding protein 1	HINT1	P49773	3074.67	-	-	A549
Histone H1.4	HIST1H1E	P10412	2912.70	-	-	A549
Histone H2A	N/A	A0A0U1RRH7	10970.97	0.79	0.00	A549/CDDP
Histone H2A.Z	H2AFZ	P0C0S5	2070.54	-	-	A549
Histone H2AX	H2AFX	P16104	8775.58	1.51	0.80	-
Histone H2B	HIST1H2BN	U3KQK0	16811.61	1.30	1.00	A549
Histone H3 (Fragment)	H3F3B	K7EK07	2307.70	2.27	1.00	A549

Histone H3.2	HIST2H3A	Q71DI3	8863.72	2.36	1.00	A549
Histone H4	HIST1H4A	P62805	20088.14	3.25	1.00	A549
Hsc70-interacting protein (Fragment)	ST13	F6VDH7	1103.01	-	-	A549/CDDP
Hydroxyacyl-coenzyme A dehydrogenase_mitochondrial	HADH	A0A0A0MS E2	1189.04	-	-	A549/CDDP
Inorganic pyrophosphatase	PPA1	Q15181	1514.83	-	-	A549
Integrin beta-1	ITGB1	P05556	1652.34	-	-	A549
Isochorismatase domain-containing protein 2 (Fragment)	ISOC2	K7EKW4	13089.19	2.01	1.00	A549
Isocitrate dehydrogenase [NADP] cytoplasmic	IDH1	O75874	1692.17	-	-	A549
Keratin_type I cytoskeletal 18	KRT18	P05783	26195.07	2.64	1.00	A549
Keratin_type II cytoskeletal 7	KRT7	P08729	5916.27	1.11	1.00	A549
Keratin_type II cytoskeletal 8	KRT8	P05787	44708.18	2.20	1.00	A549
Kynureninase	KYNU	Q16719	1026.88	1.82	1.00	A549
L-lactate dehydrogenase A chain	LDHA	P00338	20600.90	1.20	1.00	A549
L-lactate dehydrogenase B chain	LDHB	P07195	20919.42	1.72	1.00	A549
Lactoylglutathione lyase	GLO1	Q04760	1428.86	4.22	1.00	A549
Lamina-associated polypeptide 2_ isoform alpha	TMPO	P42166	1638.84	-	-	A549/CDDP
Macrophage migration inhibitory factor	MIF	P14174	25074.88	2.34	1.00	A549
Major vault protein	MVP	Q14764	1132.12	3.22	1.00	A549
Malate dehydrogenase_cytoplasmic	MDH1	P40925	1735.06	-	-	A549/CDDP
Malate dehydrogenase_mitochondrial	MDH2	P40926	16495.98	2.56	1.00	A549
Microsomal glutathione S-transferase 1	MGST1	P10620	2141.82	-	-	A549
Moesin	MSN	P26038	1321.98	-	-	A549/CDDP
Myosin light polypeptide 6	MYL6	G8JLA2	1865.80	-	-	A549
Myosin-9	MYH9	P35579	777.51	-	-	A549/CDDP
NADPH--cytochrome P450 reductase	POR	P16435	870.10	-	-	A549
NADPH:adrenodoxin oxidoreductase_mitochondrial	FDXR	P22570	1296.29	0.95	0.43	-
Neutral alpha-glucosidase AB	GANAB	F5H6X6	862.83	-	-	A549

Nicotinamide N-methyltransferase	NNMT	P40261	4745.17	3.52	1.00	A549
Nicotinamide phosphoribosyltransferase	NAMPT	P43490	4020.73	1.26	1.00	A549
Nuclear factor of-activated T-cells 5	NFAT5	H3BP21	2385.66	-	-	A549/CDDP
Nuclease-sensitive element-binding protein 1 (Fragment)	YBX1	H0Y449	1367.58	-	-	A549/CDDP
Nucleolar and coiled-body phosphoprotein 1	NOLC1	S4R341	2320.54	-	-	A549/CDDP
Nucleolin	NCL	P19338	1387.59	-	-	A549/CDDP
Nucleophosmin	NPM1	P06748	8147.96	0.95	0.00	A549/CDDP
Nucleoside diphosphate kinase	NME1-NME2	Q32Q12	2781.09	3.13	1.00	A549
Ornithine aminotransferase_mitochondrial	OAT	P04181	1109.45	-	-	A549
PDZ and LIM domain protein 1	PDLIM1	O00151	1660.00	-	-	A549
Peptidyl-prolyl cis-trans isomerase A	PPIA	P62937	32242.34	1.79	1.00	A549
Peptidyl-prolyl cis-trans isomerase B	PPIB	P23284	3398.99	3.35	1.00	A549
Peptidyl-prolyl cis-trans isomerase FKBP1A	FKBP1A	P62942	1003.11	-	-	A549/CDDP
Peptidyl-prolyl cis-trans isomerase FKBP4	FKBP4	Q02790	1332.70	-	-	A549/CDDP
Perilipin-3	PLIN3	O60664	1197.33	-	-	A549/CDDP
Peroxiredoxin-1	PRDX1	Q06830	10369.73	2.53	1.00	A549
Peroxiredoxin-4	PRDX4	Q13162	1513.33	-	-	A549/CDDP
Peroxiredoxin-5_mitochondrial	PRDX5	P30044	5435.41	2.92	1.00	A549
Peroxiredoxin-6	PRDX6	P30041	1892.71	4.53	1.00	A549
Peroxisomal multifunctional enzyme type 2	HSD17B4	P51659	1524.74	-	-	A549
Phosphatidylethanolamine-binding protein 1	PEBP1	P30086	2015.04	3.03	1.00	A549
Phosphoglucosmutase-1	PGM1	P36871	2100.78	2.77	1.00	A549
Phosphoglycerate kinase 1	PGK1	P00558	6612.81	2.86	1.00	A549
Phosphoglycerate mutase 1	PGAM1	P18669	12065.18	2.64	1.00	A549
Plastin-3	PLS3	P13797	2472.04	2.27	1.00	A549
Plectin	PLEC	Q15149	937.47	-	-	A549/CDDP
Polypyrimidine tract-binding protein 1	PTBP1	P26599	17974.43	1.31	1.00	A549
Polypyrimidine tract-binding protein 3	PTBP3	O95758	1759.77	-	-	A549/CDDP

Polyubiquitin-C (Fragment)	UBC	F5H6Q2	9778.59	-	-	A549/CDDP
Pre-mRNA-processing factor 19	PRPF19	Q9UMS4	1329.80	-	-	A549/CDDP
Profilin-1	PFN1	P07737	15102.87	1.14	1.00	A549
Prohibitin	PHB	P35232	3510.62	1.92	1.00	A549
Proliferating cell nuclear antigen	PCNA	P12004	12391.33	1.17	1.00	A549
Prosaposin	PSAP	P07602	3524.15	-	-	A549/CDDP
Prostaglandin E synthase 3	PTGES3	A0A087WYT3	2946.83	-	-	A549/CDDP
Prostaglandin reductase 1	PTGR1	Q14914	3206.07	3.63	1.00	A549
Proteasome activator complex subunit 2	PSME2	H0YM70	2543.65	-	-	A549/CDDP
Proteasome subunit alpha type	PSMA2	A0A024RA52	1143.41	-	-	A549
Proteasome subunit beta type (Fragment)	PSMA4	H0YKT8	1489.17	-	-	A549/CDDP
Proteasome subunit beta type-1	PSMB1	P20618	1858.38	-	-	A549
Protein deglycase DJ-1	PARK7	Q99497	7490.02	2.58	1.00	A549
Protein disulfide-isomerase	P4HB	P07237	12779.17	2.48	1.00	A549
Protein disulfide-isomerase A3	PDIA3	P30101	4763.27	4.22	1.00	A549
Protein disulfide-isomerase A4	PDIA4	P13667	1430.53	2.80	1.00	A549
Protein disulfide-isomerase A6	PDIA6	Q15084	8144.39	3.42	1.00	A549
Protein preY_mitochondrial	PYURF	Q96I23	2303.76	-	-	A549/CDDP
Protein S100 (Fragment)	S100A6	R4GN98	1285.13	-	-	A549/CDDP
Protein S100-A10	S100A10	P60903	2320.70	6.36	1.00	A549
Protein S100-A11	S100A11	P31949	19396.29	3.71	1.00	A549
Protein-glutamine gamma-glutamyltransferase 2	TGM2	P21980	7127.53	1.72	1.00	A549
Protein-L-isoaspartate(D-aspartate) O-methyltransferase	PCMT1	F6S8N6	1191.09	-	-	A549
Putative elongation factor 1-alpha-like 3	EEF1A1P5	Q5VTE0	23071.31	1.04	1.00	A549
Pyridoxal kinase	PDXK	O00764	3261.09	-	-	A549/CDDP
Pyruvate kinase PKM	PKM	P14618	29069.33	3.19	1.00	A549
Quinone oxidoreductase	CRYZ	Q08257	3662.09	-	-	A549
Rab GDP dissociation inhibitor beta	GDI2	P50395	5975.07	4.01	1.00	A549

Radixin	RDX	P35241	1273.63	-	-	A549
Ras GTPase-activating-like protein IQGAP1	IQGAP1	P46940	1850.76	1.84	1.00	A549
Receptor of-activated protein C kinase 1	RACK1	J3KPE3	788.18	-	-	A549/CDDP
Reticulon-4	RTN4	Q9NQC3	776.60	-	-	A549/CDDP
Retinal dehydrogenase 1	ALDH1A1	P00352	35496.59	5.21	1.00	A549
Rho GDP-dissociation inhibitor 1	ARHGDI1	J3QQX2	2320.40	2.51	1.00	A549
Ribonuclease inhibitor	RNH1	P13489	3143.41	2.12	1.00	A549
S-formylglutathione hydrolase	ESD	X6RA14	1589.46	-	-	A549
Sepiapterin reductase	SPR	P35270	1733.86	4.30	1.00	A549
Serine/threonine-protein phosphatase 2A activator (Fragment)	PTPA	Q5T948	2629.19	-	-	A549/CDDP
Serpin H1	SERPINH1	P50454	3894.59	-	-	A549
Serum albumin (Fragment)	ALB	H0YA55	792.88	-	-	A549/CDDP
Sideroflexin-1	SFXN1	Q9H9B4	6017.82	3.39	1.00	A549
Small nuclear ribonucleoprotein E	SNRPE	P62304	1714.72	-	-	A549/CDDP
Small nuclear ribonucleoprotein Sm D1	SNRPD1	J3QLI9	13351.88	1.77	1.00	A549
Spliceosome RNA helicase DDX39B	DDX39B	Q13838	948.77	-	-	A549/CDDP
Splicing factor U2AF 65 kDa subunit	U2AF2	P26368	4859.77	0.44	0.00	A549/CDDP
Splicing factor_ proline- and glutamine-rich	SFPQ	P23246	1251.97	-	-	A549/CDDP
Stomatin-like protein 2_ mitochondrial	STOML2	Q9UJZ1	9450.80	2.44	1.00	A549
Stress-70 protein_ mitochondrial	HSPA9	P38646	5041.43	1.95	1.00	A549
Stress-induced-phosphoprotein 1	STIP1	P31948	1089.04	-	-	A549/CDDP
SUMO-activating enzyme subunit 1	SAE1	Q9UBE0	2106.56	-	-	A549/CDDP
Superoxide dismutase [Cu-Zn]	SOD1	P00441	8846.47	2.01	1.00	A549
T-complex protein 1 subunit alpha	TCP1	P17987	1241.71	2.14	1.00	A549
T-complex protein 1 subunit beta	CCT2	P78371	2390.36	-	-	A549
T-complex protein 1 subunit delta	CCT4	P50991	7327.31	3.67	1.00	A549
T-complex protein 1 subunit epsilon	CCT5	P48643	2615.86	-	-	A549
T-complex protein 1 subunit gamma	CCT3	P49368	1705.68	-	-	A549

Talin-1	TLN1	Q9Y490	2047.29	1.58	1.00	A549
Thioredoxin	TXN	P10599	2030.48	2.14	1.00	A549
Thioredoxin reductase 1_ cytoplasmic	TXNRD1	A0A087WSW9	5958.18	2.46	1.00	A549
Thioredoxin-dependent peroxide reductase_ mitochondrial	PRDX3	P30048	5899.13	3.78	1.00	A549
Transaldolase	TALDO1	F2Z393	2915.81	-	-	A549/CDDP
Transcription factor BTF3	BTF3	P20290	4082.76	-	-	A549
Transgelin-2	TAGLN2	P37802	15695.73	-	-	A549/CDDP
Transitional endoplasmic reticulum ATPase	VCP	P55072	3902.94	2.53	1.00	A549
Transketolase	TKT	P29401	23749.47	2.48	1.00	A549
Transmembrane emp24 domain-containing protein 9	TMED9	Q9BVK6	2582.50	-	-	A549/CDDP
Trifunctional enzyme subunit alpha_ mitochondrial	HADHA	P40939	1159.91	4.10	1.00	A549
Triosephosphate isomerase	TPI1	P60174	29488.05	2.14	1.00	A549
Tubulin alpha-1B chain	TUBA1B	P68363	12114.35	1.86	1.00	A549
Tubulin beta chain	TUBB	P07437	32065.27	1.86	1.00	A549
Tubulin beta-3 chain	TUBB3	Q13509	1110.24	1.84	1.00	A549
Tubulin beta-4B chain	TUBB4B	P68371	3724.57	3.78	1.00	A549
Ubiquilin-1	UBQLN1	Q9UMX0	2064.87	-	-	A549/CDDP
Ubiquitin carboxyl-terminal hydrolase isozyme L1	UCHL1	P09936	5440.01	1.75	1.00	A549
Ubiquitin-40S ribosomal protein S27a	RPS27A	P62979	11788.96	-	-	A549
Ubiquitin-conjugating enzyme E2 N	UBE2N	P61088	4614.44	-	-	A549/CDDP
Ubiquitin-like modifier-activating enzyme 1	UBA1	P22314	3376.13	1.93	1.00	A549
UDP-glucose 6-dehydrogenase	UGDH	O60701	6934.43	2.80	1.00	A549
Uncharacterized protein	N/A	A0A1B0GU92	2389.41	-	-	A549
UV excision repair protein RAD23 homolog A	RAD23A	P54725	2542.46	-	-	A549/CDDP
Very-long-chain 3-oxoacyl-CoA reductase	HSD17B12	Q53GQ0	1360.96	-	-	A549
Vesicle-associated membrane protein-associated protein A	VAPA	Q9P0L0	1401.82	-	-	A549/CDDP
Vimentin	VIM	P08670	1418.23	2.10	1.00	A549

Vinculin	VCL	P18206	1009.60	2.22	1.00	A549
Voltage-dependent anion-selective channel protein 1	VDAC1	P21796	1866.67	2.36	1.00	A549
X-ray repair cross-complementing protein 5	XRCC5	P13010	3189.08	2.34	1.00	A549
X-ray repair cross-complementing protein 6	XRCC6	P12956	2360.83	-	-	A549
Zinc finger protein 331 (Fragment)	ZNF331	D6RH27	4422.31	-	-	A549
Zinc finger protein 90	ZNF90	A0A087WZ27	1705.61	-	-	A549/CDDP

N/A, not applicable

Supplementary Table 2: Functional annotation clustering and gene-term enrichment analysis for proteins found A) upregulated and B) downregulated in A549/CDDP cells in comparison to A549 cells.

S2A Table Functional annotation clustering and gene-term enrichment analysis for proteins found upregulated in A549/CDDP cells in comparison to A549 cells.

Annotation Cluster 1	Annotation Cluster 2	Count	%	PValue	Column5	Column6	Column7	Column8	Column9	Column10	Column11	Column12	Column13
Category	Term				Genes	Genes	List Total	Pop Hits	Fold Enrichment	Benferroni	Benferroni	Benferroni	FDR
GOTERM_BP_DIRECT	GO:0098641:cadherin binding involved in cell-cell adhesion	14	19.178082	1.778082	3.71201951289248E-10	AUDOA, RTM4, CAST, VAPA, RPL24, SFN, CLIC1, MYH9, TAGLN2, RACK1, BAG3, PINK3, TMPO, PLEC	73	290	1.68182775193518	5.52131996116298E-8	2.761060426746064E-8	3.17E-09	
GOTERM_BP_DIRECT	GO:0005951:cell-cell adhesion junction	12	16.498395	1.6498395	3.71201951289248E-10	AUDOA, RTM4, CAST, VAPA, RPL24, SFN, CLIC1, MYH9, TAGLN2, RACK1, BAG3, PINK3, TMPO, PLEC	73	323	1.68182775193518	7.45517460937623E-8	2.4752715951559259E-8	4.6337E-09	
GOTERM_BP_DIRECT	GO:0008603:cell-cell adhesion molecule	14	19.483835	1.6498395	3.71201951289248E-10	AUDOA, RTM4, CAST, VAPA, RPL24, SFN, CLIC1, MYH9, TAGLN2, RACK1, BAG3, PINK3, TMPO, PLEC	73	271	1.68182775193518	1.198484843185838E-5	1.198484843185838E-5	2.9305E-09	
Annotation Cluster 2	Enrichment Score: 3.02647397262263												
GOTERM_BP_DIRECT	GO:0070347:RNA binding	13	17.808219	1.7808219	3.056491960292489E-6	SFQ2, UZAF2, DDX39B, RPL8, NPM1, HSP90, PTBP3, RPL11, SNRPE, NCL, YBX1, HNRNPU	73	665	5.511423991039415	5.31689020608949E-4	5.90905267948468E-5	3.74344E-05	
GOTERM_BP_DIRECT	GO:003373:RNA binding	13	17.808219	1.7808219	3.056491960292489E-6	SFQ2, UZAF2, DDX39B, RPL8, NPM1, HSP90, PTBP3, RPL11, SNRPE, NCL, YBX1, HNRNPU	73	647	5.490805240380830	6.8844020428418E-4	1.72091507621151E-4	3.95344E-05	
UP_NEWWORDS	SFQ2	6	8.1017808219	1.7808219	3.056491960292489E-6	SFQ2, UZAF2, DDX39B, RPL8, NPM1, HSP90, PTBP3, RPL11, SNRPE, NCL, YBX1, HNRNPU	73	177	13.195384876876538	0.014315316090354572	0.0012040511819216249	0.000171745	
GOTERM_BP_DIRECT	GO:0008388:mRNA splicing, via spliceosome	6	8.1017808219	1.7808219	3.056491960292489E-6	SFQ2, UZAF2, DDX39B, RPL8, NPM1, HSP90, PTBP3, RPL11, SNRPE, NCL, YBX1, HNRNPU	73	222	7.25311612988284858	2.02110882311568582	0.05488255671290904	0.00515024	
GOTERM_BP_DIRECT	GO:0070343:cellular RNA metabolic process	4	5.47945205	1.7945205	0.025132984868816475	PRPF19, UZAF2, DDX39B, SNRPE, YBX1, HNRNPU	73	26	26.5412227608004	0.9651554347848946	0.13973847066710443	0.078386417	
GOTERM_BP_DIRECT	GO:0070343:cellular RNA metabolic process	4	5.47945205	1.7945205	0.025132984868816475	PRPF19, UZAF2, DDX39B, SNRPE, YBX1, HNRNPU	73	92	10.54407980940363	0.6859903662795129	0.05366469833850564	0.07002024	
KEGG_PATHWAY	hsa03040:Spliceosome	5	6.8493150684931505	0.01163689070241498	PRPF19, UZAF2, DDX39B, SNRPE, HNRNPU		47	133	5.502319628859382	0.777265007804622	0.351497734107759	1.24069186	
GOTERM_BP_DIRECT	GO:0006349:termination of RNA polymerase II transcription	3	4.1055890410589	0.030808163917060212	UZAF2, DDX39B, SNRPE		64	64	10.782334266575342	0.999999927649991	0.41465416673394195	0.370018113	
GOTERM_BP_DIRECT	GO:0005681:spliceosomal complex	3	4.1055890410589	0.030808163917060212	UZAF2, DDX39B, SNRPE		94	1824	7.967356458437775	0.999825505278788	0.33463246695982994	0.496727448	
GOTERM_BP_DIRECT	GO:0016077:nuclear speck	3	4.1055890410589	0.030808163917060212	PRPF19, UZAF2, DDX39B		73	201	13.7480773974607233	1.0	0.6969072733957398	0.137076921	
Annotation Cluster 4	Enrichment Score: 2.83374023468685												
UP_NEWWORDS	Ribonucleoprotein	8	10.9589041058904	1.7808219	3.056491960292489E-6	RPS28, RPL8, RPS13, SNRNP, RPL24, RPL11, SNRPE, HNRNPU	73	296	7.639770455868893	0.03575975991145805	0.001248809501687334	0.000618463	
GOTERM_BP_DIRECT	GO:0005575:structural constituent of ribosome	7	9.5890410589041	1.6498395	3.71201951289248E-10	RPS28, RPL8, RPS13, SNRNP, RPL24, RPL11	73	222	12.92533849894964	0.081545074530092	0.01971379018579497	0.00462057	
GOTERM_BP_DIRECT	GO:0005575:structural constituent of ribosome	7	9.5890410589041	1.6498395	3.71201951289248E-10	RPS28, RPL8, RPS13, SNRNP, RPL24, RPL11	73	86	12.92533849894964	0.081545074530092	0.01971379018579497	0.00462057	
GOTERM_BP_DIRECT	GO:0005575:structural constituent of ribosome	7	9.5890410589041	1.6498395	3.71201951289248E-10	RPS28, RPL8, RPS13, SNRNP, RPL24, RPL11	73	222	12.92533849894964	0.081545074530092	0.01971379018579497	0.00462057	
GOTERM_BP_DIRECT	GO:0005575:structural constituent of ribosome	7	9.5890410589041	1.6498395	3.71201951289248E-10	RPS28, RPL8, RPS13, SNRNP, RPL24, RPL11	73	222	12.92533849894964	0.081545074530092	0.01971379018579497	0.00462057	
GOTERM_BP_DIRECT	GO:0005575:structural constituent of ribosome	7	9.5890410589041	1.6498395	3.71201951289248E-10	RPS28, RPL8, RPS13, SNRNP, RPL24, RPL11	73	222	12.92533849894964	0.081545074530092	0.01971379018579497	0.00462057	
GOTERM_BP_DIRECT	GO:0005575:structural constituent of ribosome	7	9.5890410589041	1.6498395	3.71201951289248E-10	RPS28, RPL8, RPS13, SNRNP, RPL24, RPL11	73	222	12.92533849894964	0.081545074530092	0.01971379018579497	0.00462057	
GOTERM_BP_DIRECT	GO:0005575:structural constituent of ribosome	7	9.5890410589041	1.6498395	3.71201951289248E-10	RPS28, RPL8, RPS13, SNRNP, RPL24, RPL11	73	222	12.92533849894964	0.081545074530092	0.01971379018579497	0.00462057	
GOTERM_BP_DIRECT	GO:0005575:structural constituent of ribosome	7	9.5890410589041	1.6498395	3.71201951289248E-10	RPS28, RPL8, RPS13, SNRNP, RPL24, RPL11	73	222	12.92533849894964	0.081545074530092	0.01971379018579497	0.00462057	
GOTERM_BP_DIRECT	GO:0005575:structural constituent of ribosome	7	9.5890410589041	1.6498395	3.71201951289248E-10	RPS28, RPL8, RPS13, SNRNP, RPL24, RPL11	73	222	12.92533849894964	0.081545074530092	0.01971379018579497	0.00462057	
GOTERM_BP_DIRECT	GO:0005575:structural constituent of ribosome	7	9.5890410589041	1.6498395	3.71201951289248E-10	RPS28, RPL8, RPS13, SNRNP, RPL24, RPL11	73	222	12.92533849894964	0.081545074530092	0.01971379018579497	0.00462057	
GOTERM_BP_DIRECT	GO:0005575:structural constituent of ribosome	7	9.5890410589041	1.6498395	3.71201951289248E-10	RPS28, RPL8, RPS13, SNRNP, RPL24, RPL11	73	222	12.92533849894964	0.081545074530092	0.01971379018579497	0.00462057	
GOTERM_BP_DIRECT	GO:0005575:structural constituent of ribosome	7	9.5890410589041	1.6498395	3.71201951289248E-10	RPS28, RPL8, RPS13, SNRNP, RPL24, RPL11	73	222	12.92533849894964	0.081545074530092	0.01971379018579497	0.00462057	
GOTERM_BP_DIRECT	GO:0005575:structural constituent of ribosome	7	9.5890410589041	1.6498395	3.71201951289248E-10	RPS28, RPL8, RPS13, SNRNP, RPL24, RPL11	73	222	12.92533849894964	0.081545074530092	0.01971379018579497	0.00462057	
GOTERM_BP_DIRECT	GO:0005575:structural constituent of ribosome	7	9.5890410589041	1.6498395	3.71201951289248E-10	RPS28, RPL8, RPS13, SNRNP, RPL24, RPL11	73	222	12.92533849894964	0.081545074530092	0.01971379018579497	0.00462057	
GOTERM_BP_DIRECT	GO:0005575:structural constituent of ribosome	7	9.5890410589041	1.6498395	3.71201951289248E-10	RPS28, RPL8, RPS13, SNRNP, RPL24, RPL11	73	222	12.92533849894964	0.081545074530092	0.01971379018579497	0.00462057	
GOTERM_BP_DIRECT	GO:0005575:structural constituent of ribosome	7	9.5890410589041	1.6498395	3.71201951289248E-10	RPS28, RPL8, RPS13, SNRNP, RPL24, RPL11	73	222	12.92533849894964	0.081545074530092	0.01971379018579497	0.00462057	
GOTERM_BP_DIRECT	GO:0005575:structural constituent of ribosome	7	9.5890410589041	1.6498395	3.71201951289248E-10	RPS28, RPL8, RPS13, SNRNP, RPL24, RPL11	73	222	12.92533849894964	0.081545074530092	0.01971379018579497	0.00462057	
GOTERM_BP_DIRECT	GO:0005575:structural constituent of ribosome	7	9.5890410589041	1.6498395	3.71201951289248E-10	RPS28, RPL8, RPS13, SNRNP, RPL24, RPL11	73	222	12.92533849894964	0.081545074530092	0.01971379018579497	0.00462057	
GOTERM_BP_DIRECT	GO:0005575:structural constituent of ribosome	7	9.5890410589041	1.6498395	3.71201951289248E-10	RPS28, RPL8, RPS13, SNRNP, RPL24, RPL11	73	222	12.92533849894964	0.081545074530092	0.01971379018579497	0.00462057	
GOTERM_BP_DIRECT	GO:0005575:structural constituent of ribosome	7	9.5890410589041	1.6498395	3.71201951289248E-10	RPS28, RPL8, RPS13, SNRNP, RPL24, RPL11	73	222	12.92533849894964	0.081545074530092	0.01971379018579497	0.00462057	
GOTERM_BP_DIRECT	GO:0005575:structural constituent of ribosome	7	9.5890410589041	1.6498395	3.71201951289248E-10	RPS28, RPL8, RPS13, SNRNP, RPL24, RPL11	73	222	12.92533849894964	0.081545074530092	0.01971379018579497	0.00462057	
GOTERM_BP_DIRECT	GO:0005575:structural constituent of ribosome	7	9.5890410589041	1.6498395	3.71201951289248E-10	RPS28, RPL8, RPS13, SNRNP, RPL24, RPL11	73	222	12.92533849894964	0.081545074530092	0.01971379018579497	0.00462057	
GOTERM_BP_DIRECT	GO:0005575:structural constituent of ribosome	7	9.5890410589041	1.6498395	3.71201951289248E-10	RPS28, RPL8, RPS13, SNRNP, RPL24, RPL11	73	222	12.92533849894964	0.081545074530092	0.01971379018579497	0.00462057	
GOTERM_BP_DIRECT	GO:0005575:structural constituent of ribosome	7	9.5890410589041	1.6498395	3.71201951289248E-10	RPS28, RPL8, RPS13, SNRNP, RPL24, RPL11	73	222	12.92533849894964	0.081545074530092	0.01971379018579497	0.00462057	
GOTERM_BP_DIRECT	GO:0005575:structural constituent of ribosome	7	9.5890410589041	1.6498395	3.71201951289248E-10	RPS28, RPL8, RPS13, SNRNP, RPL24, RPL11	73	222	12.92533849894964	0.081545074530092	0.01971379018579497	0.00462057	
GOTERM_BP_DIRECT	GO:0005575:structural constituent of ribosome	7	9.5890410589041	1.6498395	3.71201951289248E-10	RPS28, RPL8, RPS13, SNRNP, RPL24, RPL11	73	222	12.92533849894964	0.081545074530092	0.01971379018579497	0.00462057	
GOTERM_BP_DIRECT	GO:0005575:structural constituent of ribosome	7	9.5890410589041	1.6498395	3.71201951289248E-10	RPS28, RPL8, RPS13, SNRNP, RPL24, RPL11	73	222	12.92533849894964	0.081545074530092	0.01971379018579497	0.00462057	
GOTERM_BP_DIRECT	GO:0005575:structural constituent of ribosome	7	9.5890410589041	1.6498395	3.71201951289248E-10	RPS28, RPL8, RPS13, SNRNP, RPL24, RPL11	73	222	12.92533849894964	0.081545074530092	0.01971379018579497	0.00462057	
GOTERM_BP_DIRECT	GO:0005575:structural constituent of ribosome	7	9.5890410589041	1.6498395	3.71201951289248E-10	RPS28, RPL8, RPS13, SNRNP, RPL24, RPL11	73	222	12.92533849894964	0.081545074530092	0.01971379018579497	0.00462057	
GOTERM_BP_DIRECT	GO:0005575:structural constituent of ribosome	7	9.5890410589041	1.6498395	3.71201951289248E-10	RPS28, RPL8, RPS13, SNRNP, RPL24, RPL11	73	222	12.92533849894964	0.081545074530092	0.01971379018579497	0.00462057	
GOTERM_BP_DIRECT	GO:0005575:structural constituent of ribosome	7	9.5890410589041	1.6498395	3.71201951289248E-10	RPS28, RPL8, RPS13, SNRNP, RPL24, RPL11	73	222	12.92533849894964	0.081545074530092	0.01971379018579497	0.00462057	
GOTERM_BP_DIRECT	GO:0005575:structural constituent of ribosome	7	9.5890410589041	1.6498395	3.71201951289248E-10	RPS28, RPL8, RPS13, SNRNP, RPL24, RPL11	73	222	12.92533849894964	0.081545074530092	0.01971379018579497	0.00462057	
GOTERM_BP_DIRECT	GO:0005575:structural constituent of ribosome	7	9.5890410589041	1.6498395	3.71201951289248E-10	RPS28, RPL8, RPS13, SNRNP, RPL24, RPL11	73	222	12.92533849894964	0.081545074530092	0.01971379018579497	0.00462057	
GOTERM_BP_DIRECT	GO:0005575:structural constituent of ribosome	7	9.5890410589041	1.6498395	3.71201951289248E-10	RPS28, RPL8, RPS13, SNRNP, RPL24, RPL11	73	222	12.92533849894964	0.081545074530092	0.01971379018579497	0.00462057	
GOTERM_BP_DIRECT	GO:0005575:structural constituent of ribosome	7	9.5890410589041	1.6498395	3.71201951289248E-10								

UP_KEYWORDS	Count	%	PValue	Genes	List Total	Pop Hits	Fold Enrichment	Benjamini	FDR
UP_KEYWORDS	4	5.47945205479452	0.28903324177047734	GOT2, PVUFR, ATP5O, HADH	73	536	2.10364690247931	1.0	0.834483300346771
UP_KEYWORDS	6	8.21917808219178	0.832957929716335	GOT2, SLC25A4, FRBP4, PVUFR, ATP5O, HADH	73	1119	1.5116970876638878	1.0	0.8718216889264279
UP_SEQ_FEATURE	3	4.10558904105589	0.5115469370470207	GOT2, ATP5O, HADH	72	482	1.734333386563677	1.0	0.9999973111186421
Annotation Cluster 15									
Category	Count	%	PValue	Genes	List Total	Pop Hits	Fold Enrichment	Benjamini	FDR
Term									
GOTERM_CC_DIRECT	9	12.32876712328767	0.02007572729458331	RTN4, COPA, VAPA, FRBP4, PVUFR, FRBP1A, RPN2, TMPO, TMED9	73	822	2.6064901630486603	0.9826741691981336	0.1547550054174875
GOTERM_CC_DIRECT	8	10.958990410958904	0.0468189033601083	CAS1, RTM4, VAPA, ALB, SYNCINP, RPN2, UBOLINA, TMED9	73	824	2.42027735425925	0.998892946187428	0.278560251248853
UP_SEQ_FEATURE	4	5.47945205479452	0.21328951981093558	RTN4, RPN2, TMPO, TMED9	72	450	2.4769135807469133	1.0	0.9998137173088513
UP_KEYWORDS	6	8.21917808219178	0.5115469370470207	RTN4, VAPA, SYNCINP, RPN2, UBOLINA, TMED9	73	1067	1.58539298123734	1.0	0.838484163606597
UP_KEYWORDS	20	27.307160373071603	0.931232049171268	RPN4, ALDOA, COPA, S100A6, VAPA, SLC25A4, CAL2, FRBP4, CLIC1, CLIC2, TMED9, UBOLINA, MICAL1, GOT2, PIRNA, NEAT5, ATP5O, RPN2, TMPO, WDR5	73	2104	0.7524193709377957	1.0	0.909973851545453
UP_KEYWORDS	11	15.064848150648481	0.898154502819448	ALDOA, RTM4, VAPA, SLC25A4, CAL2, NEAT5, FRBP4, CLIC1, RPN2, TMPO, TMED9	73	563	0.525046626323232	1.0	0.99999938044371
UP_KEYWORDS	11	15.064848150648481	0.898154502819448	ALDOA, RTM4, VAPA, SLC25A4, CAL2, NEAT5, FRBP4, CLIC1, RPN2, TMPO, TMED9	73	565	0.5487669671283784	1.0	0.999999392486864
UP_SEQ_FEATURE	5	6.8493150684931505	0.899468425630012	RTN4, VAPA, CAL2, RPN2, TMED9	72	3456	0.40313448636831276	1.0	1.0
UP_KEYWORDS	10	13.689630136896301	0.999419857321745	RTN4, VAPA, SLC25A4, PSAP, CAL2, NEAT5, FRBP4, RPN2, TMPO, TMED9	73	5163	0.483547639287979	1.0	0.9999959959999997
UP_SEQ_FEATURE	8	10.958990410958904	0.9995629248189227	RTN4, VAPA, SLC25A4, CAL2, CLIC1, RPN2, TMPO, TMED9	72	5056	0.44096282895217995	1.0	1.0
Annotation Cluster 16									
Category	Count	%	PValue	Genes	List Total	Pop Hits	Fold Enrichment	Benjamini	FDR
Term									
GOTERM_MF_DIRECT	4	5.47945205479452	0.8311121623931943	ACTB, ZNF90, NFAT5, YBX1	73	355	2.605585215126374	1.0	0.8965126040370899
UP_KEYWORDS	8	10.958990410958904	0.384565494445159	ZNF90, SFPQ, KHSRP, NEAT5, TMPO, NCL, YBX1, HNRNP1U	73	2050	1.100220514539123	1.0	0.760202053684374
UP_KEYWORDS	3	4.10558904105589	0.67420102530892	SFPQ, NFAT5, YBX1	73	661	1.2795831897548337	1.0	0.8987270394185274
GOTERM_MF_DIRECT	6	8.21917808219178	0.851761315058378	ALB, NPMT, KHSRP, TMPO, YBX1, HNRNP1U	73	474	0.8288407718307948	1.0	0.999995865694435
GOTERM_MF_DIRECT	4	5.47945205479452	0.8628985834453	ZNF90, MEF2B, TMPO, YBX1	73	1479	0.613744921246692	1.0	0.99999909094989
UP_KEYWORDS	5	6.8493150684931505	0.899289272789327	ZNF90, SFPQ, KHSRP, NEAT5, YBX1	73	2504	0.65444434828484662	1.0	0.99999684687762
UP_KEYWORDS	5	6.8493150684931505	0.97451337798944607	ZNF90, SFPQ, KHSRP, NEAT5, YBX1	73	2398	0.5878471285489938	1.0	0.9999971656687658
GOTERM_BP_DIRECT	3	4.10558904105589	0.898608947333871	ZNF90, SFPQ, KHSRP	73	1955	0.352893248302107	1.0	1.0
Annotation Cluster 17									
Category	Count	%	PValue	Genes	List Total	Pop Hits	Fold Enrichment	Benjamini	FDR
Term									
GOTERM_MF_DIRECT	4	5.47945205479452	0.893607602471817	S10DA6, PDK, ZNF90, CAL2	73	1169	0.7912628754232315	1.0	0.9999999607249648
UP_KEYWORDS	4	5.47945205479452	0.914563962176877	PDK, ZNF90, ALB, CAL2	73	2348	0.48029217521178036	1.0	0.9999957868782908
UP_KEYWORDS	7	9.58904109589041	0.892427265606554	S10DA6, PDK, ZNF90, ALB, CAL2, ACLY, CALM1	73	3640	0.5423759747102213	1.0	0.999999804688789
Annotation Cluster 18									
Category	Count	%	PValue	Genes	List Total	Pop Hits	Fold Enrichment	Benjamini	FDR
Term									
GOTERM_BP_DIRECT	7	9.58904109589041	0.89804109589041	ALB, RBP4, CAL2, NRM1, PRDM4, CLIC1	73	397	0.8999999333512833	1.0	0.9999999333512833
UP_SEQ_FEATURE	5	6.8493150684931505	0.89455604117656	ALB, PSAP, CAL2, PRDM4, CLIC1	72	2924	0.47765458923776586	1.0	1.0
UP_SEQ_FEATURE	6	8.21917808219178	0.995096297159648	ALB, PSAP, CAL2, PRDM4, RPN2, TMED9	72	3346	0.489862303247658	1.0	1.0
UP_KEYWORDS	7	9.58904109589041	0.898286343802203	ST13, ALB, PSAP, CAL2, PRDM4, RPN2, TMED9	73	4160	0.4744639378714436	1.0	0.999999993040236
UP_SEQ_FEATURE	5	6.8493150684931505	0.99908842563680012	RTN4, VAPA, CAL2, RPN2, TMED9	72	3456	0.40313448636831276	1.0	1.0
UP_KEYWORDS	5	6.8493150684931505	0.999976153756064	ALB, PSAP, CAL2, RPN2, TMED9	73	4551	0.3097467466479142	1.0	0.9999959959999997
UP_SEQ_FEATURE	4	5.47945205479452	0.999990529131356	PSAP, CAL2, RPN2, TMED9	72	4234	0.26322525061670078	1.0	1.0

UP_KEYWORDS	Antibiotic	5	2.564102564102564	7.115869696969696	38.46546	195	14	20581	37.694130494392	0.001862674817609145	8.47402449277208E-5	9.31198E-05
GOTERM_BP_DIRECT	GO:0196879 cellular oxidant detoxification	8	4.10256410256410256	1.5973989697000843E-5	PROX6: PRDX3, PRDX5, TXNIP1, PRDX1, PRDX4	195 <td>70</td> <td>16782</td> <td>9.841462501463200</td> <td>0.0219646474376106</td> <td>0.001090114232928283</td> <td>0.000263</td>	70	16782	9.841462501463200	0.0219646474376106	0.001090114232928283	0.000263
UP_SEQ_FEATURE	active site/cysteine sulfenic acid (SOH) intermediate	4	2.051282051282051	1.742746982048317E-5	PROX6: TXN, PROX5, TXNIP1, PROX3, MGST1, PARK7, GSTP1	195 <td>6</td> <td>20683</td> <td>68.3914282051282051</td> <td>0.0292860696725487</td> <td>9.006488826004154E-4</td> <td>0.000257006</td>	6	20683	68.3914282051282051	0.0292860696725487	9.006488826004154E-4	0.000257006
GOTERM_BP_DIRECT	GO:0051927 peroxidase activity	5	2.564102564102564	9.65403320778708E-5	PROX6: PRDX3, PRDX4, PRDX7	195 <td>6</td> <td>16881</td> <td>57.71282051282051</td> <td>0.04175118734691484</td> <td>0.001373655807371178</td> <td>0.000420098</td>	6	16881	57.71282051282051	0.04175118734691484	0.001373655807371178	0.000420098
GOTERM_CC_DIRECT	GO:0005623 cell	5	4.10256410256410256	9.65403320778708E-5	PROX6: PRDX3, PRDX6, ACO1, TXNIP1, PDIM4, PRDX1, VCL	195 <td>100</td> <td>18224</td> <td>7.47651282051282051</td> <td>0.0303268371001837</td> <td>0.0011400106902871522</td> <td>0.001301381</td>	100	18224	7.47651282051282051	0.0303268371001837	0.0011400106902871522	0.001301381
UP_SEQ_FEATURE	domain/interleukin	5	2.564102564102564	2.7841494980791953E-4	PH4B: PHN, PROX5, PROX3, PRDX1	195 <td>33</td> <td>20063</td> <td>15.58896668989868821</td> <td>0.15246678949009746</td> <td>0.001096776059621786</td> <td>0.000490959</td>	33	20063	15.58896668989868821	0.15246678949009746	0.001096776059621786	0.000490959
INTERPRO	IPRO00866:Alkyl hydroperoxide reductase subunit C/Thiol specific	3	1.5384615384615385	0.00016647871467165138	PROX6: PRDX3, PRDX1	195 <td>5</td> <td>18559</td> <td>57.104615384615385</td> <td>0.44104344129936346</td> <td>0.03015103149256374</td> <td>0.015413321</td>	5	18559	57.104615384615385	0.44104344129936346	0.03015103149256374	0.015413321
GOTERM_BP_DIRECT	GO:0003719 peroxidase, C-terminal	3	1.5384615384615385	0.00016647871467165138	PROX6: PRDX3, PRDX1	195 <td>5</td> <td>18559</td> <td>57.104615384615385</td> <td>0.44104344129936346</td> <td>0.03015103149256374</td> <td>0.015413321</td>	5	18559	57.104615384615385	0.44104344129936346	0.03015103149256374	0.015413321
GOTERM_BP_DIRECT	GO:0003719 peroxidase, N-terminal	3	1.5384615384615385	0.00016647871467165138	PROX6: PRDX3, PRDX1	195 <td>5</td> <td>18559</td> <td>57.104615384615385</td> <td>0.44104344129936346</td> <td>0.03015103149256374</td> <td>0.015413321</td>	5	18559	57.104615384615385	0.44104344129936346	0.03015103149256374	0.015413321
GOTERM_BP_DIRECT	GO:0003719 peroxidase, C-terminal	3	1.5384615384615385	0.00016647871467165138	PROX6: PRDX3, PRDX1	195 <td>5</td> <td>18559</td> <td>57.104615384615385</td> <td>0.44104344129936346</td> <td>0.03015103149256374</td> <td>0.015413321</td>	5	18559	57.104615384615385	0.44104344129936346	0.03015103149256374	0.015413321
GOTERM_BP_DIRECT	GO:0003719 peroxidase, N-terminal	3	1.5384615384615385	0.00016647871467165138	PROX6: PRDX3, PRDX1	195 <td>5</td> <td>18559</td> <td>57.104615384615385</td> <td>0.44104344129936346</td> <td>0.03015103149256374</td> <td>0.015413321</td>	5	18559	57.104615384615385	0.44104344129936346	0.03015103149256374	0.015413321
UP_KEYWORDS	Peroxidase	4	2.051282051282051	0.001627844337131217	PROX6: PRDX3, PRDX5, PRDX1	195	25	20581	16.88697435897436	0.3474338082592937	0.0121214149359550778	0.011084856
UP_KEYWORDS	Disulfide bond	25	12.82051282051282051	0.9616578985226911	PDIA3, PDIA6, PROX5, PRDX3, PDIA4, CCT3, CALR, UQCRC1, PRDX1, CANX, ITGB1, PCMT1, GLO1, APEX1, PH4B, S100A11, SLC24A1, SOD1, HSP90B1, PROX6, TXN, PEBP1, TXNIP1, AGR2, PH4B, PDIA3, SLC24A1, SOD1A11, PROX5, PDIA6, CCT3, PRDX3, PDIA4, CALR, SOD1, UQCRC1, ITGB1, CANX, PRDX1, HSP90B1, PROX6, TXN, TXNIP1, PCMT1	195	3434	20581	0.7683720860778859	1.0	0.95960220534950778	1
UP_SEQ_FEATURE	disulfide bond	20	10.256410256410256	0.93819634656898355	CANX, PRDX1, HSP90B1, PROX6, TXN, TXNIP1, PCMT1	195	2917	20063	0.70543341671723824	1.0	1.0	1
Annotation Cluster 13	Enrichment Score: 4.133771541958945											
GOTERM_BP_DIRECT	GO:0006413 Translational initiation	12	6.153846153846154	5.5300466133681087E-7	Genes: RPS15, RPS17, RPS18, RPS19, RPS20, RPS21, RPS22, RPS23, RPS24, RPS25, RPS26, RPS27, RPS28, RPS29, RPS30, RPS31, RPS32, RPS33, RPS34, RPS35, RPS36, RPS37, RPS38, RPS39, RPS40, RPS41, RPS42, RPS43, RPS44, RPS45, RPS46, RPS47, RPS48, RPS49, RPS50, RPS51, RPS52, RPS53, RPS54, RPS55, RPS56, RPS57, RPS58, RPS59, RPS60, RPS61, RPS62, RPS63, RPS64, RPS65, RPS66, RPS67, RPS68, RPS69, RPS70, RPS71, RPS72, RPS73, RPS74, RPS75, RPS76, RPS77, RPS78, RPS79, RPS80, RPS81, RPS82, RPS83, RPS84, RPS85, RPS86, RPS87, RPS88, RPS89, RPS90, RPS91, RPS92, RPS93, RPS94, RPS95, RPS96, RPS97, RPS98, RPS99, RPS100, RPS101, RPS102, RPS103, RPS104, RPS105, RPS106, RPS107, RPS108, RPS109, RPS110, RPS111, RPS112, RPS113, RPS114, RPS115, RPS116, RPS117, RPS118, RPS119, RPS120, RPS121, RPS122, RPS123, RPS124, RPS125, RPS126, RPS127, RPS128, RPS129, RPS130, RPS131, RPS132, RPS133, RPS134, RPS135, RPS136, RPS137, RPS138, RPS139, RPS140, RPS141, RPS142, RPS143, RPS144, RPS145, RPS146, RPS147, RPS148, RPS149, RPS150, RPS151, RPS152, RPS153, RPS154, RPS155, RPS156, RPS157, RPS158, RPS159, RPS160, RPS161, RPS162, RPS163, RPS164, RPS165, RPS166, RPS167, RPS168, RPS169, RPS170, RPS171, RPS172, RPS173, RPS174, RPS175, RPS176, RPS177, RPS178, RPS179, RPS180, RPS181, RPS182, RPS183, RPS184, RPS185, RPS186, RPS187, RPS188, RPS189, RPS190, RPS191, RPS192, RPS193, RPS194, RPS195, RPS196, RPS197, RPS198, RPS199, RPS200, RPS201, RPS202, RPS203, RPS204, RPS205, RPS206, RPS207, RPS208, RPS209, RPS210, RPS211, RPS212, RPS213, RPS214, RPS215, RPS216, RPS217, RPS218, RPS219, RPS220, RPS221, RPS222, RPS223, RPS224, RPS225, RPS226, RPS227, RPS228, RPS229, RPS230, RPS231, RPS232, RPS233, RPS234, RPS235, RPS236, RPS237, RPS238, RPS239, RPS240, RPS241, RPS242, RPS243, RPS244, RPS245, RPS246, RPS247, RPS248, RPS249, RPS250, RPS251, RPS252, RPS253, RPS254, RPS255, RPS256, RPS257, RPS258, RPS259, RPS260, RPS261, RPS262, RPS263, RPS264, RPS265, RPS266, RPS267, RPS268, RPS269, RPS270, RPS271, RPS272, RPS273, RPS274, RPS275, RPS276, RPS277, RPS278, RPS279, RPS280, RPS281, RPS282, RPS283, RPS284, RPS285, RPS286, RPS287, RPS288, RPS289, RPS290, RPS291, RPS292, RPS293, RPS294, RPS295, RPS296, RPS297, RPS298, RPS299, RPS300, RPS301, RPS302, RPS303, RPS304, RPS305, RPS306, RPS307, RPS308, RPS309, RPS310, RPS311, RPS312, RPS313, RPS314, RPS315, RPS316, RPS317, RPS318, RPS319, RPS320, RPS321, RPS322, RPS323, RPS324, RPS325, RPS326, RPS327, RPS328, RPS329, RPS330, RPS331, RPS332, RPS333, RPS334, RPS335, RPS336, RPS337, RPS338, RPS339, RPS340, RPS341, RPS342, RPS343, RPS344, RPS345, RPS346, RPS347, RPS348, RPS349, RPS350, RPS351, RPS352, RPS353, RPS354, RPS355, RPS356, RPS357, RPS358, RPS359, RPS360, RPS361, RPS362, RPS363, RPS364, RPS365, RPS366, RPS367, RPS368, RPS369, RPS370, RPS371, RPS372, RPS373, RPS374, RPS375, RPS376, RPS377, RPS378, RPS379, RPS380, RPS381, RPS382, RPS383, RPS384, RPS385, RPS386, RPS387, RPS388, RPS389, RPS390, RPS391, RPS392, RPS393, RPS394, RPS395, RPS396, RPS397, RPS398, RPS399, RPS400, RPS401, RPS402, RPS403, RPS404, RPS405, RPS406, RPS407, RPS408, RPS409, RPS410, RPS411, RPS412, RPS413, RPS414, RPS415, RPS416, RPS417, RPS418, RPS419, RPS420, RPS421, RPS422, RPS423, RPS424, RPS425, RPS426, RPS427, RPS428, RPS429, RPS430, RPS431, RPS432, RPS433, RPS434, RPS435, RPS436, RPS437, RPS438, RPS439, RPS440, RPS441, RPS442, RPS443, RPS444, RPS445, RPS446, RPS447, RPS448, RPS449, RPS450, RPS451, RPS452, RPS453, RPS454, RPS455, RPS456, RPS457, RPS458, RPS459, RPS460, RPS461, RPS462, RPS463, RPS464, RPS465, RPS466, RPS467, RPS468, RPS469, RPS470, RPS471, RPS472, RPS473, RPS474, RPS475, RPS476, RPS477, RPS478, RPS479, RPS480, RPS481, RPS482, RPS483, RPS484, RPS485, RPS486, RPS487, RPS488, RPS489, RPS490, RPS491, RPS492, RPS493, RPS494, RPS495, RPS496, RPS497, RPS498, RPS499, RPS500, RPS501, RPS502, RPS503, RPS504, RPS505, RPS506, RPS507, RPS508, RPS509, RPS510, RPS511, RPS512, RPS513, RPS514, RPS515, RPS516, RPS517, RPS518, RPS519, RPS520, RPS521, RPS522, RPS523, RPS524, RPS525, RPS526, RPS527, RPS528, RPS529, RPS530, RPS531, RPS532, RPS533, RPS534, RPS535, RPS536, RPS537, RPS538, RPS539, RPS540, RPS541, RPS542, RPS543, RPS544, RPS545, RPS546, RPS547, RPS548, RPS549, RPS550, RPS551, RPS552, RPS553, RPS554, RPS555, RPS556, RPS557, RPS558, RPS559, RPS560, RPS561, RPS562, RPS563, RPS564, RPS565, RPS566, RPS567, RPS568, RPS569, RPS570, RPS571, RPS572, RPS573, RPS574, RPS575, RPS576, RPS577, RPS578, RPS579, RPS580, RPS581, RPS582, RPS583, RPS584, RPS585, RPS586, RPS587, RPS588, RPS589, RPS590, RPS591, RPS592, RPS593, RPS594, RPS595, RPS596, RPS597, RPS598, RPS599, RPS600, RPS601, RPS602, RPS603, RPS604, RPS605, RPS606, RPS607, RPS608, RPS609, RPS610, RPS611, RPS612, RPS613, RPS614, RPS615, RPS616, RPS617, RPS618, RPS619, RPS620, RPS621, RPS622, RPS623, RPS624, RPS625, RPS626, RPS627, RPS628, RPS629, RPS630, RPS631, RPS632, RPS633, RPS634, RPS635, RPS636, RPS637, RPS638, RPS639, RPS640, RPS641, RPS642, RPS643, RPS644, RPS645, RPS646, RPS647, RPS648, RPS649, RPS650, RPS651, RPS652, RPS653, RPS654, RPS655, RPS656, RPS657, RPS658, RPS659, RPS660, RPS661, RPS662, RPS663, RPS664, RPS665, RPS666, RPS667, RPS668, RPS669, RPS670, RPS671, RPS672, RPS673, RPS674, RPS675, RPS676, RPS677, RPS678, RPS679, RPS680, RPS681, RPS682, RPS683, RPS684, RPS685, RPS686, RPS687, RPS688, RPS689, RPS690, RPS691, RPS692, RPS693, RPS694, RPS695, RPS696, RPS697, RPS698, RPS699, RPS700, RPS701, RPS702, RPS703, RPS704, RPS705, RPS706, RPS707, RPS708, RPS709, RPS710, RPS711, RPS712, RPS713, RPS714, RPS715, RPS716, RPS717, RPS718, RPS719, RPS720, RPS721, RPS722, RPS723, RPS724, RPS725, RPS726, RPS727, RPS728, RPS729, RPS730, RPS731, RPS732, RPS733, RPS734, RPS735, RPS736, RPS737, RPS738, RPS739, RPS740, RPS741, RPS742, RPS743, RPS744, RPS745, RPS746, RPS747, RPS748, RPS749, RPS750, RPS751, RPS752, RPS753, RPS754, RPS755, RPS756, RPS757, RPS758, RPS759, RPS760, RPS761, RPS762, RPS763, RPS764, RPS765, RPS766, RPS767, RPS768, RPS769, RPS770, RPS771, RPS772, RPS773, RPS774, RPS775, RPS776, RPS777, RPS778, RPS779, RPS780, RPS781, RPS782, RPS783, RPS784, RPS785, RPS786, RPS787, RPS788, RPS789, RPS790, RPS791, RPS792, RPS793, RPS794, RPS795, RPS796, RPS797, RPS798, RPS799, RPS800, RPS801, RPS802, RPS803, RPS804, RPS805, RPS806, RPS807, RPS808, RPS809, RPS810, RPS811, RPS812, RPS813, RPS814, RPS815, RPS816, RPS817, RPS818, RPS819, RPS820, RPS821, RPS822, RPS823, RPS824, RPS825, RPS826, RPS827, RPS828, RPS829, RPS830, RPS831, RPS832, RPS833, RPS834, RPS835, RPS836, RPS837, RPS838, RPS839, RPS840, RPS841, RPS842, RPS843, RPS844, RPS845, RPS846, RPS847, RPS848, RPS849, RPS850, RPS851, RPS852, RPS853, RPS854, RPS855, RPS856, RPS857, RPS858, RPS859, RPS860, RPS861, RPS862, RPS863, RPS864, RPS865, RPS866, RPS867, RPS868, RPS869, RPS870, RPS871, RPS872, RPS873, RPS874, RPS875, RPS876, RPS877, RPS878, RPS879, RPS880, RPS881, RPS882, RPS883, RPS884, RPS885, RPS886, RPS887, RPS888, RPS889, RPS890, RPS891, RPS892, RPS893, RPS894, RPS895, RPS896, RPS897, RPS898, RPS899, RPS900, RPS901, RPS902, RPS903, RPS904, RPS905, RPS906, RPS907, RPS908, RPS909, RPS910, RPS911, RPS912, RPS913, RPS914, RPS915, RPS916, RPS917, RPS918, RPS919, RPS920, RPS921, RPS922, RPS923, RPS924, RPS925, RPS926, RPS927, RPS928, RPS929, RPS930, RPS931, RPS932, RPS933, RPS934, RPS935, RPS936, RPS937, RPS938, RPS939, RPS940, RPS941, RPS942, RPS943, RPS944, RPS945, RPS946, RPS947, RPS948, RPS949, RPS950, RPS951, RPS952, RPS953, RPS954, RPS955, RPS956, RPS957, RPS958, RPS959, RPS960, RPS961, RPS962, RPS963, RPS964, RPS965, RPS966, RPS967, RPS968, RPS969, RPS970, RPS971, RPS972, RPS973, RPS974, RPS975, RPS976, RPS977, RPS978, RPS979, RPS980, RPS981, RPS982, RPS983, RPS984, RPS985, RPS986, RPS987, RPS988, RPS989, RPS990, RPS991, RPS992, RPS993, RPS994, RPS995, RPS996, RPS997, RPS998, RPS999, RPS1000, RPS1001, RPS1002, RPS1003, RPS1004, RPS1005, RPS1006, RPS1007, RPS1008, RPS1009, RPS1010, RPS1011, RPS1012, RPS1013, RPS1014, RPS1015, RPS1016, RPS1017, RPS1018, RPS1019, RPS1020, RPS1021, RPS1022, RPS1023, RPS1024, RPS1025, RPS1026, RPS1027, RPS1028, RPS1029, RPS1030, RPS1031, RPS1032, RPS1033, RPS1034, RPS1035, RPS1036, RPS1037, RPS1038, RPS1039, RPS1040, RPS1041, RPS1042, RPS1043, RPS1044, RPS1045, RPS1046, RPS1047, RPS1048, RPS1049, RPS1050, RPS1051, RPS1052, RPS1053, RPS1054, RPS1055, RPS1056, RPS1057, RPS1058, RPS1059, RPS1060, RPS1061, RPS1062, RPS1063, RPS1064, RPS1065, RPS1066, RPS1067, RPS1068, RPS1069, RPS1070, RPS1071, RPS1072, RPS1073, RPS1074, RPS1075, RPS1076, RPS1077, RPS1078, RPS1079, RPS1080, RPS1081, RPS1082, RPS1083, RPS1084, RPS1085, RPS1086, RPS1087, RPS1088, RPS1089, RPS1090, RPS1091, RPS1092, RPS1093, RPS1094, RPS1095, RPS1096, RPS1097, RPS1098, RPS1099, RPS1100, RPS1101, RPS1102, RPS1103, RPS1104, RPS1105, RPS1106, RPS1107, RPS1108, RPS1109, RPS1110, RPS1111, RPS1112, RPS1113, RPS1114, RPS1115, RPS1116, RPS1117, RPS1118, RPS1119, RPS1120, RPS1121, RPS1122, RPS1123, RPS1124, RPS1125, RPS1126, RPS1127, RPS1128, RPS1129, RPS1130, RPS1131, RPS1132, RPS1133, RPS1134, RPS1135, RPS1136, RPS1137, RPS1138, RPS1139, RPS1140, RPS1141, RPS1142, RPS1143, RPS1144, RPS1145, RPS1146, RPS1147, RPS1148, RPS1149, RPS1150, RPS1151, RPS1152, RPS1153, RPS1154, RPS1155, RPS1156, RPS1157, RPS1158, RPS1159, RPS1160, RPS1161, RPS1162, RPS1163, RPS1164, RPS1165, RPS1166, RPS1167, RPS1168, RPS1169, RPS1170, RPS1171, RPS1172, RPS1173, RPS1174, RPS1175, RPS1176, RPS1177, RPS1178, RPS1179, RPS1180, RPS1181, RPS1182, RPS1183, RPS1184, RPS1185, RPS1186, RPS1187, RPS1188, RPS1189, RPS1190, RPS1191, RPS1192, RPS1193, RPS1194, RPS1195, RPS1196, RPS1197, RPS1198, RPS1199, RPS1200, RPS1201, RPS1202, RPS1203, RPS1204, RPS1205, RPS1206, RPS1207, RPS1208, RPS1209, RPS1210, RPS1211, RPS1212, RPS1213, RPS1214, RPS1215, RPS1216, RPS1217, RPS1218, RPS1219, RPS1220, RPS1221, RPS1222, RPS1223, RPS1224, RPS1225, RPS1226, RPS1227, RPS1228, RPS1229, RPS1230, RPS1231, RPS1232, RPS1233, RPS1234, RPS1235, RPS1236, RPS1237, RPS1238, RPS1239, RPS1240, RPS1241, RPS1242, RPS1243, RPS1244, RPS1245, RPS1246, RPS1247, RPS1248, RPS1249, RPS1250, RPS1251, RPS1252, RPS1253, RPS1254, RPS1255, RPS1256, RPS1257, RPS1258, RPS1259, RPS1260, RPS1261, RPS1262, RPS1263, RPS1264, RPS1265, RPS1266, RPS1267, RPS1268, RPS1269, RPS1270, RPS1271, RPS1272, RPS1273, RPS1274, RPS1275, RPS1276, RPS1277, RPS1278, RPS1279, RPS1280, RPS1281, RPS1282, RPS1283, RPS1284, RPS1285, RPS1286, RPS1287, RPS1288, RPS1289, RPS1290, RPS1291, RPS1292, RPS1293, RPS1294, RPS1295, RPS1296, RPS1297, RPS1298, RPS1299, RPS1300, RPS1301, RPS1302, RPS1303, RPS1304, RPS1305, RPS1306, RPS1307, RPS1308, RPS1309, RPS1310, RPS1311, RPS1312, RPS1313, RPS1314, RPS1315, RPS1316, RPS1317, RPS1318, RPS1319, RPS1320, RPS1321, RPS1322, RPS1323, RPS1324, RPS1325, RPS1326, RPS1327, RPS1328, RPS1329, RPS1330, RPS1331, RPS1332, RPS1333, RPS1334, RPS1335, RPS1336, RPS1337, RPS1338, RPS1339, RPS1340, RPS1341, RPS1342, RPS1343, RPS1344, RPS1345, RPS1346, RPS1347, RPS1348, RPS1349, RPS1350, RPS1351, RPS1352, RPS1353, RPS1354, RPS1355, RPS1356, RPS1357, RPS1358, RPS1359, RPS1360, RPS1361, RPS1362, RPS1363, RPS1364, RPS1365, RPS1366, RPS1367, RPS1368, RPS1369, RPS1370, RPS1371, RPS1372, RPS1373, RPS1374, RPS1375, RPS1376, RPS1377, RPS1378, RPS1379, RPS1380, RPS1381, RPS1382, RPS1383, RPS1384, RPS1385, RPS1386, RPS1387, RPS1388, RPS1389, RPS1390, RPS1391, RPS1392, RPS1393, RPS1394, RPS1395, RPS1396, RPS1397, RPS1398, RPS1399, RPS1400, RPS1401, RPS1402, RPS1403, RPS1404, RPS1405, RPS1406, RPS1407, RPS1408, RPS1409, RPS1410, RPS1411, RPS1412, RPS1413, RPS1414, RPS1415, RPS1416, RPS1417, RPS1418, RPS1419, RPS1420, RPS14							

Category	Term	Count	%	PValue	Genes	Pop Hits	Pop Total	Fold Enrichment	Benfoni	Benjamini	FDR
Annotation Cluster 17	Enrichment Score: 3.141589725972605										
UP_NEWWORDS	Triacetyloxy acid cycle	5	2.564102564102564	7.01603890790846E-5	ACD1, ACO1, CS, DH1, MDH2	195	20581	33.411960132860954	0.01652477814098382	0.00829544008153153	0.002128548
KEGG_PATHWAY	tricarboxylate and dicarboxylate metabolism	6	3.0783976093077	1.78883039373958E-4	ACD1, ACO1, CS, GHRPR, ACAT1, MDH2	140	20581	10.933049630496304	0.02600109317035543	0.0183884557012897874	0.000917781
UP_NEWWORDS	tricarboxylate and dicarboxylate cycle	5	2.564102564102564	7.01603890790846E-5	ACD1, ACO1, CS, DH1, MDH2	195	20581	33.411960132860954	0.01652477814098382	0.00829544008153153	0.002128548
GOTERM_BP_DIRECT	GO:0006102 tricarboxylate metabolism	3	1.5384615384615385	0.00284838483848384	ACD1, ACO1, CS	195	6779	36.9054845654845	0.9151542321652744	0.07642321652744	0.0324242
KEGG_PATHWAY	hsa010202 Oxidation-reduction (ICAC cycle)	4	2.051282051282051	0.0049607216483961805	ACD1, ACO1, CS, DH1, MDH2	140	17	8.18928574286715	0.3213159674956568	0.03102589105470906	0.041511988
KEGG_PATHWAY	hsa010202 Oxidation-reduction (ICAC cycle)	4	2.051282051282051	0.0049607216483961805	ACD1, ACO1, CS, DH1	140	17	8.18928574286715	0.3213159674956568	0.03102589105470906	0.041511988
Annotation Cluster 18	Enrichment Score: 3.04831059050467										
SMART	SM00335A_NX	4	2.051282051282051	1.9830738077607638E-4	ANKA1, ANKAS, ANKA4, ANKA2	86	14	33.411960132860954	0.01652477814098382	0.00829544008153153	0.002128548
GOTERM_MF_DIRECT	GO:0004857 phospholipase inhibitor activity	4	2.051282051282051	1.9830738077607638E-4	ANKA1, ANKAS, ANKA4, ANKA2	195	11	33.411960132860954	0.01652477814098382	0.00829544008153153	0.002128548
UP_NEWWORDS	Annexin	4	2.051282051282051	1.9830738077607638E-4	ANKA1, ANKAS, ANKA4, ANKA2	195	11	33.411960132860954	0.01652477814098382	0.00829544008153153	0.002128548
UP_NEWWORDS	Calcium phospholipid binding	4	2.051282051282051	1.9830738077607638E-4	ANKA1, ANKAS, ANKA4, ANKA2	195	11	33.411960132860954	0.01652477814098382	0.00829544008153153	0.002128548
UP_NEWWORDS	Calcium phospholipid binding	4	2.051282051282051	1.9830738077607638E-4	ANKA1, ANKAS, ANKA4, ANKA2	195	11	33.411960132860954	0.01652477814098382	0.00829544008153153	0.002128548
UP_SEQ_FEATURE	repeat:Annexin 4	4	2.051282051282051	3.717490404646164E-4	ANKA1, ANKAS, ANKA4, ANKA2	195	15	20.063	27.436581196581198	0.18818778651541185	0.005469424
UP_SEQ_FEATURE	repeat:Annexin 3	4	2.051282051282051	3.717490404646164E-4	ANKA1, ANKAS, ANKA4, ANKA2	195	15	20.063	27.436581196581198	0.18818778651541185	0.005469424
UP_SEQ_FEATURE	repeat:Annexin 2	4	2.051282051282051	3.717490404646164E-4	ANKA1, ANKAS, ANKA4, ANKA2	195	15	20.063	27.436581196581198	0.18818778651541185	0.005469424
UP_SEQ_FEATURE	repeat:Annexin 1	4	2.051282051282051	3.717490404646164E-4	ANKA1, ANKAS, ANKA4, ANKA2	195	15	20.063	27.436581196581198	0.18818778651541185	0.005469424
INTERPRO	IPRO1464:Annexin	4	2.051282051282051	3.76040231720346E-4	ANKA1, ANKAS, ANKA4, ANKA2	195	14	18559	27.19267392673996	0.185641188278579	0.005488143
INTERPRO	IPRO1832:Annexin repeat	4	2.051282051282051	3.76040231720346E-4	ANKA1, ANKAS, ANKA4, ANKA2	195	14	18559	27.19267392673996	0.185641188278579	0.005488143
INTERPRO	IPRO1832:Annexin repeat	4	2.051282051282051	3.76040231720346E-4	ANKA1, ANKAS, ANKA4, ANKA2	195	14	18559	27.19267392673996	0.185641188278579	0.005488143
GOTERM_MF_DIRECT	GO:0005544 calcium dependent phospholipid binding	4	2.051282051282051	0.02950588710693856	ANKA1, ANKAS, ANKA4, ANKA2	195	58	16881	5.97029177788328	0.999997063376225	0.346790741
GOTERM_MF_DIRECT	GO:0043002 calcium dependent protein binding	4	2.051282051282051	0.02950588710693856	ANKA1, ANKAS, ANKA4, ANKA2	195	58	16881	5.97029177788328	0.999997063376225	0.346790741
GOTERM_BP_DIRECT	GO:0043186 negative regulation of catalytic activity	4	2.051282051282051	0.05010867540384204	RNH1, ANKAS, ANKA4, ANKA2	195	75	16792	4.59283760687605	1.0	0.51139381813253
Annotation Cluster 19	Enrichment Score: 2.7127492175232877										
UP_NEWWORDS	Stress response	10	5.128205128205128	4.4324380538114E-7	HSP90A1, HSP90B1, HSP90C1, HSP90D1, SERPINE1, PARK7, HSP89A	195	100	20581	10.543358943589435	1.161356382625156E-4	6.432333768502966E-5
GOTERM_MF_DIRECT	GO:0020202 MHC class II protein complex binding	5	2.564102564102564	2.76245463645138E-5	HSP90A1, PPIA, HSP90A2, YWHAZ, HSP89A	195	16	16881	27.022884615846158	0.01398827197718676092	0.000338881
GOTERM_BP_DIRECT	GO:0036102 protein folding	4	2.051282051282051	3.162643793644132E-5	HSP90A1, HSP90A2, YWHAZ, HSP89A	195	15	16792	27.3418804132804	0.0798248362148213	0.00210276444
KEGG_PATHWAY	hsa04612:Antigen processing and presentation	6	3.0783976093077	0.006454668313545	HSP90A1, HSP90A2, PPIA, HSP90A3, CALR, CANX, HSP89A	140	76	6879	4.52656578978842	0.4650035401480517	0.048889594
GOTERM_BP_DIRECT	GO:0048267 histone deacetylase binding	6	3.0783976093077	0.006454668313545	HSP90A1, HSP90A2, PPIA, HSP90A3, CALR, CANX, HSP89A	195	102	16881	5.092307692307693	0.0315924421129169	0.00829544008153153
GOTERM_BP_DIRECT	GO:0000903 regulation of cellular homeostasis	3	1.5384615384615385	0.0142535241194844	HSP90A1, HSP90A2, HSP89A	195	75	16792	5.7460510065701	0.999999816342387	0.03998441393536734
GOTERM_BP_DIRECT	GO:0031397 regulation of protein ubiquitination	3	1.5384615384615385	0.0142535241194844	HSP90A1, HSP90A2, HSP89A	195	16	16792	6.146153846153847	0.999999958521213	0.11426205
GOTERM_BP_DIRECT	GO:0048639 protein domain specific binding	3	1.5384615384615385	0.0142535241194844	HSP90A1, HSP90A2, HSP89A	195	16	16792	6.146153846153847	0.999999958521213	0.11426205
KEGG_PATHWAY	hsa09155:Strain signaling pathway	5	2.564102564102564	0.139175680485303	HSP90A1, HSP90B1, HSP90C1, HSP89A	140	99	6879	2.461027131617116	0.999999998186313	0.4211853807464259
Annotation Cluster 20	Enrichment Score: 2.50347166383288										
SMART	SM00101.1_4_3_3	3	1.5384615384615385	0.0029356155622E-5	YWHAZ, YWHAG, YWHAQ, YWHAZ	86	7	1057	66.823920265728073	0.00167458139058603	0.002131631
INTERPRO	IPRO038144-3_3 protein	3	1.5384615384615385	0.0029356155622E-5	YWHAZ, YWHAG, YWHAQ, YWHAZ	195	7	18559	54.3834789358479	0.0206238355601325	0.00052667
INTERPRO	IPRO2309-14-3_3 domain	4	2.051282051282051	3.162643793644132E-5	YWHAZ, YWHAG, YWHAQ, YWHAZ	195	7	18559	54.3834789358479	0.0206238355601325	0.00052667
UP_SEQ_FEATURE	site interaction with phosphoserine on interacting protein	4	2.051282051282051	4.03054402005482E-5	YWHAZ, YWHAG, YWHAQ, YWHAZ	195	8	2003	5.144338914338975	0.0281688124128202	0.002195010044818864
GOTERM_MF_DIRECT	GO:0003959 protein domain specific binding	11	5.841025641025641	1.495384848484848E-4	TUBB1, YWHAZ, YWHAG, HIST1H2B, VCP, TGM2, YWHAQ, RDX, HSPA5, YWHAZ, IGFAP1	195	208	16881	4.598380413372781	0.07942488400002042	0.00405046450333514
PIR_SUPERFAMILY	GO:0002426 protein-protein interaction into mitochondrial membrane (involved in apoptotic signaling pathway)	4	2.051282051282051	0.00489898162420613	YWHAZ, YWHAG, YWHAQ, YWHAZ	51	7	1692	18.9797819377731	0.0308235062825153	0.0715915
GOTERM_BP_DIRECT	GO:0016102 membrane organization	4	2.051282051282051	0.00489898162420613	YWHAZ, YWHAG, YWHAQ, YWHAZ	195	30	16792	11.4817096019402	0.989816481243887	0.07676778
GOTERM_BP_DIRECT	GO:0016102 membrane organization	4	2.051282051282051	0.00489898162420613	YWHAZ, YWHAG, YWHAQ, YWHAZ	195	32	16792	11.4817096019402	0.989816481243887	0.07676778
GOTERM_BP_DIRECT	GO:0006052 protein targeting	4	2.051282051282051	0.0024217008936011	YWHAZ, YWHAG, YWHAQ, YWHAZ	195	39	16792	8.83028415161079	0.999998746260678	0.197292730478335
GOTERM_CC_DIRECT	GO:0030579 cytoplasmic vesicle membrane	9	4.615384615384615	0.04579307272884	PKM, YWHAZ, YWHAG, HIST1H2B, HNRNP, HIST1H3A, ACTN1, YWHAQ, YWHAZ	195	126	18224	3.70838789878086	0.999998793891515	0.112846573686662
KEGG_PATHWAY	hsa01100:Cell cycle	5	2.564102564102564	0.24156765207063	YWHAZ, YWHAG, PCNA, YWHAQ, YWHAZ	140	205	6879	2.15717700348432	0.999793648841152	0.432846092
KEGG_PATHWAY	hsa01100:Cell cycle	5	2.564102564102564	0.24156765207063	YWHAZ, YWHAG, PCNA, YWHAQ, YWHAZ	140	124	6879	1.98178801843131	1.0	0.935010094
KEGG_PATHWAY	hsa01100:Cell cycle	5	2.564102564102564	0.24156765207063	YWHAZ, YWHAG, PCNA, YWHAQ, YWHAZ	140	151	6879	1.62701046811731	1.0	0.99509167
KEGG_PATHWAY	hsa01100:Cell cycle	5	2.564102564102564	0.24156765207063	YWHAZ, YWHAG, PCNA, YWHAQ, YWHAZ	140	111	6879	1.77065370656710	1.0	0.97924528
KEGG_PATHWAY	hsa01100:Cell cycle	5	2.564102564102564	0.24156765207063	YWHAZ, YWHAG, PCNA, YWHAQ, YWHAZ	140	345	6879	1.13931886395776	1.0	0.84021730502284
Annotation Cluster 21	Enrichment Score: 2.47839532741097										
KEGG_PATHWAY	hsa00200:Pyruvate metabolism	8	4.102564102564102	1.26280947082658E-5	PKM, LDHA, LDHB, ALDH2, GLO1, GHRPR, ACAT1, MDH2	140	40	6879	9.827142857142858	0.00187563753474439	2.6873629535370185E-4
INTERPRO	IPRO01557:L-lactate/malate dehydrogenase	5	1.5384615384615385	0.0029356155622E-5	LDHB, LDHA, MDH2	195	8	18559	35.690384615384616	0.7974637646711985	0.05956880165196188
INTERPRO	IPRO02238:Lactate/malate dehydrogenase, N-terminal	3	1.5384615384615385	0.0029356155622E-5	LDHB, LDHA, MDH2	195	8	18559	35.690384615384616	0.7974637646711985	0.05956880165196188
INTERPRO	IPRO1595:Lactate dehydrogenase/lysine hydroxylase, family 4, C-PIR_SUPERFAMILY	3	1.5384615384615385	0.003228843831941016	LDHB, LDHA, MDH2	195	8	18559	35.690384615384616	0.7974637646711985	0.05956880165196188
KEGG_PATHWAY	hsa01100:Cell cycle	5	2.564102564102564	0.24156765207063	LDHB, LDHA, MDH2	51	8	1692	12.441176470582862	0.978004914513738	0.1794565208
KEGG_PATHWAY	hsa01100:Cell cycle	5	2.564102564102564	0.24156765207063	LDHB, LDHA, MDH2	140	38	6879	3.879133338458644	0.999999999998137	0.47868971333602985
Annotation Cluster 22	Enrichment Score: 2.32678133273469										
GOTERM_MF_DIRECT	GO:0005202 structural constituent of cytoskeleton	8	4.102564102564102	2.8278908489078E-4	ACTR3, ACTG1, TUBB1, TUBA1B, TUBB3, TUBB8	195	10	16881	6.2959440594056	0.13253208586015318	0.0064416218126919
GOTERM_MF_DIRECT	GO:0003925 GTPase activity	11	5.841025641025641	3.49495978767931E-4	TUBA1B, TUBB, EFPA1A, EFPA2, EFPA3, EFPA4, TGM2, EFPA5, ARF4, TGM2, SAR1A, TUBA1B, HSP90A1, TUBF, HSP90A2, RAN, EFPA2, EFPA3, EFPA4, EFPA5, ARF4, TGM2, SAR1A, TUBA1B, TUBB3, TUBB8	195	234	16881	4.06949371109139	0.178303740714117	0.008149380814078344
GOTERM_MF_DIRECT	GO:0005202 structural constituent of cytoskeleton	8	4.102564102564102	2.8278908489078E-4	ACTR3, ACTG1, TUBB1, TUBA1B, TUBB3, TUBB8	195	10	16881	6.2959440594056	0.13253208586015318	0.0064416218126919
GOTERM_MF_DIRECT	GO:0003925 GTPase activity	11	5.841025641025641	3.49495978767931E-4	TUBA1B, TUBB, EFPA1A, EFPA2, EFPA3, EFPA4, TGM2, EFPA5, ARF4, TGM2, SAR1A, TUBA1B, HSP90A1, TUBF, HSP90A2, RAN, EFPA2, EFPA3, EFPA4, EFPA5, ARF4, TGM2, SAR1A, TUBA1						

Category	Term	Count	Enrichment Score	Gene	Pop Total	Pop Hits	Ust Total	Ust Hits	Benjamini	FDR		
Annotation Cluster 23	INTERPRO	4	2.051282051282051	0.00149590208948574	TUBB1, TUBB2, TUBB3, TUBB4B	195	22	18559	17.3044278904428013	0.5584218939862852	0.021588671	
	UP_NEWWORDS	11	5.641025610256102	0.00161481030989854	TUBB1, TUBB2, TUBB3, TUBB4B	195	343	20851	3.96477984060033355	0.344625651656628	0.0120884874	
	IPRO23123: Tubulin, C-terminal	4	2.051282051282051	0.0017078421339830296	TUBB1, TUBB2, TUBB3, TUBB4B	195	23	18559	16.5520624030233	0.606596367198885	0.04151888126643233	
	IPRO23123: Tubulin, N-terminal	4	2.051282051282051	0.0017078421339830296	TUBB1, TUBB2, TUBB3, TUBB4B	195	23	18559	16.5520624030233	0.606596367198885	0.04151888126643233	
	IPRO17975: Tubulin, conserved site	4	2.051282051282051	0.0018887676828989312	TUBB1, TUBB2, TUBB3, TUBB4B	195	23	18559	16.5520624030233	0.606596367198885	0.04151888126643233	
	IPRO00587: microtubule	4	2.051282051282051	0.0018887676828989312	TUBB1, TUBB2, TUBB3, TUBB4B	195	311	18224	3.3055121526435	0.45281327136206617	0.01708002929890544	
	IPRO0217: Tubulin	4	2.051282051282051	0.0018887676828989312	TUBB1, TUBB2, TUBB3, TUBB4B	195	24	18559	16.8239162939161	0.6529023788804076	0.0449641831662932656	
	KEGG_PATHWAY	4	2.051282051282051	0.0018887676828989312	TUBB1, TUBB2, TUBB3, TUBB4B	195	25	18559	15.27897935997953	0.6568168681378626	0.0425967538001971	
	KEGG_PATHWAY	4	2.051282051282051	0.0018887676828989312	TUBB1, TUBB2, TUBB3, TUBB4B	195	51	8879	9.786972289897963	0.60433378787287963	0.03414527704847411	
	KEGG_PATHWAY	4	2.051282051282051	0.0018887676828989312	TUBB1, TUBB2, TUBB3, TUBB4B	195	9	18559	31.7247862768326	0.689844776944849	0.020861011578897	
Annotation Cluster 24	GOTERM_BP_DIRECT	4	4.102564102564102	0.00819187133493955	TUBB1, TUBB2, TUBB3, TUBB4B	195	36	16792	9.5609161609161	0.9989891746372656	0.1735049211623828	
	KEGG_PATHWAY	8	4.102564102564102	0.00819187133493955	TUBB1, TUBB2, TUBB3, TUBB4B	195	150	6879	2.620571425874286	0.93190808434998	0.18219578952883426	
	INTERPRO	13	6.666666666666667	0.2101338647562332	TURF1, BRAN, FEAF2, ATFSB, EEF2, IGGAP1, VCP, PSMCA, EF1A1P5, EF1A2, ARA2, ATRPSA1, SARA1	195	879	18559	1.4075843781865088	1.0	0.942858101542815	
	INTERPRO	4	2.051282051282051	0.2538294527930074	RAN, ARF1, EEF2, SARA1	195	167	18559	2.7796235846653043	1.0	0.966879476127796	
	KEGG_PATHWAY	4	2.051282051282051	0.4629585913568	TUBB1, TUBB2, TUBB3, TUBB4B	195	140	88	6879	2.233441584415883	1.0	0.9735332382
	UP_NEWWORDS	4	2.051282051282051	0.490019312481669	TUBB1, TUBB2, TUBB3, TUBB4B	195	280	20581	1.5077656077656077	1.0	0.9714865963381	
	Annotation Cluster 25	GOTERM_BP_DIRECT	8	4.102564102564102	0.002722456978663196	ACTB3, TINI, ACTNA, KR18, FIMA, IGGAP1, ANKAA2, VCL	195	171	18224	4.3480979362919	0.54605656521552	0.033484322
		GOTERM_BP_DIRECT	7	3.581743580715841	0.00421207768215491	ACTB3, TINI, ACTNA, CFL1, EEF2, FIMA, PLS3	195	132	18224	4.500792540792541	0.884368071508254	0.026026444
		GOTERM_BP_DIRECT	9	4.102564102564102	0.004574746488405649	ACTB3, PFN1, ACTNA, CFL1, RDX, CAP1, FIMA, PLS3, VCL	195	274	20581	3.466762402705218	0.689446621260665	0.038200244
		UP_NEWWORDS	8	4.102564102564102	0.0083971138005369	ACTB3, ACTNA, CFL1, PGML1, STOML2, FIMA, IGGAP1, VCL	195	218	18224	3.4295930363924865	0.94294526270343	0.0616505196131001
GOTERM_CC_DIRECT		8	4.102564102564102	0.0083971138005369	ACTB3, ACTNA, CFL1, PGML1, STOML2, FIMA, IGGAP1, VCL	195	218	18224	3.4295930363924865	0.94294526270343	0.0616505196131001	
Annotation Cluster 26		Term	Count	Enrichment Score	Gene	Pop Total	Pop Hits	Ust Total	Ust Hits	Benjamini	FDR	
GOTERM_BP_DIRECT		4	2.051282051282051	0.001264574303826964	ADH1A1, ADH2, GAPDH, ADH3A1	195	19	18881	18.251012145749	0.475462011464795	0.03286463513931047	
UP_SEQ_FEATURE		4	2.051282051282051	0.0042746248387974	HNRKPK, UBA1, CALR, CANX	195	34	20683	2.104954029735233	0.921398661682194	0.1005175558708725	
UP_SEQ_FEATURE		3	1.538461538461538	0.0155338638615884	HNRKPK, UBA1, CALR, CANX	195	19	18881	15.763026929338	0.9997187185129042	0.077101519	
UP_SEQ_FEATURE		3	1.538461538461538	0.0155338638615884	HNRKPK, UBA1, CALR, CANX	195	19	18881	15.763026929338	0.9997187185129042	0.077101519	
Annotation Cluster 27	Term	Count	Enrichment Score	Gene	Pop Total	Pop Hits	Ust Total	Ust Hits	Benjamini	FDR		
GOTERM_BP_DIRECT	8	4.102564102564102	9.1548183043603E-6	HSP90AB1, HSP90AA1, IGLA51, VIM, HSPA5, CALR, CANX, FLNA	195	65	20881	10.646745621307	0.00479064344436545	0.00089407650237E-4		
UP_NEWWORDS	3	1.538461538461538	0.477915845195671	IGLAL1, CALR, CANX	195	171	20881	1.851641925413663	1.0	0.865158617204828		
INTERPRO	3	1.538461538461538	0.7001931117169962	IGLAL1, CALR, CANX	195	232	18559	1.230702917718833	1.0	0.999995860240868		
Annotation Cluster 28	GOTERM_BP_DIRECT	5	2.564102564102564	0.00125287496409886	HSP90AB1, HSP90AA1, HSD17B4, HSD17B5, HSD17B7, HSD17B8, HSD17B9, HSD17B10, HSD17B11, HSD17B12, HSD17B13, HSD17B14, HSD17B15, HSD17B16, HSD17B17, HSD17B18, HSD17B19, HSD17B20, HSD17B21, HSD17B22, HSD17B23, HSD17B24, HSD17B25, HSD17B26, HSD17B27, HSD17B28, HSD17B29, HSD17B30, HSD17B31, HSD17B32, HSD17B33, HSD17B34, HSD17B35, HSD17B36, HSD17B37, HSD17B38, HSD17B39, HSD17B40, HSD17B41, HSD17B42, HSD17B43, HSD17B44, HSD17B45, HSD17B46, HSD17B47, HSD17B48, HSD17B49, HSD17B50, HSD17B51, HSD17B52, HSD17B53, HSD17B54, HSD17B55, HSD17B56, HSD17B57, HSD17B58, HSD17B59, HSD17B60, HSD17B61, HSD17B62, HSD17B63, HSD17B64, HSD17B65, HSD17B66, HSD17B67, HSD17B68, HSD17B69, HSD17B70, HSD17B71, HSD17B72, HSD17B73, HSD17B74, HSD17B75, HSD17B76, HSD17B77, HSD17B78, HSD17B79, HSD17B80, HSD17B81, HSD17B82, HSD17B83, HSD17B84, HSD17B85, HSD17B86, HSD17B87, HSD17B88, HSD17B89, HSD17B90, HSD17B91, HSD17B92, HSD17B93, HSD17B94, HSD17B95, HSD17B96, HSD17B97, HSD17B98, HSD17B99, HSD17B100, HSD17B101, HSD17B102, HSD17B103, HSD17B104, HSD17B105, HSD17B106, HSD17B107, HSD17B108, HSD17B109, HSD17B110, HSD17B111, HSD17B112, HSD17B113, HSD17B114, HSD17B115, HSD17B116, HSD17B117, HSD17B118, HSD17B119, HSD17B120, HSD17B121, HSD17B122, HSD17B123, HSD17B124, HSD17B125, HSD17B126, HSD17B127, HSD17B128, HSD17B129, HSD17B130, HSD17B131, HSD17B132, HSD17B133, HSD17B134, HSD17B135, HSD17B136, HSD17B137, HSD17B138, HSD17B139, HSD17B140, HSD17B141, HSD17B142, HSD17B143, HSD17B144, HSD17B145, HSD17B146, HSD17B147, HSD17B148, HSD17B149, HSD17B150, HSD17B151, HSD17B152, HSD17B153, HSD17B154, HSD17B155, HSD17B156, HSD17B157, HSD17B158, HSD17B159, HSD17B160, HSD17B161, HSD17B162, HSD17B163, HSD17B164, HSD17B165, HSD17B166, HSD17B167, HSD17B168, HSD17B169, HSD17B170, HSD17B171, HSD17B172, HSD17B173, HSD17B174, HSD17B175, HSD17B176, HSD17B177, HSD17B178, HSD17B179, HSD17B180, HSD17B181, HSD17B182, HSD17B183, HSD17B184, HSD17B185, HSD17B186, HSD17B187, HSD17B188, HSD17B189, HSD17B190, HSD17B191, HSD17B192, HSD17B193, HSD17B194, HSD17B195, HSD17B196, HSD17B197, HSD17B198, HSD17B199, HSD17B200, HSD17B201, HSD17B202, HSD17B203, HSD17B204, HSD17B205, HSD17B206, HSD17B207, HSD17B208, HSD17B209, HSD17B210, HSD17B211, HSD17B212, HSD17B213, HSD17B214, HSD17B215, HSD17B216, HSD17B217, HSD17B218, HSD17B219, HSD17B220, HSD17B221, HSD17B222, HSD17B223, HSD17B224, HSD17B225, HSD17B226, HSD17B227, HSD17B228, HSD17B229, HSD17B230, HSD17B231, HSD17B232, HSD17B233, HSD17B234, HSD17B235, HSD17B236, HSD17B237, HSD17B238, HSD17B239, HSD17B240, HSD17B241, HSD17B242, HSD17B243, HSD17B244, HSD17B245, HSD17B246, HSD17B247, HSD17B248, HSD17B249, HSD17B250, HSD17B251, HSD17B252, HSD17B253, HSD17B254, HSD17B255, HSD17B256, HSD17B257, HSD17B258, HSD17B259, HSD17B260, HSD17B261, HSD17B262, HSD17B263, HSD17B264, HSD17B265, HSD17B266, HSD17B267, HSD17B268, HSD17B269, HSD17B270, HSD17B271, HSD17B272, HSD17B273, HSD17B274, HSD17B275, HSD17B276, HSD17B277, HSD17B278, HSD17B279, HSD17B280, HSD17B281, HSD17B282, HSD17B283, HSD17B284, HSD17B285, HSD17B286, HSD17B287, HSD17B288, HSD17B289, HSD17B290, HSD17B291, HSD17B292, HSD17B293, HSD17B294, HSD17B295, HSD17B296, HSD17B297, HSD17B298, HSD17B299, HSD17B300, HSD17B301, HSD17B302, HSD17B303, HSD17B304, HSD17B305, HSD17B306, HSD17B307, HSD17B308, HSD17B309, HSD17B310, HSD17B311, HSD17B312, HSD17B313, HSD17B314, HSD17B315, HSD17B316, HSD17B317, HSD17B318, HSD17B319, HSD17B320, HSD17B321, HSD17B322, HSD17B323, HSD17B324, HSD17B325, HSD17B326, HSD17B327, HSD17B328, HSD17B329, HSD17B330, HSD17B331, HSD17B332, HSD17B333, HSD17B334, HSD17B335, HSD17B336, HSD17B337, HSD17B338, HSD17B339, HSD17B340, HSD17B341, HSD17B342, HSD17B343, HSD17B344, HSD17B345, HSD17B346, HSD17B347, HSD17B348, HSD17B349, HSD17B350, HSD17B351, HSD17B352, HSD17B353, HSD17B354, HSD17B355, HSD17B356, HSD17B357, HSD17B358, HSD17B359, HSD17B360, HSD17B361, HSD17B362, HSD17B363, HSD17B364, HSD17B365, HSD17B366, HSD17B367, HSD17B368, HSD17B369, HSD17B370, HSD17B371, HSD17B372, HSD17B373, HSD17B374, HSD17B375, HSD17B376, HSD17B377, HSD17B378, HSD17B379, HSD17B380, HSD17B381, HSD17B382, HSD17B383, HSD17B384, HSD17B385, HSD17B386, HSD17B387, HSD17B388, HSD17B389, HSD17B390, HSD17B391, HSD17B392, HSD17B393, HSD17B394, HSD17B395, HSD17B396, HSD17B397, HSD17B398, HSD17B399, HSD17B400, HSD17B401, HSD17B402, HSD17B403, HSD17B404, HSD17B405, HSD17B406, HSD17B407, HSD17B408, HSD17B409, HSD17B410, HSD17B411, HSD17B412, HSD17B413, HSD17B414, HSD17B415, HSD17B416, HSD17B417, HSD17B418, HSD17B419, HSD17B420, HSD17B421, HSD17B422, HSD17B423, HSD17B424, HSD17B425, HSD17B426, HSD17B427, HSD17B428, HSD17B429, HSD17B430, HSD17B431, HSD17B432, HSD17B433, HSD17B434, HSD17B435, HSD17B436, HSD17B437, HSD17B438, HSD17B439, HSD17B440, HSD17B441, HSD17B442, HSD17B443, HSD17B444, HSD17B445, HSD17B446, HSD17B447, HSD17B448, HSD17B449, HSD17B450, HSD17B451, HSD17B452, HSD17B453, HSD17B454, HSD17B455, HSD17B456, HSD17B457, HSD17B458, HSD17B459, HSD17B460, HSD17B461, HSD17B462, HSD17B463, HSD17B464, HSD17B465, HSD17B466, HSD17B467, HSD17B468, HSD17B469, HSD17B470, HSD17B471, HSD17B472, HSD17B473, HSD17B474, HSD17B475, HSD17B476, HSD17B477, HSD17B478, HSD17B479, HSD17B480, HSD17B481, HSD17B482, HSD17B483, HSD17B484, HSD17B485, HSD17B486, HSD17B487, HSD17B488, HSD17B489, HSD17B490, HSD17B491, HSD17B492, HSD17B493, HSD17B494, HSD17B495, HSD17B496, HSD17B497, HSD17B498, HSD17B499, HSD17B500, HSD17B501, HSD17B502, HSD17B503, HSD17B504, HSD17B505, HSD17B506, HSD17B507, HSD17B508, HSD17B509, HSD17B510, HSD17B511, HSD17B512, HSD17B513, HSD17B514, HSD17B515, HSD17B516, HSD17B517, HSD17B518, HSD17B519, HSD17B520, HSD17B521, HSD17B522, HSD17B523, HSD17B524, HSD17B525, HSD17B526, HSD17B527, HSD17B528, HSD17B529, HSD17B530, HSD17B531, HSD17B532, HSD17B533, HSD17B534, HSD17B535, HSD17B536, HSD17B537, HSD17B538, HSD17B539, HSD17B540, HSD17B541, HSD17B542, HSD17B543, HSD17B544, HSD17B545, HSD17B546, HSD17B547, HSD17B548, HSD17B549, HSD17B550, HSD17B551, HSD17B552, HSD17B553, HSD17B554, HSD17B555, HSD17B556, HSD17B557, HSD17B558, HSD17B559, HSD17B560, HSD17B561, HSD17B562, HSD17B563, HSD17B564, HSD17B565, HSD17B566, HSD17B567, HSD17B568, HSD17B569, HSD17B570, HSD17B571, HSD17B572, HSD17B573, HSD17B574, HSD17B575, HSD17B576, HSD17B577, HSD17B578, HSD17B579, HSD17B580, HSD17B581, HSD17B582, HSD17B583, HSD17B584, HSD17B585, HSD17B586, HSD17B587, HSD17B588, HSD17B589, HSD17B590, HSD17B591, HSD17B592, HSD17B593, HSD17B594, HSD17B595, HSD17B596, HSD17B597, HSD17B598, HSD17B599, HSD17B600, HSD17B601, HSD17B602, HSD17B603, HSD17B604, HSD17B605, HSD17B606, HSD17B607, HSD17B608, HSD17B609, HSD17B610, HSD17B611, HSD17B612, HSD17B613, HSD17B614, HSD17B615, HSD17B616, HSD17B617, HSD17B618, HSD17B619, HSD17B620, HSD17B621, HSD17B622, HSD17B623, HSD17B624, HSD17B625, HSD17B626, HSD17B627, HSD17B628, HSD17B629, HSD17B630, HSD17B631, HSD17B632, HSD17B633, HSD17B634, HSD17B635, HSD17B636, HSD17B637, HSD17B638, HSD17B639, HSD17B640, HSD17B641, HSD17B642, HSD17B643, HSD17B644, HSD17B645, HSD17B646, HSD17B647, HSD17B648, HSD17B649, HSD17B650, HSD17B651, HSD17B652, HSD17B653, HSD17B654, HSD17B655, HSD17B656, HSD17B657, HSD17B658, HSD17B659, HSD17B660, HSD17B661, HSD17B662, HSD17B663, HSD17B664, HSD17B665, HSD17B666, HSD17B667, HSD17B668, HSD17B669, HSD17B670, HSD17B671, HSD17B672, HSD17B673, HSD17B674, HSD17B675, HSD17B676, HSD17B677, HSD17B678, HSD17B679, HSD17B680, HSD17B681, HSD17B682, HSD17B683, HSD17B684, HSD17B685, HSD17B686, HSD17B687, HSD17B688, HSD17B689, HSD17B690, HSD17B691, HSD17B692, HSD17B693, HSD17B694, HSD17B695, HSD17B696, HSD17B697, HSD17B698, HSD17B699, HSD17B700, HSD17B701, HSD17B702, HSD17B703, HSD17B704, HSD17B705, HSD17B706, HSD17B707, HSD17B708, HSD17B709, HSD17B710, HSD17B711, HSD17B712, HSD17B713, HSD17B714, HSD17B715, HSD17B716, HSD17B717, HSD17B718, HSD17B719, HSD17B720, HSD17B721, HSD17B722, HSD17B723, HSD17B724, HSD17B725, HSD17B726, HSD17B727, HSD17B728, HSD17B729, HSD17B730, HSD17B731, HSD17B732, HSD17B733, HSD17B734, HSD17B73							

Category	Term	Count	%	PValue	Genes	List Total	Pop Hts	Pop Total	Fold Enrichment	Benjamini	FDR		
Annotation Cluster 31	GOTERM_MF_DIRECT	3	1.5846	1.53861538615385	0.1088507627456972	ATP5B, ATP5A1, ATP5H	195	49	16881	5.300151698571272	1.0	0.518605947153750512	
	UP_NEWWORDS	6	3.07692	0.307692037	0.1926293	ACTL1, CYC1, SPK1, UQCRC1, COX5A	195	324	20581	1.9545109917588	1.0	0.582335752546948	
	KEGG_PATHWAY	1	1.5846	1.53861538615385	0.4500771753548116	CYC1, UQCRC1, COX5A	140	75	6879	0.9624076240807887	1.0	0.78472918689583586	
	KEGG_PATHWAY	4	1.5846	1.53861538615385	0.8144625688893323	CYC1, UQCRC1, COX5A	140	151	6879	0.9624076240807887	1.0	0.933774565567856	
	UP_NEWWORDS	5	2.564	0.2564102564	0.585759075420479	ATP5B, SPN1, ATP5A1, VDAC1	195	642	20581	0.8211900543270229	1.0	0.9337634102861157	
Annotation Cluster 31	Enrichment Score: 1.572643975394597												
Annotation Cluster 32	Category	Term	Count	%	PValue	Genes	List Total	Pop Hts	Pop Total	Fold Enrichment <td>Benjamini</td> <td>FDR</td>	Benjamini	FDR	
	INTERPRO	IPR019305:heat shock protein (Hsp90), conserved site	3	1.5846	1.53861538615385	0.0042107776815991	ACTR1, TUB1, ACTA1, CFL1, EEF2, FINA, PLS3	195	4	18859	0.8343608071508254	0.0193052025083802	0.093937595
	MIRN	MIR00527:miR-145-3-5p	4	1.5846	1.53861538615385	0.005958816881659114	ACTR1, TUB1, ACTA1, CFL1, EEF2, FINA, PLS3	195	12	18859	0.8343608071508254	0.0193052025083802	0.093937595
	INTERPRO	IPR001580:actin-1-type, actin-binding, conserved site	3	1.5846	1.53861538615385	0.0238120086769819	ACTA1, FINA, PLS3	195	23	18859	1.2444069277424376	0.9091880713264527	0.52925618699985
	PDB_SUPERFAMILY	P1R02058:heat shock protein, HSP90/HTRG types	51	4	1.692	24.88232954117647	0.7987580132168872	0.6326258537048836	0.44342928	24.88232954117647	0.7987580132168872	0.6326258537048836	0.44342928
	INTERPRO	IPR001404:heat shock protein Hsp90	51	11	18559	25.9656433566433568	0.93288974571745887	0.93747359147345887	0.717866517	25.9656433566433568	0.93288974571745887	0.93747359147345887	0.717866517
	INTERPRO	IPR020568:ribosomal protein S5 domain 2-type fold	195	44	18859	8.65214452144521	0.93747359147345887	0.93747359147345887	0.165201489901617486	0.165201489901617486	0.165201489901617486	0.165201489901617486	0.165201489901617486
	GOTERM_BP_DIRECT	GO:0009507:response to stress	195	61	16792	5.64674232709542	1.0	0.4127541020200673	0.4294139	5.64674232709542	1.0	0.4127541020200673	0.4294139
	INTERPRO	IPR003594:histidine kinase-like ATPase, ATP-binding domain	195	33	18859	8.65214452144521	0.93747359147345887	0.93747359147345887	0.4610866023286663	0.4610866023286663	0.4610866023286663	0.4610866023286663	0.4610866023286663
	KEGG_PATHWAY	h04915:estrogen signaling pathway	140	88	6879	2.48160171601716	0.93747359147345887	0.93747359147345887	0.421365887464293	0.421365887464293	0.421365887464293	0.421365887464293	0.421365887464293
KEGG_PATHWAY	h04915:estrogen signaling pathway	140	88	6879	1.6750811688116881	1.0	0.8313964376688186	0.8313964376688186	1.6750811688116881	1.0	0.8313964376688186	0.8313964376688186	
KEGG_PATHWAY	h04151P:PK-Akt signaling pathway	140	345	6879	1.193738819057576	1.0	0.404021730552284	0.404021730552284	1.193738819057576	1.0	0.404021730552284	0.404021730552284	
KEGG_PATHWAY	h04206P:Wnt signaling pathway	140	395	6879	0.626136314067617	1.0	0.9374965191840689	0.9374965191840689	0.626136314067617	1.0	0.9374965191840689	0.9374965191840689	
Annotation Cluster 33	Enrichment Score: 1.435450848985845												
Annotation Cluster 33	Category	Term	Count	%	PValue	Genes	List Total	Pop Hts	Pop Total	Fold Enrichment <td>Benjamini</td> <td>FDR</td>	Benjamini	FDR	
	KEGG_PATHWAY	h04060P:Propanoate metabolism	140	28	6879	8.77423246987549	0.2842901256343491	0.202949657034601285	0.02840732	8.77423246987549	0.2842901256343491	0.02840732	0.02840732
	KEGG_PATHWAY	h04290:Valine, leucine and isoleucine degradation	140	47	6879	6.27244376896966	0.30421515484787465	0.202974463314112992	0.202974463314112992	6.27244376896966	0.30421515484787465	0.202974463314112992	0.202974463314112992
	KEGG_PATHWAY	h04060P:Tryptophan metabolism	140	44	6879	1.142848287541286	0.1713235451131596	0.060232476206893426	0.094657444	1.142848287541286	0.1713235451131596	0.060232476206893426	0.094657444
	GOTERM_BP_DIRECT	GO:0006375:fatty acid beta-oxidation	195	40	16792	7.96483284382228975	0.93747359147345887	0.93747359147345887	0.283876688991326	0.283876688991326	0.283876688991326	0.283876688991326	0.283876688991326
	KEGG_PATHWAY	h040041:beta-Alanine metabolism	140	31	6879	6.3400921561888817	0.9373271537945431	0.1457059133988528	0.23370007	6.3400921561888817	0.9373271537945431	0.1457059133988528	0.23370007
	KEGG_PATHWAY	h040071:Fatty acid degradation	140	42	6879	4.679591838774694	0.93747359147345887	0.93747359147345887	0.2650044676865341	4.679591838774694	0.93747359147345887	0.2650044676865341	0.2650044676865341
	KEGG_PATHWAY	h040212:Fatty acid metabolism	140	48	6879	4.096464285740577	0.93747359147345887	0.93747359147345887	0.3115167022261605	4.096464285740577	0.93747359147345887	0.3115167022261605	0.3115167022261605
	KEGG_PATHWAY	h04020:Leucine degradation	140	52	6879	3.778610295030396	0.93747359147345887	0.93747359147345887	0.3378617320573956	3.778610295030396	0.93747359147345887	0.3378617320573956	0.3378617320573956
	KEGG_PATHWAY	h04056:Valine metabolism	140	27	6879	5.6562384952341	0.93747359147345887	0.93747359147345887	0.148648684062678	5.6562384952341	0.93747359147345887	0.148648684062678	0.148648684062678
Annotation Cluster 34	Enrichment Score: 1.37116055706412												
Annotation Cluster 34	Category	Term	Count	%	PValue	Genes	List Total	Pop Hts	Pop Total	Fold Enrichment <td>Benjamini</td> <td>FDR</td>	Benjamini	FDR	
	GOTERM_MF_DIRECT	GO:0097110:catalytic protein binding	195	48	16881	7.21410254102541	0.93747359147345887	0.93747359147345887	0.1523886180050119	0.1523886180050119	0.1523886180050119	0.1523886180050119	
	GOTERM_BP_DIRECT	GO:0009198:structural molecule activity	195	108	16881	2.8083861753192153	0.93747359147345887	0.93747359147345887	0.19485238152789184	0.19485238152789184	0.19485238152789184	0.19485238152789184	
	SMART	SM013915:SM01391	86	75	10057	6.23869224826201	0.8851839440013184	0.3790423250569996	0.246205981	6.23869224826201	0.8851839440013184	0.3790423250569996	0.246205981
	UP_SEQ_FEATURE	region of interest:linker 12	195	68	20063	6.052187028657617	0.93747359147345887	0.93747359147345887	0.454874786880198	6.052187028657617	0.93747359147345887	0.454874786880198	0.454874786880198
	UP_SEQ_FEATURE	region of interest:linker 11	195	64	18859	5.948397845897456	0.93747359147345887	0.93747359147345887	0.4484841310857467	5.948397845897456	0.93747359147345887	0.4484841310857467	0.4484841310857467
	INTERPRO	IPR018389:intermediate filament protein, conserved site	195	64	18859	4.1323293187656	0.93747359147345887	0.93747359147345887	0.4484841310857467	4.1323293187656	0.93747359147345887	0.4484841310857467	0.4484841310857467
	GOTERM_CC_DIRECT	GO:0005827:intermediate filament	195	113	18224	4.1323293187656	0.93747359147345887	0.93747359147345887	0.16713305192761327	4.1323293187656	0.93747359147345887	0.16713305192761327	0.16713305192761327
	UP_SEQ_FEATURE	region of interest:coil 1A	195	74	20063	5.56146161469161	0.93747359147345887	0.93747359147345887	0.4085463475	5.56146161469161	0.93747359147345887	0.4085463475	0.4085463475
	UP_SEQ_FEATURE	region of interest:coil 1B	195	74	20063	5.56146161469161	0.93747359147345887	0.93747359147345887	0.4085463475	5.56146161469161	0.93747359147345887	0.4085463475	0.4085463475
UP_SEQ_FEATURE	region of interest:linker 1	195	74	20063	5.56146161469161	0.93747359147345887	0.93747359147345887	0.4085463475	5.56146161469161	0.93747359147345887	0.4085463475	0.4085463475	
UP_SEQ_FEATURE	region of interest:head	195	75	20063	5.48731623931624	0.93747359147345887	0.93747359147345887	0.1518008183280505	5.48731623931624	0.93747359147345887	0.1518008183280505	0.1518008183280505	
UP_NEWWORDS	intermediate filament	4	20581	20581	4.82738382783883	0.93747359147345887	0.93747359147345887	0.17600624924763127	4.82738382783883	0.93747359147345887	0.17600624924763127	0.17600624924763127	
UP_SEQ_FEATURE	region of interest:head	195	77	20063	5.34478854478854	0.93747359147345887	0.93747359147345887	0.150024959769575	5.34478854478854	0.93747359147345887	0.150024959769575	0.150024959769575	
UP_SEQ_FEATURE	region of interest:tail	195	79	20063	5.208477442388855	0.93747359147345887	0.93747359147345887	0.1518008183280505	5.208477442388855	0.93747359147345887	0.1518008183280505	0.1518008183280505	
UP_SEQ_FEATURE	region of interest:coil 1B	195	36	20063	8.579318216761074	0.93747359147345887	0.93747359147345887	0.1518008183280505	8.579318216761074	0.93747359147345887	0.1518008183280505	0.1518008183280505	
UP_SEQ_FEATURE	region of interest:coil 1A	195	36	20063	8.579318216761074	0.93747359147345887	0.93747359147345887	0.1518008183280505	8.579318216761074	0.93747359147345887	0.1518008183280505	0.1518008183280505	
GOTERM_CC_DIRECT	GO:040505:weat filament	195	100	18224	2.8083927692308	1.0	0.64379751846968	0.64379751846968	2.8083927692308	1.0	0.64379751846968	0.64379751846968	
UP_NEWWORDS	Keratin	3	1.5846	1.53861538615385	0.4229262834651246	0.93747359147345887	0.93747359147345887	0.822676506888866	0.4229262834651246	0.93747359147345887	0.822676506888866	0.822676506888866	
Annotation Cluster 35	Enrichment Score: 1.27579482025114												
Annotation Cluster 35	Category	Term	Count	%	PValue	Genes	List Total	Pop Hts	Pop Total	Fold Enrichment <td>Benjamini</td> <td>FDR</td>	Benjamini	FDR	
	GOTERM_BP_DIRECT	GO:0043488:regulation of mRNA stability	9	4.615	13861	2.538770024407338E-5	PSMA2, YWHAZ, PSMB1, PSMB2, HSPB1, HSPB1, APOB1, RPS27A, HSP48	195	108	16792	7.524421209858104	0.001480756859282032	0.000431148
	GOTERM_CC_DIRECT	GO:0000502:proteinosome complex	6	2.564	10206	0.0034167160130873197	PSMA2, PSMB1, PSMB2, VCP, HSPB1	195	60	18224	7.786031418038188	0.7044877616347823	0.292951549702372
	GOTERM_BP_DIRECT	GO:0060077:Wnt signaling pathway	195	92	16792	5.66053517006666	0.93747359147345887	0.93747359147345887	0.1080656375196599	5.66053517006666	0.93747359147345887	0.1080656375196599	0.1080656375196599
	GOTERM_BP_DIRECT	GO:0032970:Wnt receptor-mediated signaling pathway	195	118	16792	4.786118921749728	0.93747359147345887	0.93747359147345887	0.1515211772149728	4.786118921749728	0.93747359147345887	0.1515211772149728	0.1515211772149728
	GOTERM_BP_DIRECT	GO:0051434:Wnt receptor-mediated signaling pathway	195	66	16792								

Category	Term	Count	%	PValue	Genes	Pop/Total	Pop/Hits	Fold Enrichment	Benfoni	FDR		
GOTERM_BP_DIRECT	GO:0002225~regulation of C-type lectin receptor signaling pathway	4	2.051282051282051	0.1218606362765141	PSMA2, PSMB1, PSMA, RPS27A	195	105	16792	3.280486004884003	1.0	0.77692127374163	0.88218897
GOTERM_BP_DIRECT	GO:0000225~positive regulation of canonical Wnt signaling pathway	4	2.051282051282051	0.1618148317891188	PSMA2, PSMB1, PSMA, RPS27A	195	100	16792	2.870427594275505	1.0	0.737952037291125	0.9452882308
GOTERM_BP_DIRECT	GO:0004779~antigen processing and presentation of exogenous peptide antigen via MHC class I, TAP-dependent	3	1.5384615384615385	0.16478853967087292	PSMA2, PSMB1, PSMA, RPS27A	195	63	16792	4.100610506105	1.0	0.8433995430084459	0.94840604
KEGG_PATHWAY	h04050~Protein processing - eukaryotic	140	44	6879	3.501398093943883	195	140	6879	2.113198093943883	1.0	0.558259477324477	0.950600655
GOTERM_BP_DIRECT	GO:0000909~negative regulation of canonical Wnt signaling pathway	4	2.051282051282051	0.29044116783884	PSMA2, PSMB1, PSMA, RPS27A	195	163	16792	1.955119562085435	1.0	0.938447885680034	0.998485022
GOTERM_BP_DIRECT	GO:0000295~Fc-epsilon receptor signaling pathway	3	1.5384615384615385	0.356739385738883	PSMA2, PSMB1, PSMA, RPS27A	195	184	16792	1.872017872528585	1.0	0.9808385935203409	0.992995579
GOTERM_BP_DIRECT	GO:0000165~NADAP-catabolic	5	2.564102564102564	0.3586957164762951	PSMA2, PSMB1, PSMA, RPS27A	195	262	16792	1.643174417267507	1.0	0.93094916785053076	0.959338244
Annotation Cluster 36												
GOTERM_MF_DIRECT	GO:0000505~electron carrier activity	7	3.589745389745389	5.962386769703426	AKR1B1, UGDH, ALDH2, TYMRD1, COX5A, POF1A	195	168	16881	6.735162391623925	0.62273941228556	0.1010434240869429012	0.008575864
GOTERM_BP_DIRECT	GO:0000378~nucleosome	6	3.076230762307623	0.00315823297112046	HST2H3A, HSTH1E, HSTH1B, HSTH1A, HZAT, HZFB, HZFC	195	125	16792	5.92481514326259	0.832851074500112	0.787611018251012	0.85047032
UP_NETWORKS	GO:0000378~nucleosome	5	2.564102564102564	0.01002829638344407	HST2H3A, HSTH1B, HSTH1A, HZAT, HZFB, HZFC	195	89	20581	5.92041514326259	0.828688852917	0.60493741160249845	0.121571332
UP_NETWORKS	GO:0000378~nucleosome	5	2.564102564102564	0.01002829638344407	HST2H3A, HSTH1B, HSTH1A, HZAT, HZFB, HZFC	195	97	20581	5.44038121866178	0.971075524623029	0.773674713595669	0.162198458
INTERPRO	IPR009072~Histone-fold	5	2.564102564102564	0.03038097585339673	HST2H3A, HSTH1B, HSTH1A, HZAT, HZFB, HZFC	195	112	18559	4.248855311305311	0.95959941378969	0.347322600556093	0.38394273
INTERPRO	IPR007125~Histone core	4	2.051282051282051	0.0343707307366978	HST2H3A, HSTH1B, HZAT, HZFB, HZFC	195	68	18559	5.98491704374057	0.95959941378969	0.379318394675919	0.39913273
UP_NETWORKS	GO:0000378~nucleosome	9	4.615384615384615	0.0363002040478886	HST2H3A, KRCC5, HST1H1E, HST1H2B, HSTH1A, KRCC6, HZAF, HZEB, BANF1	195	400	20581	2.37470709207693	0.999937944189814	0.17300105077045436	0.383811037
GOTERM_BP_DIRECT	GO:0006334~nucleosome assembly	5	2.564102564102564	0.0493514648912453	HST2H3A, HSTH1E, HSTH1B, HSTH1A, HZAT, HZFB, HZFC	195	119	16792	3.618183758327497	1.0	0.5151384097814606	0.546628083
KEGG_PATHWAY	h040325~Protein biosynthesis	7	3.589745389745389	0.053468513697094	HST2H3A, HSTH1B, HSTH1A, ACTN1, HZAT, SNRPD1, HZFB	140	134	6879	2.566791047761195	0.99972987975447	0.5432525296482045	0.646208105
GOTERM_BP_DIRECT	GO:0000332~chromatin silencing at DNA	3	1.5384615384615385	0.0679488678133699	HST2H3A, HSTH1A, HZFB	195	37	16792	6.90210582120583	1.0	0.606051322463588	0.686015733
GOTERM_BP_DIRECT	GO:0031492~transcriptional DNA binding	3	1.5384615384615385	0.079384868780993	HST2H3A, HZAT, HZFB	195	46	18881	5.64819397993312	1.0	0.5281237598338534	0.743926452
GOTERM_BP_DIRECT	GO:003104~transcription factor activity, sequence-specific	4	2.051282051282051	0.137232363096913	HST2H3A, HSTH1A, BAN, HZFB	195	51	16792	3.00510582120583	1.0	0.63150033823241	0.8161511
GOTERM_BP_DIRECT	GO:004426~cellular protein metabolic process	4	2.051282051282051	0.154550996275849	HST2H3A, HSTH1A, HZFB, RPS27A	195	118	16792	2.9102786614515427	1.0	0.832501919904514	0.90003603
GOTERM_BP_DIRECT	GO:004581~positive regulation of gene expression, epigenetic	3	1.5384615384615385	0.16071160363086726	HST2H3A, HSTH1A, HZFB	195	62	16792	4.16676897665727	1.0	0.839254561619829	0.944100823
GOTERM_MF_DIRECT	GO:0040582~protein tetramerization activity	8	4.102564102564102	0.077188484630544	HST2H3A, PAH, HSTH1B, HSTH1A, HZAT, HZFB, VMAE1, ITGB1	195	465	16881	1.489336110006274	1.0	0.8851147479240968	0.992546113
GOTERM_MF_DIRECT	GO:0042397~telomere binding	3	1.5384615384615385	0.4102677199551345	HST2H3A, HSTH1A, HZFB	195	122	16881	2.12875157629256	1.0	0.9608055024709466	0.999511112
KEGG_PATHWAY	h040340~Alcoholism	5	2.564102564102564	0.402679150033842	HST2H3A, HSTH1B, HSTH1A, HZAT, HZFB, HZFC	140	177	6879	1.388014578450362	1.0	0.80002591066707185	0.95996407
Annotation Cluster 38												
Category	Term	Count	%	PValue	Genes	Pop/Total	Pop/Hits	Fold Enrichment	Benfoni	FDR		
GOTERM_MF_DIRECT	GO:0006919~double-stranded telomeric DNA binding	3	1.5384615384615385	0.00351248752729596	KRCC5, KRCC6, APEX1	195	8	18881	32.4636153861538	0.840278533811154	0.04095375733695826	0.059580111
GOTERM_BP_DIRECT	GO:0000378~nucleosome	4	2.051282051282051	0.01764415023801908	KRCC5, KRCC6, APEX1	195	48	16792	7.1706497608876	0.999599989882697	0.784217468811725	0.27269882
GOTERM_BP_DIRECT	GO:0006848~telomeric region	3	1.5384615384615385	0.0127244341251672	KRCC5, HSTH1A, KRCC6, PCNA, HZFB, APEX1	195	30	18224	4.393474084906909	0.883303954774239	0.8431383223262	0.99816556
GOTERM_BP_DIRECT	GO:0006848~telomeric region	4	2.051282051282051	0.015828030978834	KRCC5, KRCC6, PCNA, APEX1	195	63	18881	4.498454096509695	0.9595999895956451	0.2596510692999567	0.410087474
UP_NETWORKS	GO:0006848~telomeric region	3	1.5384615384615385	0.1778208478961612	KRCC5, KRCC6, APEX1	195	81	20581	3.900218402355176	1.0	0.556500767077797	0.92158462
GOTERM_BP_DIRECT	GO:0003107~DNA recombination	3	1.5384615384615385	0.248897462829235	KRCC5, KRCC6, APEX1	195	83	16792	3.112511584807416	1.0	0.9432424348049451	0.991088421
UP_NETWORKS	GO:0006848~telomeric region	5	2.564102564102564	0.238745815784397	KRCC5, VCP, KRCC6, PCNA, APEX1	195	293	20581	1.801189149208016	1.0	0.7300774449405238	0.990385142
UP_NETWORKS	GO:0006848~telomeric region	5	2.564102564102564	0.2227326576428657	KRCC5, VCP, KRCC6, PCNA, APEX1	195	332	20581	1.469198719487818	1.0	0.819812954956688	0.999426293
UP_NETWORKS	GO:0006848~telomeric region	7	3.589745389745389	0.044116052700846	KRCC5, HNRNP, NME1, KRCC6, PTP1, TXN, APEX1	195	661	20581	1.11770821100525	1.0	0.9256888271971754	0.999992617
Annotation Cluster 39												
Category	Term	Count	%	PValue	Genes	Pop/Total	Pop/Hits	Fold Enrichment	Benfoni	FDR		
GOTERM_BP_DIRECT	GO:0000225~positive regulation of canonical Wnt signaling pathway	4	2.051282051282051	0.2110040378894	KRCC5, C10orf113, HNRPA2B1	195	105	16792	3.2110040378894	0.999599999999999	0.8117401	0.94840604
GOTERM_BP_DIRECT	GO:0000225~positive regulation of canonical Wnt signaling pathway	4	2.051282051282051	0.17044415023801908	HNRNP, HNRNP, PTP1, HNRPA2B1	195	48	16792	7.1706497608876	0.999599989882697	0.784217468811725	0.27269882
UP_NETWORKS	GO:0000225~positive regulation of canonical Wnt signaling pathway	3	1.5384615384615385	0.02864463768332715	HNRNP, HNRNP, PTP1, HNRPA2B1	195	28	20581	11.30824175824176	0.99948888327251	0.148659716518973	0.31461801
UP_NETWORKS	GO:0000225~positive regulation of canonical Wnt signaling pathway	5	2.564102564102564	0.03260626789160886	HNRNP, HNRNP, HNRPA2B1, SNRPD1, HSP48	195	127	20581	4.1525949724006	0.999816634437082	0.16104011921519001	0.349388197
GOTERM_CC_DIRECT	GO:010013~viral nucleocapsid	3	1.5384615384615385	0.0355023348523382	HNRNP, HNRNP, SNRPD1	195	28	18224	10.01318681386813	0.99990331232076	0.1777510504255532	0.386291918
UP_NETWORKS	GO:0000225~positive regulation of canonical Wnt signaling pathway	8	3.589745389745389	0.037158093542883	HNRNP, C10orf113, HNRPA2B1, SNRPD1, HSP48	195	260	20581	2.844558186404339	0.99994892728809	0.173075699041143	0.380580813
UP_NETWORKS	GO:0000225~positive regulation of canonical Wnt signaling pathway	7	3.589745389745389	0.037158093542883	HNRNP, C10orf113, HNRPA2B1, SNRPD1, HSP48	195	332	20581	2.543219079966108	0.99996454928837	0.1758018325839078	0.400610545
UP_NETWORKS	GO:0000225~positive regulation of canonical Wnt signaling pathway	3	1.5384615384615385	0.044116052700846	HNRNP, HNRNP, NUDT21, PTP1, HNRPA2B1, SNRPD1, HSP48	195	222	16792	2.7152691152691153	1.0	0.4886131562032547	0.526001169
GOTERM_CC_DIRECT	GO:0070102~catalytic step 2 spliceosome	4	2.051282051282051	0.0720797626832	HNRNP, HNRNP, SNRPD1	195	47	20581	6.7982487292409	0.999999972754791	0.1013204970578917	0.635679447
GOTERM_BP_DIRECT	GO:0000225~positive regulation of canonical Wnt signaling pathway	3	1.5384615384615385	0.07580974967629315	HNRNP, HNRNP, HNRPA2B1, SNRPD1	195	92	18224	4.08332125061331	0.999999999999999	0.3324267177129584	0.651002823
GOTERM_BP_DIRECT	GO:0000225~positive regulation of canonical Wnt signaling pathway	3	1.5384615384615385	0.07580974967629315	HNRNP, HNRNP, SNRPD1	195	92	16792	2.862381068493319	1.0	0.956601748807680	0.977186821
UP_NETWORKS	GO:0000225~positive regulation of canonical Wnt signaling pathway	4	2.051282051282051	0.141016232651739	HNRNP, HNRNP, SNRPD1	195	125	20581	2.469292027699308	1.0	0.957560810821288	0.98292009
UP_SEQ_FEATURE	domainRBM1	3	1.5384615384615385	0.3411016232651739	HNRNP, PTP1, HNRPA2B1	195	125	20063	2.469292027699308	1.0	0.957560810821288	0.98292009
UP_SEQ_FEATURE	domainRBM2	3	1.5384615384615385	0.3411016232651739	HNRNP, PTP1, HNRPA2B1	195	125	20063	2.469292027699308	1.0	0.957560810821288	0.98292009
KEGG_PATHWAY	h040405~Spliceosome	4	2.051282051282051	0.056400023209886	HNRNP, SNRPD1, HSP48, HSP48	140	133	6879	1.47776584179377	1.0	0.111353800185725	0.999781172
SMART	SM03688~RBM	3	1.5384615384615385	0.338222768633003	HNRNP, PTP1, HNRPA2B1	86	122	10057	1.654837648091268	1.0	0.997261659321173	0.999789933
GOTERM_MF_DIRECT	GO:0000378~nucleosome	5	2.564102564102564	0.059138197934282	HSP90AA1, HNT1, HNRNP, PTP1, HNRPA2B1	195	348	16881	1.24810769142352	1.0	0.931828267672	0.999994827
GOTERM_BP_DIRECT	GO:0000378~nucleosome	3	1.5384615384615385	0.077898960408883	CLBP, PTP1, SNRPD1	195	166	16792	1.5562516746562878	1.0	0.99907899203933	0.99999443
INTERPRO	IPR02054~RNA recognition motif domain	3	1.5384615384615385	0.086726929232654	HNRNP, PTP1, HNRPA2B1	195	264	18559	1.263376446562878	1.0	0.99999440491718	0.999999955
INTERPRO	IPR02077~Nucleotide-binding, alpha-beta sheet	3	1.5384615384615385	0.076593029232654	HNRNP, PTP1, HNRPA2B1	195	264	18559	1.085150805628067	1.0	0.999999976837406	0.999999955
GOTERM_MF_DIRECT	GO:0000225~positive regulation of canonical Wnt signaling pathway	6	3.076230762307623	0.08169473782654	HNRNP, EF02, PTP1, HNRPA2B1, AANS, ZNF331	195	985	18881	0.5273252525689184	1.0	0.959599999999999	0.

4. DISCUSSÃO GERAL

O câncer de pulmão é o mais incidente no mundo, sendo o líder em causa de mortes relacionada a essa patologia. Na maioria dos casos, o seu diagnóstico é realizado em estágios avançados da doença, o que gera a necessidade da utilização de agentes quimioterápicos no tratamento. A CDDP é um fármaco utilizado para diferentes tipos de câncer, incluindo o de pulmão, mas apesar de sua eficácia, a resistência tumoral à CDDP é frequente, sendo um fator relevante que limita o sucesso do tratamento. Os diferentes mecanismos de resistência incluem reparo ao dano no DNA, alteração de vias de sinalização apoptótica, detoxificação por moléculas redutoras e alterações no metabolismo bioenergético. Vias metabólicas e processos relacionados à bioenergética já foram descritos como potenciais eventos moleculares relacionados à resistência tumoral. Contudo, os diferentes *trade-offs* bioenergéticos e a regulação do metabolismo em células resistentes à CDDP ainda é pouco compreendido.

O presente estudo teve como objetivo o melhor entendimento do metabolismo e necessidades bioenergéticas de células NSCLC com resistência adquirida à CDDP, assim, caracterizando potenciais *trade-offs* envolvidos com a resistência à droga. Para isso, células da linhagem de adenocarcinoma de pulmão humano A549 foram expostas a concentrações baixas e crescentes de CDDP com o intuito de desenvolver sublinhagens com resistência adquirida à droga. Desse modo, considerando o interesse em identificar mecanismos frequentemente envolvidos com a resistência tumoral à CDDP, estas linhagens foram desenvolvidas em triplicata, sendo consideradas replicatas biológicas em todos os experimentos. Além disso, os níveis de resistência obtidos para a sublinhagem A549/CDDP foram considerados clinicamente relevantes, visto que na clínica os tumores resistentes apresentam níveis de resistência de 2 a 5 vezes maiores após o tratamento quimioterápico (MCDERMOTT et al., 2014).

Estudos proteômicos prévios do nosso grupo, utilizando o mesmo modelo de sublinhagens resistentes, identificaram um grande número de proteínas reguladas negativamente nas células A549/CDDP. Entre elas, estão proteínas relacionadas a diversas vias de obtenção de energia. Com o propósito do melhor entendimento da regulação destas vias, foram realizados ensaios de RT-qPCR, comparando a expressão gênica relativa entre as células A549 e A549/CDDP. Por essa razão, os genes escolhidos para estas análises incluíram enzimas de diferentes vias bioenergéticas e reguladores da expressão gênica.

Os ensaios de RT-qPCR revelaram uma redução significativa na expressão das enzimas HK2 e LDHA em células A549/CDDP em comparação com a linhagem sensível A549. Após a entrada da molécula de glicose na célula, HK2 é responsável por sua fosforilação, sendo considerado este o primeiro passo da glicólise (KOCH et al., 2020). Com isso, a manutenção da via glicolítica está diretamente relacionada a HK2. Enzimas homólogas a HK2, como HK1, HK3 e HK4, podem estar envolvidas nesta etapa suprindo a falta de HK2. Contudo, estas enzimas apresentam menor eficiência comparadas a HK2 por exibirem menor afinidade ao substrato ou conterem menos subunidades catalíticas. Da mesma forma, HK2 é usualmente relacionada com a regulação da via glicolítica por reguladores metabólicos em comparação com as enzimas homólogas (KRASNOV et al., 2013). A expressão de HK2 também está fortemente relacionada com o crescimento tumoral (WANG et al., 2016a), desse modo, sua regulação negativa em células A549/CDDP pode ser responsável pela reduzida taxa proliferativa e capacidade clonogênica dessa linhagem em comparação com a linhagem parental A549. A atividade de LDHA também está relacionada com a progressão e capacidade de invasão do câncer (CAI et al., 2019), e sua expressão reduzida na sublinhagem resistente pode estar relacionada com sua capacidade de proliferação reduzida. LDHA é responsável pela conversão de piruvato a lactato, acoplado com a oxidação de NADH para NAD⁺, sendo a última etapa da glicólise. Este processo reduz a dependência por O₂, regula a via glicolítica e está relacionado com a resposta a diferentes situações fisiológicas como injúria em tecidos, necrose, hipóxia, hemólise e infarto do miocárdio (MIAO et al., 2013). Além da regulação negativa destas enzimas, o transportador de glicose GLUT1 apresentou expressão reduzida em células A549/CDDP, todavia, não apresentou diferença estatística devido à variação na expressão entre as réplicas biológicas das sublinhagens resistentes. Ainda, as enzimas da via glicolítica GPI, TPI1, GAPDH, PGAM1, PGM1, PGK1, ENO1, PKM, LDHA e LDHB, foram identificadas reguladas negativamente em células A549/CDDP nas análises proteômicas. A redução da expressão constatada pelas análises de expressão gênica por RT-qPCR e proteômica geral nas células A549/CDDP confirma a regulação negativa da via glicolítica e, conseqüentemente, uma possível redução na atividade desta via em células A549/CDDP.

Entre os reguladores avaliados, o regulador negativo da glicólise *Fructose-2,6-bisphosphatase TIGAR* (TIGAR) foi encontrado regulado positivamente na linhagem A549/CDDP, indicando uma possível participação deste repressor da via glicolítica na regulação do metabolismo das células resistentes. A expressão do gene TIGAR pode estar associado com a resistência a morte celular, visto que seu silenciamento em células tumorais já

foi associado a maior susceptibilidade a estresses como hipóxia, irradiação e ao quimioterápico temozolomida (MAURER et al., 2019). Um dos fatores determinantes do efeito de TIGAR na resistência a morte celular é a diminuição de ROS associada a expressão deste gene. A maior expressão de TIGAR gera o aumento de NADPH intracelular, molécula que participa da reação de redução de glutatona, conseqüentemente aumentando a concentração de GSH na célula (BENSAAD et al., 2006). Este processo também foi relacionado com a resposta de células tumorais à epirrubicina, agente anticâncer intercalante de DNA. Ensaios *in vitro* e *in vivo* revelaram a maior citotoxicidade desta droga após o silenciamento gênico de TIGAR, levando a diminuição de NADPH, aumento de ROS e apoptose (XIE et al., 2014). Visto o importante papel deste regulador na resposta a quimioterápicos, a maior expressão de TIGAR em células A549/CDDP pode estar relacionada a resistência desta linhagem. Outros reguladores do metabolismo bioenergético também foram avaliados, mas não apresentaram diferença entre células A549 e A549/CDDP. Entre eles está o fator de transcrição HIF-1 (*hypoxia inducible factor 1*), que apresenta um papel fundamental na regulação da glicólise (MASOUD; LI, 2015); o fator de transcrição mestre *Myc proto-oncogene protein* (c-Myc), o qual está relacionado com a regulação positiva da glicólise, incluindo situações de normóxia, e glutaminólise (QU et al., 2018); e o fator de montagem do citocromo c oxidase (COX), *synthesis of cytochrome C oxidase 2* (SCO2), um dos principais reguladores positivos da obtenção de energia pela cadeia transportadora de elétrons (MADAN et al., 2011).

A ampla utilização de glutamina em diferentes processos biológicos e a alteração de enzimas relacionadas ao metabolismo deste aminoácido constatada pela análise proteômica gerou a necessidade de um melhor entendimento da expressão destes genes em células A549/CDDP. Foram avaliadas as expressões das enzimas *Aspartate aminotransferase, cytoplasmic* (GOT1), *Aspartate aminotransferase, mitochondrial* (GOT2) e *Glutamate dehydrogenase 1, mitochondrial* (GLUD1), e a proteína de ligação ao nucleotídeo guanina *GTPase KRas* (KRAS) a nível de RNA. Os genes codificadores destas proteínas apresentaram uma redução na expressão relativa em células A549/CDDP. No entanto, apenas GOT1 e GLUD1 apresentaram diferença significativa nas suas expressões. A utilização da glutamina como fonte de energia consiste na internalização do aminoácido na mitocôndria e a conversão em glutamato, podendo este ser convertido em α -cetoglutarato (α -KG) pela enzima GLUT1, liberando uma molécula de amônia e prontamente incorporado α -KG no ciclo do TCA. Aminotransferases são enzimas capazes de converter glutamato em α -KG sem a produção de amônia, entre estas enzimas então as transaminases glutâmico-oxaloacéticas (GOT), também

conhecidas como aspartato aminotransferases, que transferem o nitrogênio proveniente do glutamato para oxaloacetato (OAA) produzindo α -KG e aspartato (ALTMAN et al., 2016).

Apesar da diminuição na expressão de enzimas relacionadas ao metabolismo de glutamina a nível de RNA nas células resistentes à CDDP, os dados proteômicos foram discordantes, indicando um aumento das enzimas GOT1 e GOT2. Tendo em vista os diferentes níveis e a complexidade da regulação da expressão gênica, dados discordantes entre expressão de RNA e proteína são frequentes, e esta falta de correlação já foi descrita em células de adenocarcinoma de pulmão (CHEN et al., 2002). O aumento da presença das enzimas GOT1 e GOT2 em células A549/CDDP, enquanto a expressão de RNA está reduzida, pode ser efeito do aumento da estabilidade destas proteínas. Este evento pode ser dado por fatores como alteração em processos de ubiquitinação e desubiquitinação, e alteração na regulação da montagem e atividade do proteassomo (CAI et al., 2018; ROUSSEAU; BERTOLOTTI, 2018). Os resultados obtidos no presente estudo não permitiram inferir uma diminuição ou aumento da participação desta via no metabolismo de células A549/CDDP. Contudo, os dados apresentaram uma alteração na regulação da expressão gênica em níveis de RNA e proteína.

A análise de respirometria de alta resolução foi realizada utilizando Oxygraph-2k (O2k, OROBOROS INSTRUMENTS, Austria), um respirômetro de alta precisão que permite a análise em tempo real da variação de O₂ no meio em uma resolução na escala de pmol de O₂. O instrumento é dotado de duas câmaras onde permite a avaliação de duas amostras simultaneamente (LONG et al., 2019). Neste contexto, foram realizados ensaios de respirometria analisando simultaneamente o consumo de O₂ por células A549 e A549/CDDP a fim de minimizar possíveis erros experimentais.

A respiração basal - ou de rotina - de células A549/CDDP se apresentou diminuída. Estes dados indicam uma possível redução na atividade mitocondrial ou uma possível redução em massa mitocondrial da célula. Além disso, foi identificada a redução em consumo de oxigênio ligado a síntese de ATP (ATP-linked), indicando uma redução em OXPHOS. A diminuição da atividade mitocondrial em células de câncer é frequentemente associada à disfunção e ao dano mitocondrial, resultando na permeabilidade da membrana interna da mitocôndria (BRISTON et al., 2019). Contudo, o vazamento de prótons, consequente da permeabilidade da membrana interna (*proton leak*), foi encontrado diminuído em células A549/CDDP. *Proton leak* é resultado de diversos fatores, entre eles está a participação de mecanismos envolvidos com regulação da homeostase mitocondrial como proteínas de

desacoplamento (UCPs, do inglês *uncoupling proteins*) e poro de transição de permeabilidade mitocondrial (mPTP, do inglês *mitochondrial permeability transition pore*). O desemparelhamento da transferência de elétrons pelos complexos I-IV e a atividade do complexo V, ou ATP sintase, pode gerar um aumento na diferença de potencial mitocondrial o que leva ao aumento de ROS. Este aumento da diferença no potencial mitocondrial pode ser remediado por UCPs, visto sua função de diminuição do potencial mitocondrial (BAFFY, 2017). Além de UCPs, outro mecanismo relacionado à permeabilidade da membrana interna da mitocôndria é a ativação de mPTP. Esta ativação é mediada principalmente por ROS, compostos nítricos oxidativos e íons Ca^{2+} (ZOROV et al., 2014). Considerando a relação destes mecanismos com desequilíbrio na homeostase mitocondrial, a diminuição de *proton leak* células A549/CDDP indica uma ausência destes mecanismos e, conseqüentemente, uma atividade mitocondrial regulada.

A capacidade de respiração máxima teórica não apresentou diferença entre as linhagens, o que indica uma possível similaridade no conteúdo mitocondrial das células A549 e A549/CDDP. Ainda, a capacidade reserva de respiração não apresentou diferença entre as linhagens, sendo um indício de que células A549/CDDP não apresentam maiores demandas de energia pela respiração mitocondrial comparada com células A549. Outro parâmetro similar entre as linhagens foi o consumo de oxigênio residual (ROX). A taxa de ROX pode ser influenciada principalmente pela quantidade de ROS da célula ou por enzimas que consomem oxigênio, como NADPH-oxidase, monoaminoxidase, enzimas da família citocromo P450, heme oxidase e xantina oxidase (WAGNER et al., 2011). Sendo ROS um dos principais fatores de alteração de ROX, pode ser inferido uma semelhança em quantidade de ROS entre as linhagens.

A capacidade clonogênica reduzida de células resistentes à CDDP já foi relacionada com a maior presença de ROS intracelular, e este efeito pode ser reduzido pela presença de GSH no meio de cultivo (DUAN et al., 2017). Com isso, foram realizados ensaios clonogênicos na presença de GSH para avaliar a participação de ROS na capacidade clonogênica reduzida de células A549/CDDP. As linhagens A549 e A549/CDDP não apresentaram aumento de clonogenicidade na presença deste antioxidante, o que indica que a capacidade clonogênica reduzida de A549/CDDP não é proveniente de um efeito de ROS. Além disso, o tratamento de células A549 e A549/CDDP com agentes pró-oxidantes apresentou efeito similar em ambas as linhagens. As moléculas DEM e BSO estão diretamente relacionados com o controle da presença de GSH na célula, e o seu efeito citotóxico é resultado do estresse oxidativo gerado

pela ausência desta molécula e, conseqüentemente, ativação de vias apoptóticas (LI et al., 2016; PRIYA et al., 2014). Os dados obtidos indicam similaridade no equilíbrio redox e manutenção de GSH nas diferentes linhagens. Conjuntamente com a similaridade de ROX entre células A549 e A549/CDDP, estas evidências corroboram a hipótese de uma similaridade em ROS e moléculas oxidantes nas linhagens, além da similaridade de resposta ao estresse.

A vulnerabilidade metabólica vem sendo frequentemente associada a células resistentes a CDDP, visto a maior sensibilidade a inibidores metabólicos e a desvantagem no crescimento em ambiente com nutrientes reduzidos, e este fenótipo já foi descrito tanto *in vitro* quanto *in vivo* (CATANZARO et al., 2015; OBRIST et al., 2018; XU et al., 2018). A sublinhagem desenvolvida no presente estudo mostrou este fenótipo de vulnerabilidade quando cultivada na ausência de glicose e L-glutamina. As células A549 e A549/CDDP foram afetadas pela ausência destas fontes bioenergéticas, contudo, a sublinhagem resistente foi significativamente mais afetada. A menor habilidade de adaptação a variação de fontes essenciais de energia pode representar uma redução da capacidade de plasticidade metabólica nas células resistentes (LEHÚEDE et al., 2016). Mecanismos de regulação da expressão gênica em células A549/CDDP podem gerar uma limitação quanto a plasticidade e reprogramação metabólica nestas células, sendo uma possível consequência de *trade-offs* selecionados durante a exposição à CDDP. Com vias metabólicas essenciais menos ativas, a variação destes substratos pode ser determinante para a sobrevivência da célula. Além disso, a presença de 2-DG, molécula análoga a glicose, apresentou maior citotoxicidade em células A549/CDDP. 2-DG é amplamente conhecido pelo seu efeito específico de inibição da via glicolítica, sendo um inibidor análogo a glicose. Esta molécula inibe a fosforilação de glicose pela hexokinase, reduzindo a disponibilidade de energia na célula e ativando vias apoptóticas (ZHANG et al., 2006). Com a menor expressão de HK2 nas células A549/CDDP, identificada pela análise proteômica e RT-qPCR, acredita-se que a inibição da via glicolítica utilizando 2-DG seja mais efetiva nestas células. A menor expressão de HK1 e 2, e sua correlação com a maior citotoxicidade de 2-DG, já foi descrita em células de SCLC e NSCLC resistentes à CDDP (SULLIVAN et al., 2014). Os resultados obtidos nesse trabalho reforçam o indício da potencial utilização desse composto inibidor de glicólise combinado com CDDP como um tratamento promissor. O inibidor 3-BrP, por sua vez, apesar de inibir a atividade de enzimas glicolíticas, não é limitado a esta via, podendo atuar como inibidor da atividade mitocondrial (SHOSHAN, 2012). Este fator pode ter sido determinante na citotoxicidade deste inibidor nas células A549 e A549/CDDP. Com isso, a diferença de citotoxicidade deste inibidor da via glicolítica não foi apresentada entre as

linhagens. Visto que células A549 apresentaram maior respiração mitocondrial e respiração ligada a síntese de ATP, 3-BrP pode ter afetado esta atividade essencial nas células sensíveis à CDDP.

A análise proteômica identificou uma vasta gama de processos biológicos regulados negativamente em células A549/CDDP. Entre estes mecanismos, também foram encontrados termos funcionais envolvidos com a tradução de RNA como “*translation*”, “*translational initiation*” e “*translational elongation*”. Considerando estes resultados e a regulação negativa de diferentes processos bioenergéticos em células A549/CDDP, uma possível regulação global da tradução nestas células foi investigada. A regulação global da tradução pode ser resultado da alteração do complexo de iniciação da tradução ou através da modulação do alongamento (ZHAO et al., 2019). Estes tipos de alterações podem ser determinantes para o desenvolvimento e progressão do câncer, visto a potencialidade de conferir características consideradas *hallmarks* do câncer - como o aumento do crescimento da proliferação, a resistência à morte celular e a desregulação de mecanismos controle de crescimento (PELLETIER et al., 2015). Fatores de iniciação eucarióticos eIF2 α e eIF4E participam diretamente da montagem do complexo de tradução de RNA e a regulação destes já foi relacionada como a resistência à CDDP (JU et al., 2017; ZHANG et al., 2018). Neste cenário, a expressão de eIF2 α e *eIF4E-binding protein 1* (4E-BP1) foi avaliada, assim como a fosforilação destas, no intuito de entender uma possível alteração na tradução global de células A549/CDDP.

A regulação da expressão de eIF2 α pode ser determinante na regulação da tradução global da célula. Além disso, a fosforilação deste fator por diferentes quinases tendo como alvo Ser51 altera sua afinidade com o complexo eIF2 e influencia em sua atividade, regulando a iniciação da tradução (OHNO, 2018). O complexo eIF2 é composto pelas subunidades α , β e γ , combinada com guanossina trifosfato (GTP), eIF2-GTP. Este complexo fornece o tRNA iniciador para a iniciação da tradução e, após este processo, é liberado como eIF2-GDP (guanossina difosfato). O complexo eIF2 pode ser reciclado pela substituição de GDP por GTP, que é catalisada por eIF2 β . A fosforilação de eIF2 α altera a sua afinidade por eIF2 β que impede sua atividade (WEK, 2018). O impedimento da reciclagem deste complexo diminui sua disponibilidade para o início da tradução, reduzindo a ocorrência deste evento. eIF2 α apresentou uma expressão similar entre as linhagens A549 e A549/CDDP, assim como sua forma fosforilada. A razão entre proteína fosforilada e não fosforilada também não apresentou diferença entre as linhagens A549 e A549/CDDP. Estes resultados indicaram que eIF2 α não

está diferentemente regulado em células sensíveis e resistentes. Além disso, sua fosforilação não estaria associada a uma eventual redução na tradução de RNA em células A549/CDDP.

Além de eIF2 α , 4E-BP1 é um dos principais reguladores da tradução dependente de cap. O efeito regulador de 4E-BP1 é resultado da sequestro de eIF4E, impedindo a participação deste no processo de iniciação da tradução (QIN et al., 2016). Visto que eIF4E é um fator limitante no recrutamento do RNA para o complexo de iniciação, a sua captura pode ser responsável pela diminuição na tradução global da célula. A interação de eIF4E e 4E-BP1 também pode ser regulada por eventos de fosforilação. A fosforilação de resíduos como Thr37 e Thr46 em 4E-BP1 reduz a afinidade entre estas proteínas, impedindo a sua interação (GINGRAS et al., 1999). Apesar de não apresentar diferença significativa entre as linhagens, 4E-BP1 foi encontrado duas vezes aumentado em células A549/CDDP. Além disso, a razão entre phospho-4E-BP1 (Thr37/46) e 4E-BP1 não fosforilada foi significativamente diminuída em células A549/CDDP. O possível aumento da expressão desta proteína e a menor razão entre sua isoforma fosforilada e hipofosforilada nas células resistentes indicam uma maior presença de 4E-BP1 na sua isoforma ativa para a interação com eIF4E. Com isso, estes resultados indicam uma participação de 4E-BP1 na inibição global da tradução em células resistentes à CDDP.

Por fim, os resultados obtidos por este trabalho permitiram a identificação de alterações metabólicas e bioenergéticas em células de adenocarcinoma de pulmão sensíveis e resistentes à CDDP, assim como propor uma possível regulação global da tradução em células A549/CDDP mediada por 4E-BP1. Contudo, a validação da diminuição global da tradução em células A549/CDDP se faz necessária. Ademais, estudos posteriores são essenciais para elucidar outros possíveis mecanismos de regulação envolvidos neste processo. A identificação destas vias regulatórias determinantes para células A549/CDDP proporcionará uma maior compreensão de possíveis mecanismos de resistência recorrentes no tratamento do câncer de pulmão.

5. PERSPECTIVAS

- I. Ensaio de validação de redução global da tradução nas células A549/CDDP utilizando *Bioorthogonal Click Chemistry*;
- II. Confirmação do envolvimento da redução global da tradução na resistência à CDDP;
- III. realização de endo- e exo- metabolômica para o melhor entendimento do metabolismo das células A549/CDDP;

6. REFERÊNCIAS

- AI, Zhihong; LU, Yang; QIU, Songbo; FAN, Zhen. Overcoming cisplatin resistance of ovarian cancer cells by targeting HIF-1-regulated cancer metabolism. **Cancer Letters**, [S. l.], v. 373, n. 1, p. 36–44, 2016. DOI: 10.1016/j.canlet.2016.01.009.
- AKTIPIIS, C. Athena; BODDY, Amy M.; GATENBY, Robert A.; BROWN, Joel S.; MALEY, Carlo C. Life history trade-offs in cancer evolution. **Nature reviews. Cancer**, [S. l.], v. 13, n. 12, p. 883–92, 2013. DOI: 10.1038/nrc3606. Disponível em: <http://www.ncbi.nlm.nih.gov/pubmed/24213474>. Acesso em: 12 out. 2018.
- ALOYZ, Raquel et al. Regulation of cisplatin resistance and homologous recombinational repair by the TFIIH subunit XPD. **Cancer research**, [S. l.], v. 62, n. 19, p. 5457–62, 2002. Disponível em: <http://www.ncbi.nlm.nih.gov/pubmed/12359753>.
- ALTMAN, Brian J.; STINE, Zachary E.; DANG, Chi V. From Krebs to clinic: Glutamine metabolism to cancer therapy. **Nature Reviews Cancer**, [S. l.], v. 16, n. 10, p. 619–634, 2016. DOI: 10.1038/nrc.2016.71. Disponível em: [/pmc/articles/PMC5484415/?report=abstract](http://pmc/articles/PMC5484415/?report=abstract). Acesso em: 30 ago. 2020.
- BAFFY, Gyorgy. Mitochondrial uncoupling in cancer cells: Liabilities and opportunities. **Biochimica et Biophysica Acta - Bioenergetics**, [S. l.], v. 1858, n. 8, p. 655–664, 2017. DOI: 10.1016/j.bbabi.2017.01.005.
- BENAM, Kambez H. et al. Engineered In Vitro Disease Models. **Annual Review of Pathology: Mechanisms of Disease**, [S. l.], v. 10, n. 1, p. 195–262, 2015. DOI: 10.1146/annurev-pathol-012414-040418. Disponível em: <http://www.annualreviews.org/doi/10.1146/annurev-pathol-012414-040418>. Acesso em: 12 ago. 2020.
- BENSAAD, Karim; TSURUTA, Atsushi; SELAK, Mary A.; VIDAL, M. Nieves Calvo; NAKANO, Katsunori; BARTRONS, Ramon; GOTTLIEB, Eyal; VOUSDEN, Karen H. TIGAR, a p53-Inducible Regulator of Glycolysis and Apoptosis. **Cell**, [S. l.], v. 126, n. 1, p. 107–120, 2006. DOI: 10.1016/j.cell.2006.05.036.
- BERGSTROM, J.; FURST, P.; NOREE, L. O.; VINNARS, E. Intracellular free amino acid concentration in human muscle tissue. **Journal of Applied Physiology**, [S. l.], v. 36, n. 6, p. 693–697, 1974. DOI: 10.1152/jappl.1974.36.6.693. Disponível em: <https://pubmed.ncbi.nlm.nih.gov/4829908/>. Acesso em: 29 ago. 2020.
- BODDY, Amy M.; HUANG, Weini; AKTIPIIS, Athena. **Life History Trade-Offs in Tumors** **Current Pathobiology Reports** Springer, , 2018. DOI: 10.1007/s40139-018-0188-4. Disponível em: [/pmc/articles/PMC6290708/?report=abstract](http://pmc/articles/PMC6290708/?report=abstract). Acesso em: 16 ago. 2020.
- BRISTON, Thomas; SELWOOD, David L.; SZABADKAI, Gyorgy; DUCHEN, Michael R. Mitochondrial Permeability Transition: A Molecular Lesion with Multiple Drug Targets. **Trends in Pharmacological Sciences**, [S. l.], v. 40, n. 1, p. 50–70, 2019. DOI: 10.1016/j.tips.2018.11.004.
- BUTLER, Stacey J.; RICHARDSON, Lisa; FARIAS, Nathan; MORRISON, Jodi; COOMBER, Brenda L. Characterization of cancer stem cell drug resistance in the human colorectal cancer cell lines HCT116 and SW480. **Biochemical and Biophysical Research Communications**, [S. l.], v. 490, n. 1, p. 29–35, 2017. DOI: 10.1016/j.bbrc.2017.05.176.

Disponível em: <https://pubmed.ncbi.nlm.nih.gov/28576498/>. Acesso em: 12 ago. 2020.

CAI, Hongshi; LI, Jiaxin; ZHANG, Yadong; LIAO, Yan; ZHU, Yue; WANG, Cheng; HOU, Jinsong. LDHA Promotes Oral Squamous Cell Carcinoma Progression Through Facilitating Glycolysis and Epithelial–Mesenchymal Transition. **Frontiers in Oncology**, [S. l.], v. 9, p. 1446, 2019. DOI: 10.3389/fonc.2019.01446. Disponível em: </pmc/articles/PMC6930919/?report=abstract>. Acesso em: 30 ago. 2020.

CAI, Junting; CULLEY, Miranda K.; ZHAO, Yutong; ZHAO, Jing. The role of ubiquitination and deubiquitination in the regulation of cell junctions. **Protein and Cell**, [S. l.], v. 9, n. 9, p. 754–769, 2018. DOI: 10.1007/s13238-017-0486-3. Disponível em: </pmc/articles/PMC6107491/?report=abstract>. Acesso em: 17 set. 2020.

CANTOR, Jason R.; SABATINI, David M. Cancer cell metabolism: One hallmark, many faces. **Cancer Discovery**, [S. l.], v. 2, n. 10, p. 881–898, 2012. DOI: 10.1158/2159-8290.CD-12-0345. Disponível em: www.aacrjournals.org. Acesso em: 29 ago. 2020.

CARONIA, D. et al. Common variations in ERCC2 are associated with response to cisplatin chemotherapy and clinical outcome in osteosarcoma patients. **The pharmacogenomics journal**, [S. l.], v. 9, n. 5, p. 347–53, 2009. DOI: 10.1038/tpj.2009.19. Disponível em: <http://www.ncbi.nlm.nih.gov/pubmed/19434073>.

CASTRACANI, Carlo Castruccio et al. Role of 17 β -Estradiol on Cell Proliferation and Mitochondrial Fitness in Glioblastoma Cells. **Journal of Oncology**, [S. l.], v. 2020, 2020. DOI: 10.1155/2020/2314693. Disponível em: </pmc/articles/PMC7042539/?report=abstract>. Acesso em: 11 ago. 2020.

CATANZARO, Daniela et al. Inhibition of glucose-6-phosphate dehydrogenase sensitizes cisplatin-resistant cells to death. **Oncotarget**, [S. l.], v. 6, n. 30, p. 30102–30114, 2015. DOI: 10.18632/oncotarget.4945. Disponível em: <http://www.oncotarget.com/fulltext/4945>. Acesso em: 17 nov. 2018.

CHEN, Guoan et al. Discordant protein and mRNA expression in lung adenocarcinomas. **Molecular & cellular proteomics : MCP**, [S. l.], v. 1, n. 4, p. 304–313, 2002. DOI: 10.1074/mcp.M200008-MCP200. Disponível em: <http://www.mcponline.org>. Acesso em: 24 set. 2020.

CHO, William C. **Mass spectrometry-based proteomics in cancer research** *Expert Review of Proteomics* Taylor and Francis Ltd, , 2017. DOI: 10.1080/14789450.2017.1365604. Disponível em: <https://pubmed.ncbi.nlm.nih.gov/28783987/>. Acesso em: 10 ago. 2020.

CORBET, Cyril; FERON, Olivier. Cancer cell metabolism and mitochondria: Nutrient plasticity for TCA cycle fueling. **Biochimica et Biophysica Acta - Reviews on Cancer**, [S. l.], v. 1868, n. 1, p. 7–15, 2017. DOI: 10.1016/j.bbcan.2017.01.002.

DANIAL, Nika N.; KORSMEYER, Stanley J. Cell death: critical control points. **Cell**, [S. l.], v. 116, n. 2, p. 205–19, 2004. DOI: 10.1016/s0092-8674(04)00046-7. Disponível em: <http://www.ncbi.nlm.nih.gov/pubmed/14744432>.

DASARI, Shaloam; BERNARD TCHOUNWOU, Paul. **Cisplatin in cancer therapy: Molecular mechanisms of action** *European Journal of Pharmacology* Elsevier, , 2014. DOI: 10.1016/j.ejphar.2014.07.025. Disponível em: </pmc/articles/PMC4146684/?report=abstract>. Acesso em: 7 ago. 2020.

DASARI, Shaloam; TCHOUNWOU, Paul Bernard. Cisplatin in cancer therapy: molecular

mechanisms of action. **European journal of pharmacology**, [S. l.], v. 740, p. 364–78, 2014. DOI: 10.1016/j.ejphar.2014.07.025. Disponível em: <http://www.ncbi.nlm.nih.gov/pubmed/25058905>.

DENISENKO, Tatiana V.; BUDKEVICH, Inna N.; ZHIVOTOVSKY, Boris. Cell death-based treatment of lung adenocarcinoma. **Cell Death and Disease**, [S. l.], v. 9, n. 2, 2018. DOI: 10.1038/s41419-017-0063-y. Disponível em: </pmc/articles/PMC5833343/?report=abstract>. Acesso em: 7 ago. 2020.

DI GREGORIO, Aida; BOWLING, Sarah; RODRIGUEZ, Tristan Argeo. Cell Competition and Its Role in the Regulation of Cell Fitness from Development to Cancer. **Developmental Cell**, [S. l.], v. 38, n. 6, p. 621–634, 2016. DOI: 10.1016/j.devcel.2016.08.012. Disponível em: <http://www.ncbi.nlm.nih.gov/pubmed/27676435>. Acesso em: 25 nov. 2018.

DING, Dalian; JIANG, Haiyan; ZHANG, Jianhui; XU, Xianrong; QI, Weidong; SHI, Haibo; YIN, Shankai; SALVI, Richard. Cisplatin-induced vestibular hair cell lesion-less damage at high doses. **Journal of Otology**, [S. l.], v. 13, n. 4, p. 115–121, 2018. DOI: 10.1016/j.joto.2018.08.002. Disponível em: </pmc/articles/PMC6335437/?report=abstract>. Acesso em: 12 ago. 2020.

DU, Pei; WANG, Yifeng; CHEN, Liquan; GAN, Yaping; WU, Qinian. High ERCC1 expression is associated with platinum-resistance, but not survival in patients with epithelial ovarian cancer. **Oncology Letters**, [S. l.], v. 12, n. 2, p. 857–862, 2016. DOI: 10.3892/ol.2016.4732. Disponível em: </pmc/articles/PMC4950824/?report=abstract>. Acesso em: 27 jan. 2021.

DUAN, Guihua et al. A Strategy to Delay the Development of Cisplatin Resistance by Maintaining a Certain Amount of Cisplatin-Sensitive Cells. **Scientific Reports**, [S. l.], v. 7, n. 1, p. 432, 2017. DOI: 10.1038/s41598-017-00422-2. Disponível em: <http://www.nature.com/articles/s41598-017-00422-2>. Acesso em: 14 mar. 2018.

DUAN, Mingrui; ULIBARRI, Jenna; LIU, Ke Jian; MAO, Peng. Role of nucleotide excision repair in cisplatin resistance. **International Journal of Molecular Sciences**, [S. l.], v. 21, n. 23, p. 1–13, 2020. DOI: 10.3390/ijms21239248. Disponível em: </pmc/articles/PMC7730652/?report=abstract>. Acesso em: 27 jan. 2021.

Estimativa 2020: incidência de câncer no Brasil. Rio de Janeiro: / Instituto Nacional de Câncer José Alencar Gomes da Silva, 2019. Disponível em: <https://www.inca.gov.br/sites/ufu.sti.inca.local/files//media/document//estimativa-2020-incidencia-de-cancer-no-brasil.pdf>.

FERRER, Irene; ZUGAZAGOITIA, Jon; HERBERTZ, Stephan; JOHN, William; PAZ-ARES, Luis; SCHMID-BINDERT, Gerald. KRAS-Mutant non-small cell lung cancer: From biology to therapy. **Lung Cancer**, [S. l.], v. 124, p. 53–64, 2018. DOI: 10.1016/j.lungcan.2018.07.013.

FURUTA, Takahisa; UEDA, Takahiro; AUNE, Gregory; SARASIN, Alain; KRAEMER, Kenneth H.; POMMIER, Yves. Transcription-coupled Nucleotide Excision Repair as a Determinant of Cisplatin Sensitivity of Human Cells. **Cancer Research**, [S. l.], v. 62, n. 17, 2002.

GALLUZZI, L.; SENOVILLA, L.; VITALE, I.; MICHELS, J.; MARTINS, I.; KEPP, O.; CASTEDO, M.; KROEMER, G. **Molecular mechanisms of cisplatin resistance**. *Oncogene* Nature Publishing Group, , 2012. DOI: 10.1038/onc.2011.384.

Disponível em: www.nature.com/onc. Acesso em: 8 ago. 2020.

GALLUZZI, L.; VITALE, I.; MICHELS, J.; BRENNER, C.; SZABADKAI, G.; HAREL-BELLAN, A.; CASTEDO, M.; KROEMER, G. **Systems biology of cisplatin resistance: Past, present and future** *Cell Death and Disease* Nature Publishing Group, , 2014. DOI: 10.1038/cddis.2013.428. Disponível em: <https://pubmed.ncbi.nlm.nih.gov/24874729/>. Acesso em: 12 ago. 2020.

GAO, Yanyun; DORN, Patrick; LIU, Shengchen; DENG, Haibin; HALL, Sean R. R.; PENG, Ren-Wang; SCHMID, Ralph A.; MARTI, Thomas M. Cisplatin-resistant A549 non-small cell lung cancer cells can be identified by increased mitochondrial mass and are sensitive to pemetrexed treatment. **Cancer cell international**, [S. l.], v. 19, p. 317, 2019. DOI: 10.1186/s12935-019-1037-1. Disponível em: <http://www.ncbi.nlm.nih.gov/pubmed/31798346>.

GARRAWAY, Levi A.; JÄNNE, Pasi A. **Circumventing cancer drug resistance in the era of personalized medicine** *Cancer Discovery* Cancer Discov, , 2012. DOI: 10.1158/2159-8290.CD-12-0012. Disponível em: <https://pubmed.ncbi.nlm.nih.gov/22585993/>. Acesso em: 15 ago. 2020.

GINGRAS, Anne Claude; GYGI, Steven P.; RAUGHT, Brian; POLAKIEWICZ, Roberto D.; ABRAHAM, Robert T.; HOEKSTRA, Merl F.; AEBERSOLD, Ruedi; SONENBERG, Nahum. Regulation of 4E-BP1 phosphorylation: A novel two step mechanism. **Genes and Development**, [S. l.], v. 13, n. 11, p. 1422–1437, 1999. DOI: 10.1101/gad.13.11.1422. Disponível em: [/pmc/articles/PMC316780/?report=abstract](http://pmc/articles/PMC316780/?report=abstract). Acesso em: 18 set. 2020.

GUO, Jiwei et al. The miR 495-UBE2C-ABCG2/ERCC1 axis reverses cisplatin resistance by downregulating drug resistance genes in cisplatin-resistant non-small cell lung cancer cells. **EBioMedicine**, [S. l.], v. 35, p. 204–221, 2018. a. DOI: 10.1016/j.ebiom.2018.08.001. Disponível em: <https://pubmed.ncbi.nlm.nih.gov/30146342/>. Acesso em: 9 ago. 2020.

GUO, Xiang-Feng; LIU, Ji-Peng; MA, Si-Quan; ZHANG, Peng; SUN, Wen-De. Avicularin reversed multidrug-resistance in human gastric cancer through enhancing Bax and BOK expressions. **Biomedicine & pharmacotherapy = Biomedecine & pharmacotherapie**, [S. l.], v. 103, p. 67–74, 2018. b. DOI: 10.1016/j.biopha.2018.03.110. Disponível em: <http://www.ncbi.nlm.nih.gov/pubmed/29635130>.

HANAHAH, Douglas; WEINBERG, Robert A. **Hallmarks of cancer: The next generation** *Cell* Elsevier, , 2011. DOI: 10.1016/j.cell.2011.02.013. Disponível em: <http://www.cell.com/article/S0092867411001279/fulltext>. Acesso em: 6 ago. 2020.

HEIDEN, Matthew G. Vande.; CANTLEY, Lewis C.; THOMPSON, Craig B. **Understanding the warburg effect: The metabolic requirements of cell proliferation** *Science* NIH Public Access, , 2009. DOI: 10.1126/science.1160809. Disponível em: [/pmc/articles/PMC2849637/?report=abstract](http://pmc/articles/PMC2849637/?report=abstract). Acesso em: 15 ago. 2020.

HENSLEY, Christopher T.; WASTI, Ajla T.; DEBERARDINIS, Ralph J. Glutamine and cancer: Cell biology, physiology, and clinical opportunities. **Journal of Clinical Investigation**, [S. l.], v. 123, n. 9, p. 3678–3684, 2013. DOI: 10.1172/JCI69600. Disponível em: <https://pubmed.ncbi.nlm.nih.gov/23999442/>. Acesso em: 3 set. 2020.

HORIBE, Sayo; KAWAUCHI, Shoji; TANAHASHI, Toshihito; SASAKI, Naoto; MIZUNO, Shigeto; RIKITAKE, Yoshiyuki. CD44v-dependent upregulation of α CT is involved in the acquisition of cisplatin-resistance in human lung cancer A549 cells. **Biochemical and**

Biophysical Research Communications, [S. l.], v. 507, n. 1–4, p. 426–432, 2018. DOI: 10.1016/j.bbrc.2018.11.055. Disponível em: <https://pubmed.ncbi.nlm.nih.gov/30448176/>. Acesso em: 12 ago. 2020.

HOSSEINI, Mohsen et al. Targeting myeloperoxidase disrupts mitochondrial redox balance and overcomes cytarabine resistance in human acute myeloid leukemia. **Cancer Research**, [S. l.], v. 79, n. 20, p. 5191–5203, 2019. DOI: 10.1158/0008-5472.CAN-19-0515. Disponível em: <https://pubmed.ncbi.nlm.nih.gov/31358527/>. Acesso em: 11 ago. 2020.

HU, Jinchuan; LIEB, Jason D.; SANCAR, Aziz; ADAR, Sheera. Cisplatin DNA damage and repair maps of the human genome at single-nucleotide resolution. **Proceedings of the National Academy of Sciences of the United States of America**, [S. l.], v. 113, n. 41, p. 11507–11512, 2016. DOI: 10.1073/pnas.1614430113. Disponível em: </pmc/articles/PMC5068337/?report=abstract>. Acesso em: 9 ago. 2020.

ICARD, Philippe; SHULMAN, Seth; FARHAT, Diana; STEYAERT, Jean Marc; ALIFANO, Marco; LINCET, Hubert. How the Warburg effect supports aggressiveness and drug resistance of cancer cells? **Drug Resistance Updates**, [S. l.], v. 38, p. 1–11, 2018. DOI: 10.1016/j.drug.2018.03.001.

INTERNATIONAL AGENCY FOR RESEARCH ON CANCER. **Cancer Today**. 2020. Disponível em: http://gco.iarc.fr/today/online-analysis-multi-bars?v=2018&mode=cancer&mode_population=countries&population=900&populations=900&key=total&sex=0&cancer=39&type=0&statistic=5&prevalence=0&population_group=0&ages_group%5B%5D=0&ages_group%5B%5D=17&nb_items=10. Acesso em: 31 mar. 2020.

JACOBSEN, Margo M.; SILVERSTEIN, Sophie C.; QUINN, Michael; WATERSTON, Leo B.; THOMAS, Christian A.; BENNEYAN, James C.; HAN, Paul K. J. **Timeliness of access to lung cancer diagnosis and treatment: A scoping literature review** *Lung Cancer* Elsevier Ireland Ltd, , 2017. DOI: 10.1016/j.lungcan.2017.08.011. Disponível em: <https://pubmed.ncbi.nlm.nih.gov/29191588/>. Acesso em: 7 ago. 2020.

JU, Sung Min; JO, Yong Seok; JEON, Yoo Min; PAE, Hyun Ock; KANG, Dae Gill; LEE, Ho Sub; BAE, Jun Sang; JEON, Byung Hun. Phosphorylation of eIF2 α suppresses cisplatin-induced p53 activation and apoptosis by attenuating oxidative stress via ATF4-mediated HO-1 expression in human renal proximal tubular cells. **International Journal of Molecular Medicine**, [S. l.], v. 40, n. 6, p. 1957–1964, 2017. DOI: 10.3892/ijmm.2017.3181. Disponível em: <https://pubmed.ncbi.nlm.nih.gov/29039478/>. Acesso em: 18 set. 2020.

JUN, H. J. et al. ERCC1 expression as a predictive marker of squamous cell carcinoma of the head and neck treated with cisplatin-based concurrent chemoradiation. **British Journal of Cancer**, [S. l.], v. 99, n. 1, p. 167–172, 2008. DOI: 10.1038/sj.bjc.6604464. Disponível em: </pmc/articles/PMC2453006/?report=abstract>. Acesso em: 27 jan. 2021.

KELLAND, Lloyd. The resurgence of platinum-based cancer chemotherapy. **Nature reviews. Cancer**, [S. l.], v. 7, n. 8, p. 573–84, 2007. DOI: 10.1038/nrc2167. Disponível em: <http://www.ncbi.nlm.nih.gov/pubmed/17625587>.

KNIGHT, Tristan; LUEDTKE, Daniel; EDWARDS, Holly; TAUB, Jeffrey W.; GE, Yubin. A delicate balance - The BCL-2 family and its role in apoptosis, oncogenesis, and cancer therapeutics. **Biochemical pharmacology**, [S. l.], v. 162, p. 250–261, 2019. DOI: 10.1016/j.bcp.2019.01.015. Disponível em: <http://www.ncbi.nlm.nih.gov/pubmed/30668936>.

KOCH, Andreas; EBERT, Eva Vanessa; SEITZ, Tatjana; DIETRICH, Peter; BERNEBURG,

Mark; BOSSERHOFF, Anja; HELLERBRAND, Claus. Characterization of glycolysis-related gene expression in malignant melanoma. **Pathology Research and Practice**, [S. l.], v. 216, n. 1, 2020. DOI: 10.1016/j.prp.2019.152752. Disponível em: <https://pubmed.ncbi.nlm.nih.gov/31791701/>. Acesso em: 3 set. 2020.

KOPPENOL, Willem H.; BOUNDS, Patricia L.; DANG, Chi V. Otto Warburg's contributions to current concepts of cancer metabolism. **Nature Reviews Cancer**, [S. l.], v. 11, n. 5, p. 325–337, 2011. DOI: 10.1038/nrc3038. Disponível em: <http://www.ncbi.nlm.nih.gov/pubmed/21508971>. Acesso em: 16 nov. 2018.

KRASNOV, George S.; DMITRIEV, Alexey A.; LAKUNINA, Valentina A.; KIRPIY, Alexander A.; KUDRYAVTSEVA, Anna V. **Targeting VDAC-bound hexokinase II: A promising approach for concomitant anti-cancer therapy**Expert Opinion on Therapeutic TargetsExpert Opin Ther Targets, , 2013. DOI: 10.1517/14728222.2013.833607. Disponível em: <https://pubmed.ncbi.nlm.nih.gov/23984984/>. Acesso em: 30 ago. 2020.

LAN, Dong; WANG, Li; HE, Rongquan; MA, Jie; BIN, Yehong; CHI, Xiaojv; CHEN, Gang; CAI, Zhengwen. Exogenous glutathione contributes to cisplatin resistance in lung cancer A549 cells. **American journal of translational research**, [S. l.], v. 10, n. 5, p. 1295–1309, 2018. Disponível em: <http://www.ncbi.nlm.nih.gov/pubmed/29887946>.

LEHÚEDE, Camille; DUPUY, Fanny; RABINOVITCH, Rebecca; JONES, Russell G.; SIEGEL, Peter M. **Metabolic plasticity as a determinant of tumor growth and metastasis**Cancer ResearchAmerican Association for Cancer Research Inc., , 2016. DOI: 10.1158/0008-5472.CAN-16-0266. Disponível em: www.aacrjournals.org. Acesso em: 17 set. 2020.

LEMJABBAR-ALAOUI, Hassan; HASSAN, Omer U. I.; YANG, Yi Wei; BUCHANAN, Petra. **Lung cancer: Biology and treatment options**Biochimica et Biophysica Acta - Reviews on CancerElsevier B.V., , 2015. DOI: 10.1016/j.bbcan.2015.08.002. Disponível em: </pmc/articles/PMC4663145/?report=abstract>. Acesso em: 7 ago. 2020.

LI, Qiwei; YIN, Xiaobin; WANG, Wei; ZHAN, Ming; ZHAO, Benpeng; HOU, Zhaoyuan; WANG, Jian. The effects of buthionine sulfoximine on the proliferation and apoptosis of biliary tract cancer cells induced by cisplatin and gemcitabine. **Oncology Letters**, [S. l.], v. 11, n. 1, p. 474–480, 2016. DOI: 10.3892/ol.2015.3879. Disponível em: <https://pubmed.ncbi.nlm.nih.gov/26870236/>. Acesso em: 24 set. 2020.

LONG, Qinqiang; HUANG, Lizhen; HUANG, Kai; YANG, Qinglin. Assessing mitochondrial bioenergetics in isolated mitochondria from mouse heart tissues using oroboros 2k-oxygraph. **Methods in Molecular Biology**, [S. l.], v. 1966, p. 237–246, 2019. DOI: 10.1007/978-1-4939-9195-2_19. Disponível em: </pmc/articles/PMC7388157/?report=abstract>. Acesso em: 30 ago. 2020.

MAKOVEC, Tomaz. **Cisplatin and beyond: Molecular mechanisms of action and drug resistance development in cancer chemotherapy**Radiology and OncologySciendo, , 2019. DOI: 10.2478/raon-2019-0018. Disponível em: </pmc/articles/PMC6572495/?report=abstract>. Acesso em: 9 ago. 2020.

MAO, Yousheng; YANG, Ding; HE, Jie; KRASNA, Mark J. Epidemiology of Lung Cancer. **Surgical Oncology Clinics of North America**, [S. l.], v. 25, n. 3, p. 439–445, 2016. DOI: 10.1016/j.soc.2016.02.001. Disponível em: <https://pubmed.ncbi.nlm.nih.gov/27261907/>. Acesso em: 27 jan. 2021.

MARTINHO, Nuno; SANTOS, Tânia C. B.; FLORINDO, Helena F.; SILVA, Liana C. Cisplatin-Membrane Interactions and Their Influence on Platinum Complexes Activity and Toxicity. **Frontiers in physiology**, [S. l.], v. 9, p. 1898, 2018. DOI: 10.3389/fphys.2018.01898. Disponível em: <http://www.ncbi.nlm.nih.gov/pubmed/30687116>.

MASOUD, Georgina N.; LI, Wei. **HIF-1 α pathway: Role, regulation and intervention for cancer therapy** *Acta Pharmaceutica Sinica B* Chinese Academy of Medical Sciences, , 2015. DOI: 10.1016/j.apsb.2015.05.007. Disponível em: <https://pubmed.ncbi.nlm.nih.gov/27206315/>. Acesso em: 23 ago. 2020.

MATASSA, D. S. et al. Oxidative metabolism drives inflammation-induced platinum resistance in human ovarian cancer. **Cell Death and Differentiation**, [S. l.], v. 23, n. 9, p. 1542–1554, 2016. DOI: 10.1038/cdd.2016.39. Disponível em: <https://pubmed.ncbi.nlm.nih.gov/27206315/>. Acesso em: 21 ago. 2020.

MAURER, Gabriele D.; HELLER, Sonja; WANKA, Christina; RIEGER, Johannes; STEINBACH, Joachim P. Knockdown of the TP53-induced glycolysis and apoptosis regulator (TIGAR) sensitizes glioma cells to hypoxia, irradiation and temozolomide. **International Journal of Molecular Sciences**, [S. l.], v. 20, n. 5, 2019. DOI: 10.3390/ijms20051061. Disponível em: <https://pubmed.ncbi.nlm.nih.gov/27206315/>. Acesso em: 23 set. 2020.

MCDERMOTT, Martina; EUSTACE, Alex J.; BUSSCHOTS, Steven; BREEN, Laura; CROWN, John; CLYNES, Martin; O'DONOVAN, Norma; STORDAL, Britta. In vitro Development of Chemotherapy and Targeted Therapy Drug-Resistant Cancer Cell Lines: A Practical Guide with Case Studies. **Frontiers in oncology**, [S. l.], v. 4, p. 40, 2014. DOI: 10.3389/fonc.2014.00040. Disponível em: <http://www.ncbi.nlm.nih.gov/pubmed/24639951>.

MCGRANAHAN, Nicholas; SWANTON, Charles. **Clonal Heterogeneity and Tumor Evolution: Past, Present, and the Future** Cell Press, , 2017. DOI: 10.1016/j.cell.2017.01.018. Disponível em: <https://pubmed.ncbi.nlm.nih.gov/28187284/>. Acesso em: 11 ago. 2020.

MIAO, Ping; SHENG, Shile; SUN, Xiaoguang; LIU, Jianjun; HUANG, Gang. Lactate dehydrogenase a in cancer: A promising target for diagnosis and therapy. **IUBMB Life**, [S. l.], v. 65, n. 11, p. 904–910, 2013. DOI: 10.1002/iub.1216. Disponível em: <https://pubmed.ncbi.nlm.nih.gov/24265197/>. Acesso em: 30 ago. 2020.

NASIM, Faria; SABATH, Bruce F.; EAPEN, George A. **Lung Cancer** *Medical Clinics of North America* W.B. Saunders, , 2019. DOI: 10.1016/j.mcna.2018.12.006. Disponível em: <https://pubmed.ncbi.nlm.nih.gov/30955514/>. Acesso em: 7 ago. 2020.

NATURE. **Cancer**. 2020. Disponível em: <https://www.nature.com/subjects/cancer/#:~:text=Definition,causing local damage and inflammation>. Acesso em: 6 ago. 2020.

NEVE, Richard M. et al. A collection of breast cancer cell lines for the study of functionally distinct cancer subtypes. **Cancer Cell**, [S. l.], v. 10, n. 6, p. 515–527, 2006. DOI: 10.1016/j.ccr.2006.10.008. Disponível em: <https://pubmed.ncbi.nlm.nih.gov/17157791/>. Acesso em: 12 ago. 2020.

NIU, Nifang; WANG, Liewei. In vitro human cell line models to predict clinical response to anticancer drugs. **Pharmacogenomics**, [S. l.], v. 16, n. 3, p. 273–285, 2015. DOI: 10.2217/pgs.14.170. Disponível em: <https://pubmed.ncbi.nlm.nih.gov/25712190/>. Acesso em:

12 ago. 2020.

OBRIST, Florine et al. Metabolic vulnerability of cisplatin-resistant cancers. **The EMBO Journal**, [S. l.], v. 37, n. 14, 2018. DOI: 10.15252/embj.201798597. Disponível em: /pmc/articles/PMC6043854/?report=abstract. Acesso em: 3 set. 2020.

OCAÑA, Ma Carmen; MARTÍNEZ-POVEDA, Beatriz; QUESADA, Ana R.; MEDINA, Miguel Ángel. Metabolism within the tumor microenvironment and its implication on cancer progression: An ongoing therapeutic target. **Medicinal Research Reviews**, [S. l.], v. 39, n. 1, p. 70–113, 2019. DOI: 10.1002/med.21511. Disponível em: <https://pubmed.ncbi.nlm.nih.gov/29785785/>. Acesso em: 29 ago. 2020.

OHNO, Masuo. PERK as a hub of multiple pathogenic pathways leading to memory deficits and neurodegeneration in Alzheimer's disease. **Brain Research Bulletin**, [S. l.], v. 141, p. 72–78, 2018. DOI: 10.1016/j.brainresbull.2017.08.007. Disponível em: <https://pubmed.ncbi.nlm.nih.gov/28804008/>. Acesso em: 18 set. 2020.

OLAUSSEN, Ken A. et al. DNA Repair by ERCC1 in Non-Small-Cell Lung Cancer and Cisplatin-Based Adjuvant Chemotherapy. **New England Journal of Medicine**, [S. l.], v. 355, n. 10, p. 983–991, 2006. DOI: 10.1056/nejmoa060570. Disponível em: <https://pubmed.ncbi.nlm.nih.gov/16957145/>. Acesso em: 27 jan. 2021.

PAJUELO-LOZANO, Natalia; BARGIELA-IPARRAGUIRRE, Jone; DOMINGUEZ, Gemma; QUIROGA, Adoracion G.; PERONA, Rosario; SANCHEZ-PEREZ, Isabel. XPA, XPC, and XPD modulate sensitivity in gastric cisplatin resistance cancer cells. **Frontiers in Pharmacology**, [S. l.], v. 9, n. OCT, p. 1197, 2018. DOI: 10.3389/fphar.2018.01197. Disponível em: /pmc/articles/PMC6199368/?report=abstract. Acesso em: 27 jan. 2021.

PATHAK, Rakesh K.; DHAR, Shanta. Unique Use of Alkylation for Chemo-Redox Activity by a PtIV Prodrug. **Chemistry - A European Journal**, [S. l.], v. 22, n. 9, p. 3029–3036, 2016. DOI: 10.1002/chem.201503866. Disponível em: <https://pubmed.ncbi.nlm.nih.gov/26807548/>. Acesso em: 8 ago. 2020.

PELLETIER, Jerry; GRAFF, Jeremy; RUGGERO, Davide; SONENBERG, Nahum. Targeting the eIF4F translation initiation complex: A critical nexus for cancer development. **Cancer Research**, [S. l.], v. 75, n. 2, p. 250–263, 2015. DOI: 10.1158/0008-5472.CAN-14-2789. Disponível em: <https://pubmed.ncbi.nlm.nih.gov/25593033/>. Acesso em: 18 set. 2020.

PRIYA, Shivam; NIGAM, Akanksha; BAJPAI, Preeti; KUMAR, Sushil. Diethyl maleate inhibits MCA+TPA transformed cell growth via modulation of GSH, MAPK, and cancer pathways. **Chemico-Biological Interactions**, [S. l.], v. 219, p. 37–47, 2014. DOI: 10.1016/j.cbi.2014.04.018. Disponível em: <https://pubmed.ncbi.nlm.nih.gov/24814887/>. Acesso em: 24 set. 2020.

PRYCZYNICZ, Anna; GRYKO, Mariusz; NIEWIAROWSKA, Katarzyna; CEPOWICZ, Dariusz; USTYMOWICZ, Marek; KEMONA, Andrzej; GUZIŃSKA-USTYMOWICZ, Katarzyna. Bax protein may influence the invasion of colorectal cancer. **World Journal of Gastroenterology**, [S. l.], v. 20, n. 5, p. 1305–1310, 2014. DOI: 10.3748/wjg.v20.i5.1305. Disponível em: /pmc/articles/PMC3921512/?report=abstract. Acesso em: 9 ago. 2020.

QIN, Xiaoyu; JIANG, Bin; ZHANG, Yanjie. 4E-BP1, a multifactor regulated multifunctional protein. **Cell Cycle**, [S. l.], v. 15, n. 6, p. 781–786, 2016. DOI: 10.1080/15384101.2016.1151581. Disponível em: /pmc/articles/PMC4845917/?report=abstract. Acesso em: 24 set. 2020.

QU, Xuan; SUN, Jing; ZHANG, Yami; LI, Jun; HU, Junbi; LI, Kai; GAO, Lei; SHEN, Liangliang. c-Myc-driven glycolysis via TXNIP suppression is dependent on glutaminase-MondoA axis in prostate cancer. **Biochemical and Biophysical Research Communications**, [S. l.], v. 504, n. 2, p. 415–421, 2018. DOI: 10.1016/j.bbrc.2018.08.069.

RACKER, E. Bioenergetics and the problem of tumor growth. **American scientist**, [S. l.], v. 60, n. 1, p. 56–63, 1972. Disponível em: <https://pubmed.ncbi.nlm.nih.gov/4332766/>. Acesso em: 10 ago. 2020.

RAFF, M. C. Social controls on cell survival and cell death. **Nature**, [S. l.], v. 356, n. 6368, p. 397–400, 1992. DOI: 10.1038/356397a0. Disponível em: <http://www.ncbi.nlm.nih.gov/pubmed/1557121>.

RAHIB, Lola; SMITH, Benjamin D.; AIZENBERG, Rhonda; ROSENZWEIG, Allison B.; FLESHMAN, Julie M.; MATRISIAN, Lynn M. Projecting cancer incidence and deaths to 2030: the unexpected burden of thyroid, liver, and pancreas cancers in the United States. **Cancer research**, [S. l.], v. 74, n. 11, p. 2913–21, 2014. DOI: 10.1158/0008-5472.CAN-14-0155. Disponível em: <http://www.ncbi.nlm.nih.gov/pubmed/24840647>. Acesso em: 25 set. 2018.

REN, Jing Hua; HE, Wen Shan; NONG, Li; ZHU, Qing Yao; HU, Kai; ZHANG, Rui Guang; HUANG, Li Li; ZHU, Fang; WU, Gang. Acquired cisplatin resistance in human lung adenocarcinoma cells is associated with enhanced autophagy. **Cancer Biotherapy and Radiopharmaceuticals**, [S. l.], v. 25, n. 1, p. 75–80, 2010. DOI: 10.1089/cbr.2009.0701. Disponível em: <https://pubmed.ncbi.nlm.nih.gov/20187799/>. Acesso em: 11 ago. 2020.

ROSENBERG, B.; VANCAMP, L.; KRIGAS, T. INHIBITION OF CELL DIVISION IN ESCHERICHIA COLI BY ELECTROLYSIS PRODUCTS FROM A PLATINUM ELECTRODE. **Nature**, [S. l.], v. 205, p. 698–9, 1965. Disponível em: <http://www.ncbi.nlm.nih.gov/pubmed/14287410>. Acesso em: 6 out. 2018.

ROSENBERG, BARNETT; VANCAMP, LORETTA; TROSKO, JAMES E.; MANSOUR, VIRGINIA H. Platinum Compounds: a New Class of Potent Antitumour Agents. **Nature**, [S. l.], v. 222, n. 5191, p. 385–386, 1969. DOI: 10.1038/222385a0. Disponível em: <http://www.nature.com/doi/10.1038/222385a0>. Acesso em: 2 out. 2018.

ROUSSEAU, Adrien; BERTOLOTI, Anne. Regulation of proteasome assembly and activity in health and disease. **Nature Reviews Molecular Cell Biology**, [S. l.], v. 19, n. 11, p. 697–712, 2018. DOI: 10.1038/s41580-018-0040-z. Disponível em: www.nature.com/nrm. Acesso em: 17 set. 2020.

SARIN, Navin et al. Cisplatin resistance in non-small cell lung cancer cells is associated with an abrogation of cisplatin-induced G2/M cell cycle arrest. **PLoS ONE**, [S. l.], v. 12, n. 7, 2017. DOI: 10.1371/journal.pone.0181081. Disponível em: <https://pubmed.ncbi.nlm.nih.gov/28746345/>. Acesso em: 11 ago. 2020.

SHOSHAN, Maria C. **3-bromopyruvate: Targets and outcomes** *Journal of Bioenergetics and Biomembranes* *J Bioenerg Biomembr*, , 2012. DOI: 10.1007/s10863-012-9419-2. Disponível em: <https://pubmed.ncbi.nlm.nih.gov/22298255/>. Acesso em: 3 set. 2020.

SHUCK, Sarah C.; SHORT, Emily A.; TURCHI, John J. **Eukaryotic nucleotide excision repair: From understanding mechanisms to influencing biology** *Cell Research* *Cell Res*, , 2008. DOI: 10.1038/cr.2008.2. Disponível em: <https://pubmed.ncbi.nlm.nih.gov/18166981/>. Acesso em: 9 ago. 2020.

SIDDIK, Zahid H. Cisplatin: mode of cytotoxic action and molecular basis of resistance. **Oncogene**, [S. l.], v. 22, n. 47, p. 7265–79, 2003. DOI: 10.1038/sj.onc.1206933. Disponível em: <http://www.ncbi.nlm.nih.gov/pubmed/14576837>.

SIEGEL, Rebecca L.; MILLER, Kimberly D.; JEMAL, Ahmedin. Cancer statistics. **CA Cancer J Clin**, [S. l.], v. 66, n. 1, p. 7–30, 2016. DOI: 10.3322/caac.21332.

SINGH, Rumani; LETAI, Anthony; SAROSIEK, Kristopher. Regulation of apoptosis in health and disease: the balancing act of BCL-2 family proteins. **Nature reviews. Molecular cell biology**, [S. l.], v. 20, n. 3, p. 175–193, 2019. DOI: 10.1038/s41580-018-0089-8. Disponível em: <http://www.ncbi.nlm.nih.gov/pubmed/30655609>.

SKOWRON, Margaretha A. et al. Distinctive mutational spectrum and karyotype disruption in long-term cisplatin-treated urothelial carcinoma cell lines. **Scientific reports**, [S. l.], v. 9, n. 1, p. 14476, 2019. DOI: 10.1038/s41598-019-50891-w. Disponível em: <http://www.ncbi.nlm.nih.gov/pubmed/31597922>.

SOCINSKI, M. A. Cytotoxic Chemotherapy in Advanced Non-Small Cell Lung Cancer: A Review of Standard Treatment Paradigms. **Clinical Cancer Research**, [S. l.], v. 10, n. 12, p. 4210S–4214S, 2004. DOI: 10.1158/1078-0432.CCR-040009. Disponível em: <http://www.ncbi.nlm.nih.gov/pubmed/15217960>. Acesso em: 5 out. 2018.

SULLIVAN, Elizabeth J.; KURTOGLU, Metin; BRENNEMAN, Randall; LIU, Huaping; LAMPIDIS, Theodore J. Targeting cisplatin-resistant human tumor cells with metabolic inhibitors. **Cancer Chemotherapy and Pharmacology**, [S. l.], v. 73, n. 2, p. 417–427, 2014. DOI: 10.1007/s00280-013-2366-8. Disponível em: <https://pubmed.ncbi.nlm.nih.gov/24352250/>. Acesso em: 3 set. 2020.

SUN, Wei; ZU, Yukun; FU, Xiangning; DENG, Yu. Knockdown of lncRNA-XIST enhances the chemosensitivity of NSCLC cells via suppression of autophagy. **Oncology Reports**, [S. l.], v. 38, n. 6, p. 3347–3354, 2017. DOI: 10.3892/or.2017.6056. Disponível em: </pmc/articles/PMC5783579/?report=abstract>. Acesso em: 12 ago. 2020.

TORRE, Lindsey A.; BRAY, Freddie; SIEGEL, Rebecca L.; FERLAY, Jacques; LORTET-TIEULENT, Joannie; JEMAL, Ahmedin. Global cancer statistics, 2012. **CA: A Cancer Journal for Clinicians**, [S. l.], v. 65, n. 2, p. 87–108, 2015. DOI: 10.3322/caac.21262. Disponível em: <http://doi.wiley.com/10.3322/caac.21262>. Acesso em: 13 mar. 2018.

VAUPEL, Peter; SCHMIDBERGER, Heinz; MAYER, Arnulf. The Warburg effect: essential part of metabolic reprogramming and central contributor to cancer progression. **International Journal of Radiation Biology**, [S. l.], v. 95, n. 7, p. 912–919, 2019. DOI: 10.1080/09553002.2019.1589653. Disponível em: <https://www.tandfonline.com/doi/abs/10.1080/09553002.2019.1589653>. Acesso em: 10 ago. 2020.

VAZQUEZ, Francisca et al. PGC1 α Expression Defines a Subset of Human Melanoma Tumors with Increased Mitochondrial Capacity and Resistance to Oxidative Stress. **Cancer Cell**, [S. l.], v. 23, n. 3, p. 287–301, 2013. DOI: 10.1016/j.ccr.2012.11.020. Disponível em: </pmc/articles/PMC3708305/?report=abstract>. Acesso em: 21 ago. 2020.

WAGNER, Brett A.; VENKATARAMAN, Sujatha; BUETTNER, Garry R. The rate of oxygen utilization by cells. **Free Radical Biology and Medicine**, [S. l.], v. 51, n. 3, p. 700–712, 2011. DOI: 10.1016/j.freeradbiomed.2011.05.024. Disponível em: <http://www.ncbi.nlm.nih.gov/pubmed/21664270>. Acesso em: 21 nov. 2018.

WAKAI. Multidrug resistance-associated protein 2 determines the efficacy of cisplatin in patients with hepatocellular carcinoma. **Oncology Reports**, [S. l.], v. 23, n. 4, 2010. DOI: 10.3892/or_00000721. Disponível em: <https://pubmed.ncbi.nlm.nih.gov/20204280/>. Acesso em: 8 ago. 2020.

WAKELEE, Heather; KELLY, Karen; EDELMAN, Martin J. 50 Years of Progress in the Systemic Therapy of Non–Small Cell Lung Cancer. **American Society of Clinical Oncology Educational Book**, [S. l.], n. 34, p. 177–189, 2014. DOI: 10.14694/edbook_am.2014.34.177. Disponível em: </pmc/articles/PMC5600272/?report=abstract>. Acesso em: 7 ago. 2020.

WANG, Huanan; WANG, Lei; ZHANG, Yingjie; WANG, Ji; DENG, Yibin; LIN, Degui. Inhibition of glycolytic enzyme hexokinase II (HK2) suppresses lung tumor growth. **Cancer Cell International**, [S. l.], v. 16, n. 1, p. 9, 2016. a. DOI: 10.1186/s12935-016-0280-y. Disponível em: </pmc/articles/PMC4755025/?report=abstract>. Acesso em: 30 ago. 2020.

WANG, Sheng Fan; CHEN, Meng Shian; CHOU, Yueh Ching; UENG, Yune Fang; YIN, Pen Hui; YEH, Tien Shun; LEE, Hsin Chen. Mitochondrial dysfunction enhances cisplatin resistance in human gastric cancer cells via the ROS-activated GCN2-eIF2 α - ATF4-xCT pathway. **Oncotarget**, [S. l.], v. 7, n. 45, p. 74132–74151, 2016. b. DOI: 10.18632/oncotarget.12356.

WANG, Tianyi et al. JAK/STAT3-Regulated Fatty Acid β -Oxidation Is Critical for Breast Cancer Stem Cell Self-Renewal and Chemoresistance. **Cell Metabolism**, [S. l.], v. 27, n. 1, p. 136- 150.e5, 2018. DOI: 10.1016/j.cmet.2017.11.001. Disponível em: </pmc/articles/PMC5777338/?report=abstract>. Acesso em: 10 ago. 2020.

WANGPAICHITR, Medhi; SULLIVAN, Elizabeth J.; THEODOROPOULOS, George; WU, Chunjing; YOU, Min; FEUN, Lynn G.; LAMPIDIS, Theodore J.; KUO, Macus T.; SAVARAJ, Niramol. The relationship of thioredoxin-1 and cisplatin resistance: Its impact on ROS and oxidative metabolism in lung cancer cells. **Molecular Cancer Therapeutics**, [S. l.], v. 11, n. 3, p. 604–615, 2012. DOI: 10.1158/1535-7163.MCT-11-0599. Disponível em: </pmc/articles/PMC3326609/?report=abstract>. Acesso em: 12 set. 2020.

WARBURG, Otto. The metabolism of carcinoma cells . **The Journal of Cancer Research**, [S. l.], v. 9, n. 1, p. 148–163, 1925. DOI: 10.1158/jcr.1925.148. Disponível em: <https://cancerres.aacrjournals.org/content/9/1/148>. Acesso em: 12 set. 2020.

WEEDEN, Clare E.; ASSELIN-LABAT, Marie Liesse. Mechanisms of DNA damage repair in adult stem cells and implications for cancer formation. **Biochimica et Biophysica Acta - Molecular Basis of Disease**, [S. l.], v. 1864, n. 1, p. 89–101, 2018. DOI: 10.1016/j.bbadis.2017.10.015. Disponível em: <https://pubmed.ncbi.nlm.nih.gov/29038050/>. Acesso em: 11 ago. 2020.

WEK, Ronald C. Role of eIF2 α kinases in translational control and adaptation to cellular stress. **Cold Spring Harbor Perspectives in Biology**, [S. l.], v. 10, n. 7, 2018. DOI: 10.1101/cshperspect.a032870. Disponível em: </pmc/articles/PMC6028073/?report=abstract>. Acesso em: 24 set. 2020.

XAVIER, Cristina P. R.; PESIC, Milica; VASCONCELOS, M. Helena. Understanding Cancer Drug Resistance by Developing and Studying Resistant Cell Line Models. **Current Cancer Drug Targets**, [S. l.], v. 16, n. 3, p. 226–237, 2016. DOI: 10.2174/1568009616666151113120705. Disponível em: <https://pubmed.ncbi.nlm.nih.gov/26563882/>. Acesso em: 15 ago. 2020.

XIE, Jia Ming; LI, Bin; YU, Hong Pei; GAO, Quan Geng; LI, Wei; WU, Hao Rong; QIN, Zheng Hong. TIGAR has a dual role in cancer cell survival through regulating apoptosis and autophagy. **Cancer Research**, [S. l.], v. 74, n. 18, p. 5127–5138, 2014. DOI: 10.1158/0008-5472.CAN-13-3517. Disponível em: <https://pubmed.ncbi.nlm.nih.gov/25085248/>. Acesso em: 24 set. 2020.

XU, Yunjie et al. ABT737 reverses cisplatin resistance by targeting glucose metabolism of human ovarian cancer cells. **International Journal of Oncology**, [S. l.], v. 53, n. 3, p. 1055–1068, 2018. DOI: 10.3892/ijo.2018.4476. Disponível em: <http://www.ncbi.nlm.nih.gov/pubmed/30015875>. Acesso em: 2 abr. 2020.

YONESAKA, Kimio et al. An HER3-targeting antibody–drug conjugate incorporating a DNA topoisomerase I inhibitor U3-1402 conquers EGFR tyrosine kinase inhibitor-resistant NSCLC. **Oncogene**, [S. l.], v. 38, n. 9, p. 1398–1409, 2019. DOI: 10.1038/s41388-018-0517-4. Disponível em: <https://pubmed.ncbi.nlm.nih.gov/30302022/>. Acesso em: 12 ago. 2020.

YU, Meiling; QI, Benquan; XIAOXIANG, Wu; XU, Jian; LIU, Xiaolin. Baicalein increases cisplatin sensitivity of A549 lung adenocarcinoma cells via PI3K/Akt/NF- κ B pathway. **Biomedicine and Pharmacotherapy**, [S. l.], v. 90, p. 677–685, 2017. DOI: 10.1016/j.biopha.2017.04.001. Disponível em: <https://pubmed.ncbi.nlm.nih.gov/28415048/>. Acesso em: 12 ago. 2020.

YU, Mengxue et al. YAP1 contributes to NSCLC invasion and migration by promoting Slug transcription via the transcription co-factor TEAD. **Cell Death and Disease**, [S. l.], v. 9, n. 5, 2018. DOI: 10.1038/s41419-018-0515-z. Disponível em: </pmc/articles/PMC5920099/?report=abstract>. Acesso em: 12 ago. 2020.

ZEESHAN, Rabia; MUTAHIR, Zeeshan. **Cancer metastasis - Tricks of the trade** **Bosnian Journal of Basic Medical Sciences** Association of Basic Medical Sciences of FBiH, , 2017. DOI: 10.17305/bjbms.2017.1908. Disponível em: </pmc/articles/PMC5581965/?report=abstract>. Acesso em: 6 ago. 2020.

ZELCER, Noam; SAEKI, Tohru; REID, Glen; BEIJNEN, Jos H.; BORST, Piet. Characterization of Drug Transport by the Human Multidrug Resistance Protein 3 (ABCC3). **Journal of Biological Chemistry**, [S. l.], v. 276, n. 49, p. 46400–46407, 2001. DOI: 10.1074/jbc.M107041200. Disponível em: <http://www.jbc.org/>. Acesso em: 8 ago. 2020.

ZHANG, Jin; LIU, Jie; LI, Hui; WANG, Jun. β -catenin signaling pathway regulates cisplatin resistance in lung adenocarcinoma cells by upregulating Bcl-xl. **Molecular Medicine Reports**, [S. l.], v. 13, n. 3, p. 2543–2551, 2016. DOI: 10.3892/mmr.2016.4882. Disponível em: </pmc/articles/PMC4768989/?report=abstract>. Acesso em: 27 jan. 2021.

ZHANG, Xiao Dong; DESLANDES, Edwige; VILLEDIEU, Marie; POULAIN, Laurent; DUVAL, Marilyne; GAUDUCHON, Pascal; SCHWARTZ, Laurent; ICARD, Philippe. Effect of 2-deoxy-D-glucose on various malignant cell lines in vitro - PubMed. **Anticancer research**, [S. l.], v. 26, n. 5A, p. 3561–6, 2006. Disponível em: <https://pubmed.ncbi.nlm.nih.gov/17094483/>. Acesso em: 3 set. 2020.

ZHANG, Yu; CHEN, Shiguo; WEI, Chaoyang; RANKIN, Gary O.; ROJANASAKUL, Yon; REN, Ning; YE, Xingqian; CHEN, Yi Charlie. Dietary compound proanthocyanidins from Chinese bayberry (*Myrica rubra* Sieb. et Zucc.) leaves inhibit angiogenesis and regulate cell cycle of cisplatin-resistant ovarian cancer cells via targeting Akt pathway. **Journal of Functional Foods**, [S. l.], v. 40, p. 573–581, 2018. DOI: 10.1016/j.jff.2017.11.045. Disponível em: <https://pubmed.ncbi.nlm.nih.gov/29576805/>. Acesso em: 18 set. 2020.

ZHAO, Henan et al. MiR-770-5p inhibits cisplatin chemoresistance in human ovarian cancer by targeting ERCC2. **Oncotarget**, [S. l.], v. 7, n. 33, p. 53254–53268, 2016. DOI: 10.18632/oncotarget.10736. Disponível em: <https://pubmed.ncbi.nlm.nih.gov/27449101/>. Acesso em: 9 ago. 2020.

ZHAO, Jing; QIN, Bo; NIKOLAY, Rainer; SPAHN, Christian M. T.; ZHANG, Gong. Translatomics: The global view of translation. . **International Journal of Molecular Sciences**, [S. l.], v. 20, n. 1, 2019. DOI: 10.3390/ijms20010212. Disponível em: [/pmc/articles/PMC6337585/?report=abstract](https://pubmed.ncbi.nlm.nih.gov/34811111/). Acesso em: 18 set. 2020.

ZOROV, Dmitry B.; JUHASZOVA, Magdalena; SOLLITT, Steven J. **Mitochondrial reactive oxygen species (ROS) and ROS-induced ROS release** *Physiological Reviews* American Physiological Society, , 2014. DOI: 10.1152/physrev.00026.2013.

7. CURRÍCULO VITAE RESUMIDO

CADORE, NATHAN A.

DADOS PESSOAIS

Nome: Nathan Araujo Cadore

Local e data de nascimento: Sapucaia do Sul, 17 de julho de 1998

Endereço profissional: CBiot/UFRGS, Av. Bento Gonçalves, 9500, Bloco IV, prédio 43-421, Sala 204/206, 91501-970, Porto Alegre, Rio Grande do Sul, Brasil.

Telefone profissional: +55 51 3308 6070

E-mail: cadorenathan@gmail.com

FORMAÇÃO ACADÊMICA

2019 – atual: Mestrado em Biologia Celular e Molecular, Universidade Federal do Rio Grande do Sul, UFRGS, Brasil.

2015 – 2018: Graduação em Biotecnologia, Universidade Federal do Rio Grande do Sul, UFRGS, Brasil. Título “Análise comparativa do perfil metabólico de células humanas de adenocarcinoma de pulmão sensíveis e resistentes à cisplatina”. Orientadora: Profa. Dra. Karina Mariante Monteiro.

ATUAÇÃO PROFISSIONAL

2018 – 2018: Estagiário. Departamento de Química e Bioquímica, Medical University of Lodz, Polônia. Carga horária: 40 h/semana

2018 – 2018: Voluntário de Iniciação Científica. Laboratório de Genômica Estrutural e Funcional, Centro de Biotecnologia, Universidade Federal do Rio Grande do Sul, Brasil. Projeto: Análise do perfil metabólico e bioenergético de células de adenocarcinoma de pulmão sensíveis e resistentes à cisplatina

2017 – 2018: Bolsista de Iniciação Científica. Laboratório de Biotecnologia, Instituto de Ciência e Tecnologia de Alimentos, Universidade Federal do Rio Grande do Sul, Brasil. Projeto: Produção de ácido graxos poli-insaturados pela levedura *Meyerozyma guilliermondii* utilizando resíduos agro-industriais como substrato. Carga horária: 20 h/semana.

2015 – 2017: Bolsista Iniciação Científica. Laboratório de Genômica Estrutural e Funcional, Centro de Biotecnologia, Universidade Federal do Rio Grande do Sul, Brasil. Projeto: Desenvolvimento de resistência à cisplatina em células humanas de adenocarcinoma de pulmão e caracterização celular e molecular das linhagens celulares. Carga horária: 20 h/semana.

FORMAÇÃO COMPLEMENTAR

2019: Biologia Estrutural para Iniciantes. Universidade Federal do Rio Grande do Sul, Brasil. (Carga horária: 15h).

PROJETOS DE EXTENSÃO

2020 – atual: Ação COVID-19. Ação voluntária para o diagnóstico de COVID-19 em amostras do Sistema Único de Saúde do estado do RS. Universidade Federal do Rio Grande do Sul, Brasil.

2015 – 2018: Falaí Biotec. Projeto de divulgação científica na área da biotecnologia para o público leigo. Universidade Federal do Rio Grande do Sul, Brasil.

PARTICIPAÇÃO EM EVENTOS

2019: Escola Gaúcha de Bioinformática

2018: Congresso SulBiotec 2018. Pôster: Validação de proteínas e mecanismos moleculares envolvidos na resistência à cisplatina em células humanas de câncer de pulmão.

2017: 37ª Semana Científica do Hospital de Clínicas de Porto Alegre. Apresentação oral: Desenvolvimento de resistência à cisplatina em células humanas de adenocarcinoma de pulmão e caracterização celular e molecular das linhagens celulares.

2017: Salão UFRGS 2017: SIC - XXIX Salão de Iniciação Científica da UFRGS. Pôster e apresentação oral: Desenvolvimento de resistência à cisplatina em células humanas de adenocarcinoma de pulmão e caracterização celular e molecular das linhagens celulares.

2016: XXVIII Salão de Iniciação Científica - UFRGS. Pôster e apresentação oral: Desenvolvimento de resistência à cisplatina em células humanas de adenocarcinoma de pulmão e análise da capacidade de reparo ao dano no DNA causado pela droga.

PRODUÇÃO BIBLIOGRÁFICA

Artigos completos publicados

BALBINOTTI, HELIER; CADORE, NATHAN A.; DUTRA, CRISTINE S.; DA SILVA, EDILEUZA D.; FERREIRA, HENRIQUE B.; ZAHA, ARNALDO; MONTEIRO, KARINA M.; Protein Profiling of Extracellular Vesicles Associated With Cisplatin Resistance in Lung Cancer. *Anticancer Res.* Outubro 2020, 40 (10) 5509-5516; DOI: <https://doi.org/10.21873/anticancer.14563>